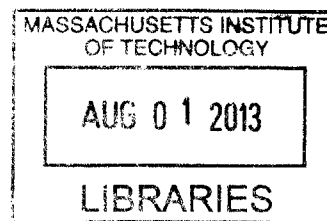


# A Generic Pathogen Capture Technology for Sepsis Diagnosis

By  
Ryan Mcomber Cooper

B.S. Bioengineering  
University of California at Berkeley, 2008

**ARCHIVES**



SUBMITTED TO THE DEPARTMENT OF CHEMICAL ENGINEERING IN  
PARTIAL FULFILLMENT OF THE REQUIREMENTS FOR THE DEGREE OF  
  
DOCTOR OF PHILOSOPHY IN MEDICAL AND ENGINEERING PHYSICS  
AT THE  
MASSACHUSETTS INSTITUTE OF TECHNOLOGY

MAY 2013  
[JUNE 2013]

© Massachusetts Institute of Technology 2009. All rights reserved.

Signature of Author: \_\_\_\_\_  
HST Department  
May 1, 2013

Certified by: \_\_\_\_\_  
Donald E. Ingber  
Judah Folkman Professor of Vascular Biology, Harvard Medical School & Boston Children's Hospital  
Professor of Bioengineering, Harvard School of Engineering and Applied Sciences  
Thesis Supervisor

Accepted by: \_\_\_\_\_  
Emery N. Brown, MD, PhD  
Director, Harvard-MIT Program in Health Sciences and Technology  
Professor of Computational Neuroscience and Health Sciences and Technology

# **A Generic Pathogen Capture Technology for Sepsis Diagnosis**

by

Ryan Mcomber Cooper

Submitted to the Department of Health Sciences and Technology

on May 1, 2013, in partial fulfillment of the

requirements for the degree of

Doctor of Philosophy in Medical and Engineering Physics

## **Abstract**

Sepsis is a systemic inflammatory response that results the presence and persistence of microorganisms or their toxins in the bloodstream and it is diagnosed by detecting the presence of pathogens in blood. Despite improvements in modern medicine, sepsis has a high mortality rate that increases rapidly with every hour the patient does not receive optimal antibiotic therapy. Thus, there is a great demand for technologies that can accelerate pathogen detection and sepsis diagnosis. Our lab previously developed a micromagnetic-microfluidic pathogen isolation technology that can selectively remove pathogens from flowing whole human blood with high efficiency using micro- or nano-sized magnetic beads coated with microbe-specific antibodies [1, 2]. However, the identity of the pathogen is not known when a patient first presents with the clinical symptoms of sepsis, and currently, it can take days to a week to identify the specific pathogen type. The goal of this dissertation is to develop a generic pathogen collection technology that can be used to pull bacteria and fungi out of blood or other fluids without first knowing their identity, and to concentrate them for analysis and rapid identification. In Chapter 1, I will review the field of sepsis diagnostics and methods that have been employed to confront this challenge. In Chapter 2, I describe the development of a natural human opsonin - Mannose Binding Lectin (MBL) – as a generic pathogen capture molecule. MBL is found in human blood and is part of the innate immune system; it has been previously shown to bind over 90 different types of pathogens, including gram negative and positive bacteria, fungi, viruses and parasites [3-5]. The studies described in this chapter include development and optimization of methods to coat magnetic beads with MBL and demonstration that MBL beads bind to wide range of pathogens with high efficiency in saline and blood. The binding of MBL beads to sample pathogens is tested under a wide range of conditions to determine optimal bead concentration, binding time and sample treatments to maximize binding in blood. In Chapter 3, I describe development of a device that efficiently concentrates and visualizes fungi tagged with the magnetic MBL micro beads. Visualization is made possible by controlling the balance of fluidic shear stress and magnetic force on the tagged pathogens in the device, which enables spreading of the beads and bound fungi into a uniform

layer that can be quickly quantified with fluorescent microscopy. Chapter 4 describes tools that I have developed to rapidly concentrate and purify magnetically tagged bacteria from blood and other complex samples for polymerase chain reaction (PCR) detection. The MBL-bead approach is used to pull out and concentrate pathogens from large sample volumes, and to remove contaminating human DNA, so that sensitive detection can be carried out using PCR amplification. The efficiency of this new MBL-based, sample pre-concentration method is compared to existing commercial isolation methods for analysis of both blood and food samples. Finally, I discuss the implications of these findings in Chapter 5.

Thesis Supervisor: Donald E. Ingber

Title: Professor of Vascular Biology & Bioengineering

## **TABLE OF CONTENTS**

<b><u>ABSTRACT</u></b>	<b>2</b>
<b><u>TABLE OF FIGURES</u></b>	<b>7</b>
<b><u>ACKNOWLEDGEMENTS</u></b>	<b>8</b>
<b><u>GLOSSARY</u></b>	<b>9</b>
<b><u>CHAPTER 1 INTRODUCTION</u></b>	<b>10</b>
1.1 WHAT IS SEPSIS	10
1.2 ROLE OF DIAGNOSTICS	11
1.3 CURRENT DIAGNOSTICS FOR SEPSIS	13
1.4 ALTERNATIVE DIAGNOSTIC METHODS BEING RESEARCHED	16
1.5 BINDING OF RARE CELLS	18
1.6 CONCENTRATION OF MAGNETICALLY TAGGED CELLS	18
1.7 GENERIC OPSONINS	19
1.8 SUMMARY	22
1.9 AIMS	23
<b><u>CHAPTER 2 GENERAL MAGNETIC OPSONINS</u></b>	<b>25</b>
2.1 INTRODUCTION	25
2.2 MATERIALS AND METHODS	26
2.2.1 FUNCTIONALIZING MAGNETIC BEADS	26
2.2.2 PATHOGEN STOCKS	26
2.2.3 BINDING QUANTIFICATION (DEPLETION ASSAY)	27
2.2.4 RECOMBINANT MBL (FcMBL) PRODUCTION	28
2.2.5 CALCIUM DEPENDENCE	28
2.2.6 BINDING IN BLOOD	29
2.3 RESULTS	32
2.3.1 BINDING IN SALINE	32
2.3.2 BINDING IN BLOOD	39
2.4 BEAD BINDING THEORY	52
2.5 DISCUSSION	55
<b><u>CHAPTER 3 OPTICAL DETECTION OF FUNGI</u></b>	<b>59</b>
3.1 INTRODUCTION	59
3.2 MATERIALS AND METHODS	59

3.2.1 MICRODEVICE FABRICATION	59
3.2.2 TESTING EARLY PROTOTYPES	61
3.2.3 MASS BALANCE STUDY	63
3.2.4 MAGNETIC FLUX CONCENTRATION CHARACTERIZATION	64
3.2.5 BEAD ISOLATION	65
3.2.6 RUNNING THE DIAGNOSTIC DEVICE	65
3.2.7 AUTOMATED DETECTION	67
<b>3.3 RESULTS</b>	<b>67</b>
3.3.1 INITIAL PROTOTYPES AND MASS BALANCE EXPERIMENT	67
3.3.2 SEPARATION THEORY	69
3.3.3 ALTERING THE MAGNETIC FIELD	72
3.3.4 MFC CHARACTERIZATION	75
3.3.5 DETECTION OF PATHOGENS	75
3.3.6 AUTOMATED COUNTING	78
<b>3.4 DISCUSSION</b>	<b>78</b>
<b><u>CHAPTER 4 PCR DETECTION OF BACTERIA</u></b>	<b><u>82</u></b>
<b>4.1 INTRODUCTION</b>	<b>82</b>
<b>4.2 MATERIALS AND METHODS</b>	<b>82</b>
4.2.1 MAKING A BETTER MAGNETIC RACK	83
4.2.2 MAGNETIC ENHANCEMENT BEADS (MEB)	84
4.2.3 FCMBL SAMPLE PREPARATION PROCEDURE	85
4.2.4 MOLYSIS SAMPLE PREPARATION PROCEDURE	87
4.2.5 HYBRID SAMPLE PREPARATION PROCEDURE	88
4.2.6 DNA EXTRACTION	89
4.2.7 BEAD INTERFERENCE WITH DNA EXTRACTION	90
4.2.8 PCR AND QUALITATIVE ANALYSIS	90
4.2.9 PRIMER EVALUATIONS	91
4.2.10 QPCR ANALYSIS	92
4.2.11 PCR DETECTION OF BACTERIA FROM FOOD	93
<b>4.3 RESULTS</b>	<b>95</b>
4.3.1 BUILDING A BETTER MAGNETIC RACK	95
4.3.2 MEB AND IMPROVING PATHOGEN SEPARATION	97
4.3.3 RESULTS IN SALINE	101
4.3.4 SAMPLE PREPARATION IN BLOOD AND COMPARISON TO COMMERCIAL KIT	102
4.3.5 OTHER COMPLEX SAMPLES	106
<b>4.4 DISCUSSION</b>	<b>110</b>
<b><u>CHAPTER 5 CONCLUSIONS</u></b>	<b><u>116</u></b>
<b>5.1 THESIS CONTRIBUTIONS</b>	<b>116</b>
5.1.1 GENERAL MAGNETIC OPSONINS	116

5.1.2 OPTICAL DETECTION OF FUNGI	117
5.1.3 RAPID PCR DETECTION OF BACTERIA	117
<b>5.2 FUTURE DIRECTIONS</b>	<b>118</b>
<b><u>CHAPTER 6 REFERENCES</u></b>	<b><u>121</u></b>

---

## Table of Figures

Figure 1.1 Stages of Sepsis .....	11
Figure 1.2 Time required for sepsis diagnosis .....	12
Figure 1.3 Pros and Cons of different methods to detect pathogens in blood.....	15
Figure 1.4 Structure of MBL .....	20
Figure 1.5 Using general magnetic opsonins of detect pathogens in blood.....	23
Figure 2.1 Procedure for Depletion assay to measure bead binding.....	27
Figure 2.2 Antibody vs. MBL beads.....	32
Figure 2.3 Calcium Dependence of MBL Binding.....	34
Figure 2.4 WtMBL Bead Binding in Saline (both 1 $\mu$ m and 128 nm beads) .....	35
Figure 2.5 Recombinant MBL (FcMBL).....	37
Figure 2.6 Role of bead size, concentration and FcMBL density in binding of E. coli in saline.....	38
Figure 2.7 Complexity of Blood .....	40
Figure 2.8 Effect of Dilution on binding of C. albicans with 1 $\mu$ m beads in heparinized blood .....	41
Figure 2.9 Effect of Temperature on phagocytosis.....	44
Figure 2.10 Effect of Salicylic Acid on Coagulation and binding in blood.....	46
Figure 2.11 Binding and separation of magnetically tagged fungi and bacteria from diluted blood.....	47
Figure 2.13 Binding of C. albicans in diluted and undiluted blood with different concentrations of 1 $\mu$ m FcMBL beads.....	50
Figure 2.14 Testing multiple species of pathogens with FcMBL beads .....	51
Figure 3.1 Fabrication of microdevice mold.....	60
Figure 3.2 Initial Diagnostic Prototype.....	62
Figure 3.3 Initial Diagnostic Prototype.....	63
Figure 3.4 Experimental Layout of Optical Diagnostic System .....	66
Figure 3.5 Results from early device prototypes .....	68
Figure 3.6 Problem with magnetic beads and optical detection.....	69
Figure 3.7 Forces at work during the separation process.....	71
Figure 3.8 Layout of MFC and microfluidic device .....	73
Figure 3.9 Characterization of the MFC .....	74
Figure 3.10 Detection of C. albicans in microdevice vs. bead concentration .....	76
Figure 3.11 Detection of C. albicans in Saline and Blood.....	77
Figure 4.1 The Hex Rack .....	84
Figure 4.2 FcMBL sample preparation method .....	87
Figure 4.3 MoLYsis sample preparation method.....	88
Figure 4.4 Hybrid sample preparation method .....	88
Figure 4.5 Modified FcMBL sample preparation method for isolating bacteria from food samples .....	94
Figure 4.6 Magnetic Enhancement Beads.....	98
Figure 4.7 MEB Theory.....	99
Figure 4.8 Effectiveness of the MEB and Hex Rack .....	100
Figure 4.9: Effect of FcMBL beads and MEB on DNA extraction .....	102
Figure 4.10 FcMBL vs. MoLYsis Sample Preparation Methods, n=7, error bars: SEM.....	105
Figure 4.11 PCR detection of E. coli in different dilutions of food using FcMBL Sample Prep .....	107
Figure 4.12 : Bacteria Detection in Food using FcMBL Sample Prep Procedure .....	109

# Acknowledgements

---

I would like to start by thanking my thesis adviser, Don Ingber, who made this project possible. He reminded me to keep track of the big picture and taught me how to effectively present my ideas. I would also like to thank Chong Yung, who got me started in the lab and helped get the diagnostic part of the project started. I would also like to thank Joel Voldman and Alexander McAdam, the other members of my thesis committee, both for reading through this document and their advice along the way.

I would also like to thank Mike Super and the rest of sepsis group for their help in making the FcMBL beads and their advice and feedback as we moved forward. In particular, I would like to thank Dan Leslie, Karel Domansky and Abhishek Jain for helping to develop the magnetic simulations and optical systems for the MFC and optical detection microdevice. Nazita Gamini, Martin Rottman, Alex Watters, Anna Waterhouse and Julia Bellows provided valuable advice and expertise for creating the PCR assays used to test the FcMBL sample preparation methods, work on improving binding and helping me troubleshoot the assays.

I would like to thank Jay Lee and Dina Super (for collecting) and the blood donors (for contributing) to the project. I owe special thanks to Eileen Lowe and the IV staff at Mt Auburn Hospital for training me to collect the blood samples so that we were never short on phlebotomists.

The multitalented team at the Wyss Institute merits thanks for creating the collaborative, creative environment that made this projects and others like it possible. I want to particularly thank Jeannie and Susan for helping a poor grad student find his way through the place as it rapidly evolved, putting up with all the stupid questions I had.

Finally I would like to thank all my family and friends, who kept me going through this whole process and believed in me, even when I didn't. They kept life interesting, sharing the joys and helping me to get through the sorrows and pains associated with life in grad school.



## Glossary

$\rho_{2d}$	Density of bead packing on two dimensional surfaces
$\mu$	Magnetic Dipole
$\eta$	Fluid viscosity
AST	Antibiotic Susceptibility Testing
B	Magnetic Field
$C_b$	Concentration of magnetic beads
$C_c$	Concentration of target pathogens
$C_q$	Threshold cycle for sample in qPCR amplification
D	Diffusivity
$D_c$	Diffusivity of target pathogens
$D_b$	Diffusivity of magnetic beads
EDTA	Ethylenediaminetetraacetic acid, a common anticoagulant that chelates calcium
$F_m$	Magnetic force on the beads induced by the magnetic field
$F_d$	Drag force on beads and/or pathogens
IgG	Immunoglobulin G
FcMBL	Recombinant version of FcMBL
MRSA	Methicillin Resistant <i>Staphylococcus aureus</i>
MBL	Mannose Binding Lectin
N	Number of beads of attached to the pathogens
PCR	Polymerase Chain Reaction
PDMS	polydimethylsiloxane (PDMS), also called Sylgard 184 (Dow Corning)
Pe	Peclet number
qPCR	Quantitative Polymerase Chain Reaction
$R_{cb}$	Collision rate between magnetic bead and pathogen
$r_c$	Radius of target pathogen
$r_b$	Radius of target bead
SU-8	Negative photoresist used to make molds for soft lithography
t	time
T	Absolute temperature
TBS	Tris Buffered Saline
$v_{cb}$	Relative velocity of bead and pathogen relative to each other
$v_{diff}$	Diffusion velocity of the beads towards the pathogen
$v_s$	Settling velocity of magnetic bead toward the ceiling of the microchannel
VRE	Vancomycin-Resistant <i>Enterococcus</i>
WtMBL	Wild type mannose binding lectin
u	Representative velocity

## Chapter 1 Introduction

### 1.1 What is Sepsis

The Center for Disease Control defines sepsis as a systemic disease associated with the presence and persistence of pathogenic microorganisms or their toxins in the bloodstream [6]. The infection itself is usually caused by a single species that manages to escape eradication by the immune system and begins to spread throughout the entire body, causing widespread release of cytokines that begins the immune dysregulation which drives the downward spiral [7]. As a disease, sepsis progresses through several stages (**Figure 1.1**). The first stage is systemic inflammatory response syndrome (SIRS), characterized by abnormal temperature, tachycardia, tachypnea and abnormal white blood cell counts, all caused by large scale dysregulation of inflammatory cytokines, commonly known as a ‘cytokine storm.’ In addition to live bacteria, fragments of bacteria such as peptidoglycan, lipoteichoic acid, lipopolysaccharide (LPS) and endotoxins in the bloodstream can elicit a strong immune response, contributing to SIRS [8]. SIRS itself is a non-specific symptom and can be caused by a range of underlying etiologies, including sepsis, so diagnostic tests are required to confirm the cause [9]. If a patient has sepsis and remains untreated, they may progress to severe sepsis where their organ systems stop working (such as renal or respiratory failure) as a result of the widespread dysregulation of inflammatory cytokines, driven by the systemic infection. Assuming their failing organs can be temporarily supported in an intensive care unit, they may progress to the final stage of the continuum: septic shock. Septic shock occurs when multiple organs fail and hypotension that cannot be reversed even with fluid resuscitation occurs, often resulting in death [6, 10].

Because of these severe effects of systemic infections, sepsis has a very high mortality rate, ranging between 20-50% [6-8] for bacterial sepsis but it can be as high as 60% mortality if a fungal pathogen is the cause. The incidence of sepsis is actually increasing as more and more antibiotic resistant pathogens evolve, more immunocompromised patients emerge (due to HIV, chemotherapy, organ transplants, etc) and more invasive surgical procedures are performed [11-13]. It is currently the leading killer in intensive care units, causing 17% of total hospital related deaths in the US [14]. In the United States alone, the incidence of sepsis has more than doubled since 2000 and costs \$15 billion per year to treat [14] The problem is even more devastating in

the developing world where 98% of infant deaths due to sepsis occur, primarily due to lack of diagnostic technologies [13].

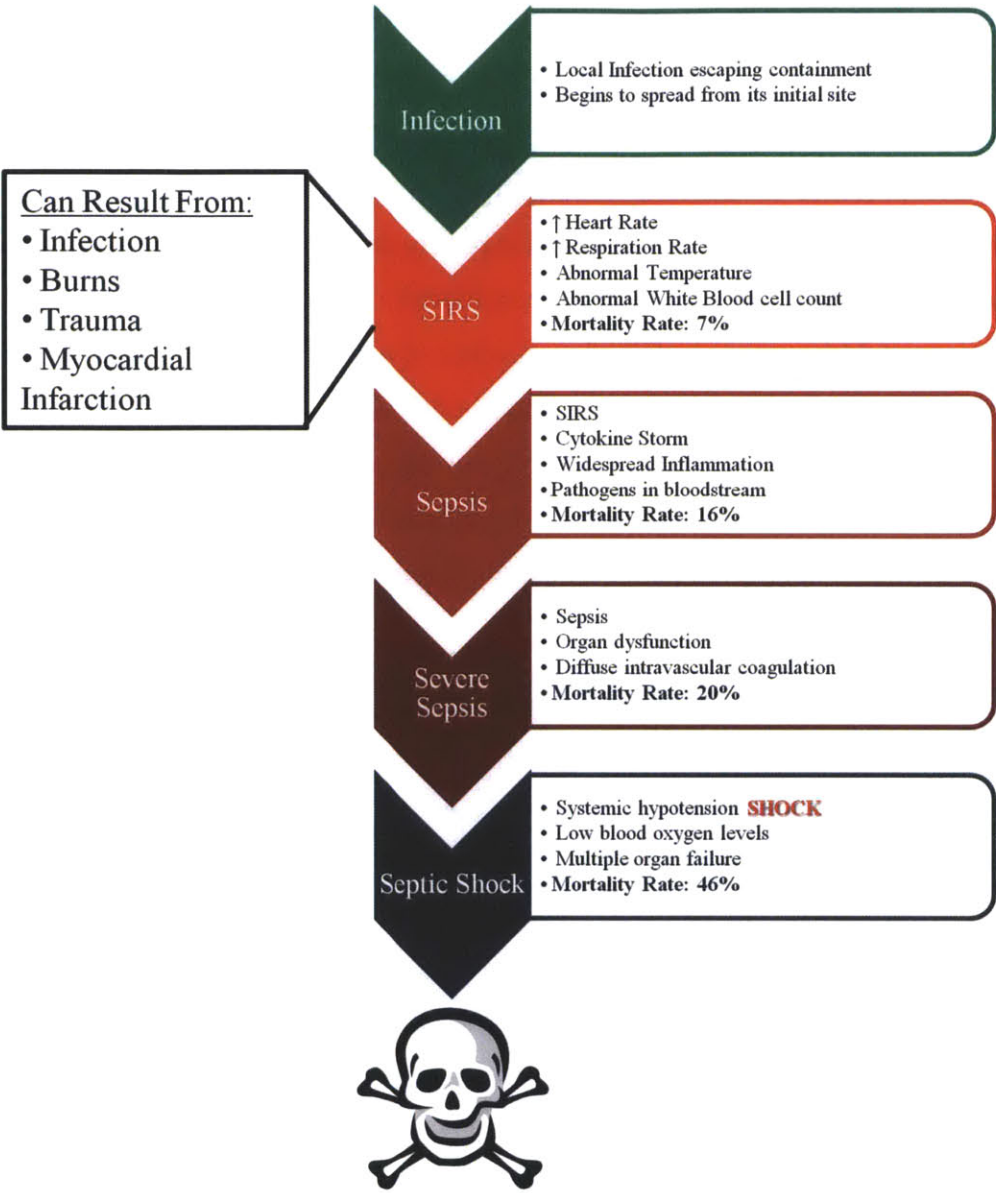






*Figure 1.1 Stages of Sepsis*  
*Sepsis starts as a local infection that the immune system cannot contain which spreads and triggers a systemic inflammatory reaction that spirals out of control, culminating in multiple organ failure, shock and death if the immune system and antibiotics cannot bring it under control. The risk of death increases as the disease progresses [15]*

**1.2 Role of Diagnostics**

While the incidence of sepsis has increased steadily over the last thirty years, sepsis diagnostic technology has changed little in the last 100 years. The primary challenge in diagnosing sepsis is that the circulating pathogen load in blood is actually very low despite its dramatic effect, typically ranging from 1 to 10 colony forming units (cfu)/ml of blood, although some patients can have loads over 1000 cfu/ml [16]. Currently ‘sepsis’ is a clinical diagnosis that results from the presence of bacteria (bacteremia) or fungi (fungemia) in the bloodstream. However, the precise circulating pathogen load is poorly defined since current measurements are relatively insensitive [10]. Currently sepsis is considered a clinical diagnosis because it typically takes a minimum of 24 hours to confirm the presence of a pathogen, so the clinicians will begin empirical treatment with broad spectrum antibiotics, which may or may not be effective depending on the pathogen. Once the data on the causative organism is obtained from the microbiology lab, the antibiotic treatment can be tailored to maximize its effectiveness. If this information is available before the patient’s organ system begin failing, they have a much better chance of survival.

	Testing Phase	Time	Information
1	Sample Arrives		
2	Automated Blood Culture	12-72 hours	Infection present
3	Plating & Gram stain	5 minutes	Gram +/-
4	Sub-culturing	24-48 hours	
5	Plate Inspection	1 minute	Probable genus
6	Automated AST and Gram Negative Identification	12-24 hours	Species and susceptibilities

**Total: 1-7 days**

*Figure 1.2 Time required for sepsis diagnosis*  
*This is the standard workflow for Mt. Auburn Hospital in Cambridge, MA, which handles about 10,000 samples per a year. Automated monitoring of the blood culture bottles has decreased the diagnosis time slightly, but a dedicated lab and a trained staff are still required*

Several studies have confirmed that a faster diagnosis time and therefore a faster time to optimal antimicrobial therapy significantly decreases both the cost of treatment and the mortality rate of sepsis [17]. The risk of death can increase as much as 9% for every hour that effective treatment is delayed in sepsis [18, 19]. Faster diagnostic times also help prevent the use of ineffective antimicrobial therapies, reducing the risks of creating drug resistant pathogens and causing adverse drug reactions, which is particularly important for highly cytotoxic antifungal

medications [20]. Treatment can be ineffective for many reasons including no coverage of the pathogen (such as treating a fungal infection with antibiotics), resistance of the pathogen to the medication, poor penetration of the drug into the infection site and underdosing [21]. Antifungal medications are toxic enough that most clinicians will not start their use without definitive microbiological data, so the patient can go days without effective treatment, contributing to the higher mortality rate of fungal sepsis [19, 22]. Therefore, rapid confirmation of the clinical diagnosis, particularly information on which antibiotics would be most effective, can save lives and reduce treatment costs. However, the current diagnosis technologies available to clinicians cannot provide this.

### **1.3 Current Diagnostics for Bacteremia and Fungemia**

Blood culture is the current state-of-the-art method for detecting low levels of pathogens in blood and has been so since the technique was first pioneered in the early 20th century. There are several stages for blood culture (**figure 1.2**): first, a blood sample is collected aseptically into a culture bottle containing growth media. Second, the sample is placed in an incubator and monitored for signs of growth. Third, if any signs of growth appear, the cultured pathogen is subcultured on several different types of agar plates to obtain a pure colony. Finally, the pure colony is used to identify the pathogen and determine its antibiotic susceptibility of that pathogen in an automated microdilution system. The entire process typically takes between 24 to 72 hours, depending on the pathogen and each different stage is vulnerable to errors. The standard workflow for a medium-sized hospital is quite elaborate and illustrates why the process is prone to errors and is difficult to implement in lower resource settings, where the need for sepsis diagnostics are often much greater.

The initial collection of the blood sample is perhaps the most difficult part of the process because sterile technique, proper growth media and timing can all be critical. Blood culture can only detect viable pathogens in the blood, which are at their highest concentration immediately after the septic patient spikes a fever [7]. Recent administration of antibiotics can bias the results by killing the viable circulating bacteria in the bloodstream but not wiping out the focus of the infection, creating a false negative result [23]. After a fever spike, two or more 10 ml samples are collected from different veins in the patient's body after the skin at the venipunctures site has been thoroughly sterilized by the phlebotomist performing the draw [24, 25]. A decision must also be made about what type of culture bottles to use; whether the presumed pathogen requires

aerobic, anaerobic or fungal media to culture; a decision that must currently be inferred from the patient's history and physical symptoms. The sample volume must be reduced for children to 1 to 2 ml of blood, but in neonates it can be difficult to obtain even that much [26].

After collection, the blood culture bottles are placed in an incubator and monitored for signs of metabolism (such as production of carbon dioxide). This step is also highly variable because the optimal growing conditions and growth rate of pathogens varies from species to species; some bacteria take as little as 12 hours while other organisms can take days and some organisms cannot be cultured at all by this method, particularly if the wrong type of culture media was used. Consequently, many patients suspected to have sepsis never have the diagnosis confirmed [27]. If the bottle does show growth, the patient likely has an infection (assuming skin flora did not contaminate the sample), but the clinicians still don't know what the organism is or what will be treat it.

If the culture becomes positive, there are enough microorganisms to identify directly, so they undergo Gram staining to differentiate between the two major classes of bacteria. The positive culture broth is plated on a range of different agar plates that favor growth of particular species or strains, which are then cultured for 24 hours so that individual bacterial colonies are visible. Skilled microbiologists can identify the genus and species of some pathogens based on its growth conditions and colony morphology, but antibiotic susceptibility testing (AST) provides the most useful information for treatment.

AST produces the most critical information that clinicians require for treatment; which antibiotics the pathogen is most vulnerable to. Bacteria from one of the subcultured plates are suspended in media and then grown for between 4 to 24 hours in the presence of a range of different antibiotics and several metabolic indicators that can be used to identify its species. This process has been simplified with 96 well plates preloaded with the different reagents that can be placed in an automated incubator with a built in colorimetric readout system (automated microdilution system). Alternatively, the bacteria can be plated once more on dishes that contain different antibiotic bearing discs or strips of paper to determine which of the drug impregnated disks inhibits the growth of adjacent bacteria [28].

Blood culture diagnostic systems tend to be slow and expensive. The system typically takes 24-72 hours to return a diagnosis in a disease that can progress in a matter of hours [29]. The diagnosis itself is not very reliable either, since the system is prone to false positives from

contamination and false negatives from incorrect culture conditions for fastidious microbes [7, 28]. In more than 50% of the cases where sepsis is strongly suspected, blood cultures never return a positive reading [30]. The high cost of maintaining a microbiology lab currently means that only hospitals with central labs can afford to operate one, since they require a large amount of resources, a trained staff and millions of dollars in equipment to run. As a result of all these shortcomings, clinicians often can never verify their diagnosis of sepsis and must rely on epidemiology and experience to try and guess the best antimicrobial treatment (**figure 1.3 a**).

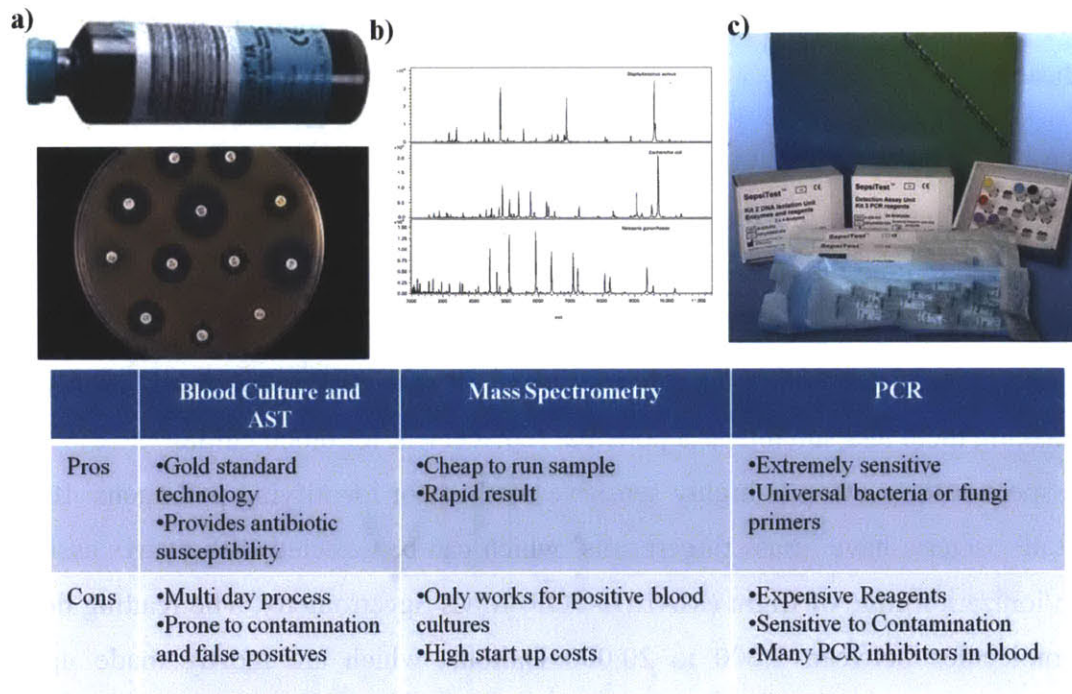


*Figure 1.3 Pros and Cons of different methods to detect pathogens in blood (a) Blood culture bottle and Petri dish with antibiotic impregnated disks used to test AST (Bauer-Kirby procedure). Reprinted from [36] (b) Mass fingerprint of different bacteria from MALDI-TOF analysis. Reprinted from [37](c) SepsisTest qPCR kit (Molzylm) for identifying pathogens. Reprinted from [38]*

This microbiological culture detection method is used widely in several other types of samples, ranging from concentrated platelets for transfusion to food samples [31, 32]. Platelet concentrates are especially vulnerable to bacterial contamination because they must be stored at room temperature, allowing uninhibited growth of bacteria in the concentrate bags, so they must be screened for contamination with microbial cultures, a process which roughly cuts the useful half life of the concentrates in half [33]. Detection of pathogenic bacterial contamination in food

is also culture based; even PCR detection assays often require culture for 1-2 days to sufficiently enrich the bacteria from food for detection, during which time the food must be stored at great expense [34, 35].

Faster, cheaper and more reliable methods for detecting rare bacteria in complex samples such as blood samples could potentially save millions of lives around the world and billions of dollars, so a variety of approaches to speed up the process are currently being investigated. These alternatives are also running into the difficulty of detecting fewer than ten pathogens among billions of red blood cells and millions of white blood cells per milliliter of blood. It's roughly equivalent to trying to find a single infectious grain of sand somewhere in four dump truck loads from the beach.

#### **1.4 Alternative Diagnostic Methods Being Researched**

Mass spectrometry and molecular diagnostics such as polymerase chain reaction (PCR) are currently believed to hold the future of sepsis diagnostics, but both systems have had difficulty in overcoming the signal to noise created by low pathogen counts in human blood. Biomarkers have also been investigated but their role in sepsis still remains undefined and highly variable [10, 39], making them less suitable as a potential replacement for blood culture.

Mass spectrometry offers a highly sensitive method for identifying pathogens. It has been found that all bacteria have 'mass fingerprints' which can be detected with matrix assisted laser desorption/ionization time of flight (MALDI-TOF) Mass Spectrometry. The reading detects and analyzes molecules between 2,000 to 20,000 Daltons, which are mostly made up of high abundance ribosomal proteins that vary from species to species, creating the specificity of the fingerprint [37]. A single machine can run several tests per hour at very little cost per a sample, although the machine itself is quite expensive [40]. The main limitation of mass spectrometry is that all the current systems require at least 5000 bacteria (although 100,000 or more is preferred for a better signal) in the sample matrix for a high enough signal to noise ratio to accurately determine the species, particularly if the sample is polymicrobial [41, 42]. This has limited mass spectrometry to identifying pathogens from positive blood cultures, which is still highly useful since it reduces the average diagnostic time by 26.5 hours at a comparable cost of existing AST methods, but it still suffers from some of the same limitations as standard blood culture [42-47]. Mass spectrometry is also a reliable method for differentiating between different types of yeasts, whose macro and microscopic characteristics are highly subjective and DNA extraction from



fungi for PCR is difficult due to their extremely tough cell walls [48-51]. So mass spectrometry is a very promising method for identifying pathogens out of blood cultures, but the high bacteria count required for a reliable mass fingerprint makes it unlikely it can detect pathogens directly from blood samples, since even in very septic patients the size of the blood draw required to have a sample with 5,000 microbes or more would require a very large volume of blood (**figure 1.3 b**).

PCR has the ability to amplify a single gene several million-fold and is capable of detecting single cells. Because this assay relies on DNA, it can pick up not only viable pathogens, but also dead ones or even phagocytosed pathogens, giving it a larger population to detect than is possible by blood culture [52]. Universal primers targeting highly conserved regions of 16s ribosomal DNA for bacteria and internal transcribed spacer region for fungi, are available [9, 53]. Therefore, with one or two primer sets, it should be possible to amplify DNA from nearly all known microbial pathogens. The amplified PCR product can then be sequenced to determine the species of the microbe. Microfluidic PCR systems can completely run an entire PCR reaction in less than 30 minutes using far less reagents than bench top systems, offering a truly rapid detection method [54-63]. However, several practical difficulties of working in blood have so far prevented the full potential of PCR diagnostics from being realized.

Extracting pathogen DNA currently has low efficiency and the reaction chemistry of PCR itself is delicate and vulnerable to a large number of inhibitors which abound in blood [28], so sample preparation has been problematic for both bench top and microfluidic systems [55, 59, 62, 64-68]. Furthermore, anticoagulants, hemoglobin, calcium, human DNA and immunoglobulin G all interfere with the reaction as well, and these are millions of times more abundant than the target pathogen in most blood samples [28, 69]. A robust sample preparation method to remove the majority of inhibitors found in blood is of paramount importance to make PCR a viable sepsis diagnostic technology, but no robust system has yet emerged. Some commercial companies have developed methods such as VYOO and MolYsis to try and enrich pathogen DNA in the sample, but none are currently approved for clinical use by the FDA. The MolYsis sample prep kit is arguably the most reliable, but its sensitivity is 50 cfu/ml, which is not sufficient to detect bacteria in the majority of septic samples [21] (**figure 1.3c**). Some groups have reported reaching down to 1 cfu/ml sensitivity through a variety of techniques such as nested PCR but reproducibility has been problematic [53]. General opsonin magnetic beads

potentially offer a simple way bind, concentrate and purify pathogens out of blood, greatly increasing the reliability of PCR for use as a diagnostic.

### **1.5 Binding of Rare Cells**

The use of immunomagnetic beads for binding and concentrating a large variety of cells and molecules have been growing in recent years. They were first used in 1977 when Molday et al. used lectin-functionalized iron oxide particles to bind and isolate red blood cells [70]. The majority of beads now used for this form of purification are superparamagnetic, meaning that they become magnetized when placed in a magnetic field but unlike ferromagnetic materials such as iron, they are not magnetic when the magnetic field is removed [71]. This makes it very easy to resuspend the beads in solution after magnetic concentration, which has led to their widespread adoption.

The force on these beads created by the magnetic field is directed parallel to the local magnetic field lines and proportional to the strength of the local magnetic field gradient [72]. Once the beads are attached to target cells, they can be used to apply a variable amount of force to a cell for purification or mechanical testing [73-75] or even more delicate operations such as rotation [76, 77]. The majority of beads used for biological applications are on the scale of micron or nanometers, meaning that they have a very large surface area to volume ratio, which gives rise to their greatest strength. A large number of beads can be added into a large fluid volume and mixed so that the beads rapidly probe every microliter of that volume and come in contact with its entire contents in a matter of minutes. If the large surface area of the beads is functionalized with a protein that can bind to a population of interest, such as a pathogen, this population will be rapidly tagged with magnetic beads that can then be magnetized to pull that population out of the tagged fluid [74, 78].

### **1.6 Concentration of Magnetically Tagged Cells**

Once the population of interest is magnetically tagged, several bulk and microfluidic separation systems are available for purification. The majority of bulk systems are essentially a test tube rack with permanent magnets in place next to the tubes that can generate enough force to pull out the micron scale beads such as Invitrogen Dynabeads, popular for binding mammalian cells. Miltenyi Biotech produces the MACS separation column, which is a column packed with steel wool that generates magnetic gradients strong enough to capture nanometer scale beads

when magnetized [79]. Microfluidic systems with external permanent magnets or micro fabricated electromagnets offer much finer control over separation conditions than bulk systems and have been widely employed to study the finer aspects magnetic cell separation [78, 80-83] with both simulations and experimental observations. Precise calculations are difficult because magnetization, convection, diffusion, collision theory and reaction chemistry all need to be taken into account when dealing with magnetically tagged cells, which restricts the majority of problems to finite element solver programs using either particle tracking or continuum models to represent the beads and bound cells [84-86]. The models can then be confirmed with experiment in the microfluidic device. The primary advantage of a microfluidic separation system is that it can offer a way to transition bulk bead binding to a small volume for detection because the magnetically tagged pathogens can be concentrated in a small area on the device, going from milliliter volumes in a tube to microliter volumes in a microfluidic chip.

Since 1977, several groups have employed primarily antibody-functionalized beads for a wide variety of different applications, including isolation of circulating tumor cells [73, 87, 88], endothelial progenitor cells [75], CD56+ cytotoxic cells [89], *E. coli* [90], and *C. albicans* [91] from blood and even bacteria out of food samples [92]. The Ingber Lab's previous work with *E. coli* and *C. albicans* showed that magnetic beads could be used to reliably remove pathogens out of human blood. Virtually any population to which an antibody or other binding protein can be created is a candidate for this magnetic tagging method, giving it a great deal of flexibility for biological assays. However, the use of antibody functionalized beads for a diagnostic system to bind rare pathogens out of a complex sample such as blood is intrinsically limited because the beads can only bind a limited group of pathogens. This would work well if there was only one population of interest, such as tumor cells or methicillin resistant *S. aureus* (MRSA), but is not sufficient for sepsis diagnostics, which must be able to pick up at least 20 different species. General opsonins are single molecules that have the ability to bind a wide range of different target cell types, so magnetic beads coated with these molecules should overcome this limitation.

## **1.7 Generic Opsonins**

Antibodies such as immunoglobulin G are important effectors of the adaptive immune system; this system is a relatively recent evolutionary development. General opsonins form an integral part of the primitive immune system, which evolved millions of years before the adaptive immune system and relies heavily on a class of sugar binding molecules called lectins

for defense against invading organisms [93]. In many invertebrates such as the Japanese horseshoe crab *Tachypleus tridentatus* [94], the silkworm *Bombyx mori* [95], and the cockroach [96], the primitive immune system is their primary form of defense. In mammals such as humans, the primitive immune system and its lectins form the first line of defense, giving time for the adaptive immune system to produce specific antibodies against an insult [93, 97]. The lectins of the innate immune system play key roles in the opsonization, activation of prophenol oxidation, phagocytosis, agglutination, activation of complement and lysis of foreign cells [98-100]. Many lectins can recognize pathogen associated molecular patterns (PAMPs) such as peptidoglycans, lipoteichoic acid and lipopolysaccharide, which are produced by bacteria but not by eukaryotic hosts. There is a wide range of lectins available that can bind to bacteria, but relatively few of them are suitable for working in blood, since most invertebrate and plant lectins see mammalian red blood cells as foreign and will attach to them, which has made some useful for blood typing [101-103]. To find a general opsonin that could bind a wide range of pathogens but is also compatible with human blood, we turned to the human primitive immune system, of which the most prevalent molecule is a polymer called mannose binding lectin (MBL), sometime also known as mannan binding lectin (**figure 1.4a**).

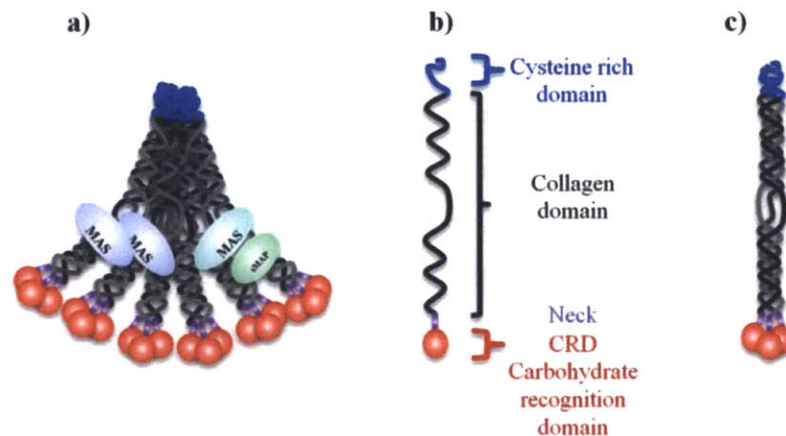


*Figure 1.4 Structure of MBL*

(a) Full polymeric form of the protein with MASP's attached to the collagen-like stalks, which are responsible for sensing MBL binding and initiating the complement cascade, coagulation and phagocytosis. (b) Single monomer of MBL. The CRD contains the actual binding pocket for the target sugar residues and the collagen domain and cysteine rich domain control polymerization of the protein. (c) Three monomers combining so that their collagen-like domains form a triple helix. These trimers assemble into the full protein.

MBL was first discovered in serum as a molecule that could inhibit influenza A virus, but it was not actually identified for another 40 years until immunologists began to realize the

importance of the primitive immune system [104]. The molecule itself is part of the calcium-dependent lectin family, along with surfactant proteins A and D (SP-A and SP-D) [99]. It is primarily a serum protein but is also found in amniotic fluid, nasal secretions, middle ear fluid and inflamed sites such as rheumatic joints [105]. MBL is able to bind and recognize the terminal sugar residues on a wide range of bacteria, fungi, viruses and some protozoa, but not human cells, unless they are damaged or mutated [106, 107]. The basic binding subunit of MBL is composed of a carbohydrate recognition domain (CRD), which is on the end of a long collagen-like stalk that twines together with two other strands to form a triple helix with a cluster of the three CRD's at the end [108] (**figure 1.4b-c**). Oligomers of these triple helices (usually a tetramer or more) attach together forming a bouquet-like arrangement that makes up the functional MBL protein [109]. MBL associated serine proteases (MASPs) bind to specific sites on the collagen-like stalks and can sense the conformational change in MBL when it binds to a pathogen and then proceed to cleave and activate complement and other effector molecules [110]. The CRD contains a highly conserved amino acid sequence that has the ability to recognize and bind to hydroxyl groups on sugars such as D-mannose, L-fucose and N-acetyl-D-glucosamine (GlcNAc) found on pathogens [111, 112]. Normal human cells have D-galactose or sialic acid as the terminal sugars on most of their glycoproteins, which fit poorly in CRD, allowing differentiation of self from non-self [105]. In addition to sugar structures, it has been shown that MBL can also bind to phospholipids [113], nucleic acids [114, 115], and non-glycosylated proteins, a feature which probably plays a role in MBL's ability to bind and help clear apoptotic and necrotic cells. These dead or mutated cells expose neo-epitopes not found on healthy human cells. So unlike invertebrate and plant lectins, MBL does not bind to human cells and unlike surfactant proteins A and D (which are usually found in the alveoli of the lung), it has evolved specifically to function in blood, making it well suited for magnetically opsonizing pathogens in blood.

The actual binding strength of each CRD in MBL is relatively weak (only  $K_d$  of  $10^{-3}$ ), but it overcomes this by using avidity-based binding, with several of the CRD's from a single MBL attaching at once to the surface of the pathogen, giving the protein binding strength comparable to most antibodies on many pathogens [109, 116-118]. Recent studies have shown that MBL can bind to fungi such as *Candida* and *Aspergillus* species and bacteria such as *S. aureus*, non-encapsulated *Listeria monocytogenes*, *Haemophilus influenzae* B, *Neisseria meningitidis*,

*Neisseria cinera*, *Neisseria subflava*, streptococci, *Escherichia coli*, and *Neisseria meningitidis* serogroup A [105, 109]. The one class of pathogens that MBL has difficulty binding is encapsulated pathogens such as *N. meningitidis*, *H. influenza*, *Streptococcus agalactiae* and some *Salmonella* strains [3, 106] because these organisms shield their terminal sugar residues so there are fewer targets for MBL to bind. MBL serum deficiency, caused by mutations in the MBL gene, has been shown to increase the risk of mortality in *pneumococcal* infections and the risk of developing serious complications in sepsis such as disseminated intravascular coagulation (DIC) [119, 120]. Phase I clinical trials are currently in progress to see if recombinant MBL therapy can reduce the risk of infections in deficient patients [121]. So, MBL is a single, blood compatible molecule that can bind to *E. coli*, *S. aureus*, and *Candida albicans*, three of the major pathogens implicated in sepsis and many more besides. We propose to take advantage of this versatile molecule, which can bind pathogens from different species, geneses, or even kingdoms, and attach it to magnetic beads. This should provide a single set of beads that can bind to the majority of pathogens that can cause sepsis, forming the foundation for a rapid diagnostic system.

## **1.8 Summary**

Sepsis is a serious problem in hospitals around the world, taking thousands of lives and costing billions of dollars every year, and it is projected to become more common as more immunocompromised patients and drug resistant pathogens emerge. In some patients, the disease can progress from fever and chills to organ failure and shock in a matter of hours, creating a great need for a rapid diagnostic that can allow clinicians to implement effective antimicrobial treatment as quickly as possible. However, the current, state-of-the-art blood culture identification and antibiotic susceptibility testing systems fall short of this mark, typically taking between 24-72 hours for most pathogens. As many as 50% septic patients never have their infection confirmed due to the poor sensitivity of these culture-based approaches. Technologies such as PCR have the potential sensitivity to detect pathogens directly in blood if the inhibitors and contaminating human DNA in blood can be removed. Towards this end, I have worked with other researchers at the Wyss Institute to develop and characterize general opsonin magnetic beads which can bind to pathogens in blood, giving us the ability to concentrate them out of blood for analysis and identification. We believe that this bead technology can create a robust sample preparation method for isolating pathogens out of blood for a plethora of different

detection technologies that can avoid the pitfalls of blood culture by directly detecting pathogens in blood. In the remainder of this thesis, I will discuss my progress in characterizing their ability to bind a wide range of different pathogens, developing a microdevice that can concentrate and display tagged pathogens for optical detection and using these beads to concentrate and purify pathogens out of blood and other complex samples for rapid identification with PCR.

### 1.9 Aims

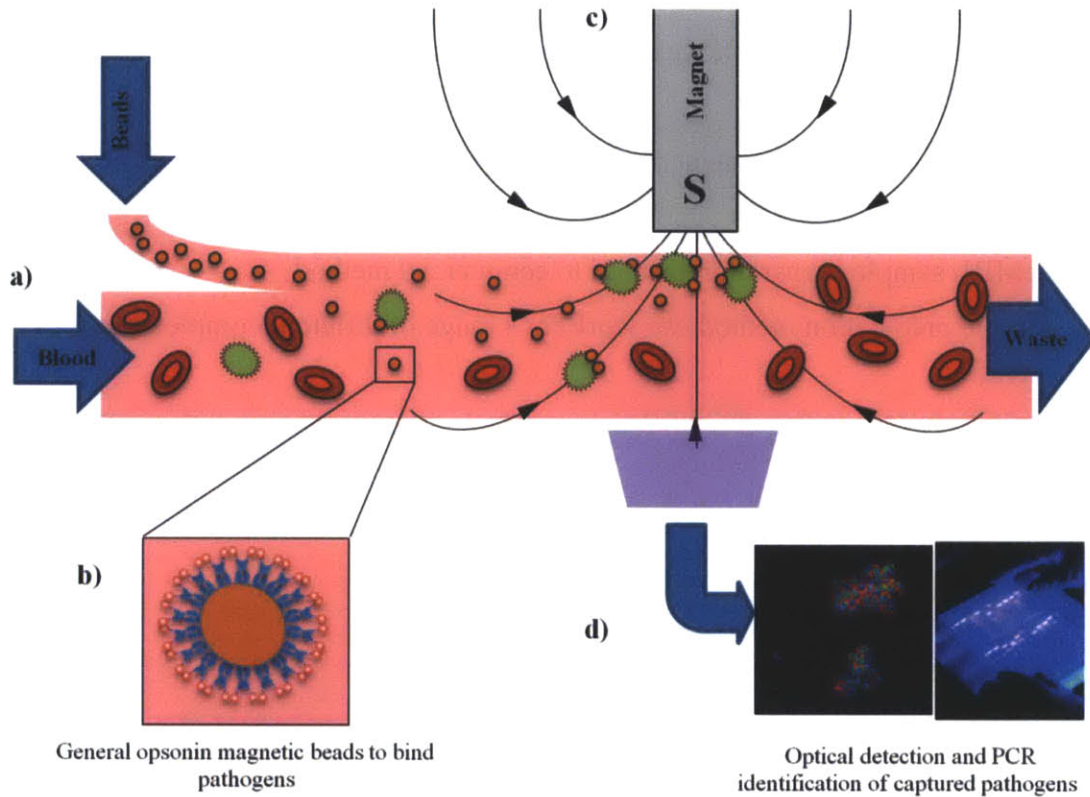


*Figure 1.5 Using general magnetic opsonins of detect pathogens in blood (a) Blood containing pathogens (green) enter the detection system (b) Magnetic beads coated with MBL bind to the pathogens but not the blood cells (c) A magnet concentrates the beads and tagged pathogens out of the blood (d) The concentrated pathogens can be detected optically or with PCR, creating a rapid sepsis diagnostic. Gel image reprinted from [122]*

Aim 1: To develop magnetic opsonins that bind pathogens with high efficiency (figure 1.5a-b)

1. Develop MBL coated magnetic beads
2. Show that MBL beads bind to wide range of pathogens in saline
3. Show that MBL beads bind to pathogens in blood

Aim 2: To engineer devices that concentrate and visualize captured pathogens (figure 1.5c-d)

1. Develop a device that can isolate magnetically tagged *C. albicans* from a large volume of blood
2. Develop a method to optically detect the presence of captured fungi in the device
3. Investigate whether the system can detect other pathogens, such as *S. aureus*

Aim 3: To develop tools to identify the specific type of pathogen captured (figure 1.5c-d)

1. Develop an effective method to remove and concentrate magnetically-tagged bacteria from blood
2. Use the FcMBL beads to isolate magnetically tagged bacteria out of blood for PCR identification
3. Compare FcMBL sample preparation method to commercial method
4. Show the sample preparation method can work for a range of different complex samples



## Chapter 2 General Magnetic Opsonins

### 2.1 Introduction

Our lab previously developed magnetic beads coated with specific antibodies against pathogens which allowed us to bind *C. albicans* and *E. coli* and concentrate them from blood [90, 91]. The beads have the ability to rapidly circulate through milliliter-size fluid volumes and bind to their target pathogen, giving us a magnetic handle on the pathogens which we can then exploit to concentrate the pathogens for direct identification rather than having to rely on culturing the organisms first to obtain enough for identification, as is currently done in the clinic [28].

However, for sepsis, the species of the organism causing the illness is not known, so species-specific immunomagnetic beads are of very little use in binding the causative pathogen, which can be one or more of over 20 species [109]. To overcome this limitation of what is otherwise a very promising method to rapidly isolate rare pathogens out of blood samples, the magnetic beads were coated with a general opsonin derived from the innate immune system to give us a single set of beads that can bind a wide range of pathogens. For this purpose, mannose binding lectin (MBL) was selected, which is a circulating serum protein that can recognize the sugar motifs found on a wide range of human pathogens, including gram positive and negative bacteria, fungi, protozoa and some viruses [3]. The primary advantage of human MBL over other lectins is that it will not bind to normal blood cells, which is the case with lectins derived from non-mammalian species [102, 103]. By coating this protein rather than a species-specific antibody onto the magnetic beads, a much more versatile capture method is created, giving us a single set of beads that can bind to the majority of pathogens recognized by the human body. Therefore, prior knowledge of the causative organism in a septic patient is not required to bind and concentrate it from blood for identification. Consequently, we hypothesized that the MBL-functionalized magnetic beads could form the core technology for a rapid sepsis diagnostic system.

The remainder of this chapter will discuss the results of my research into developing and characterizing MBL-functionalized beads for binding pathogens in both saline and blood. We

began by adapting the procedure we had used to create antibody beads for use with commercial wild type MBL (WtMBL) for capturing a range of pathogens and compared it to a recombinant form of the protein (FcMBL) produced in house at the Wyss Institute. Once we had established a basic recipe for producing the MBL beads, I then investigated how to optimize binding in saline by varying the bead size, concentration and MBL density on the beads with a variety of pathogen species. I then used the knowledge gained from binding in saline to study pathogen binding in blood while dealing with the additional challenges posed by phagocytosis, coagulation and high hematocrit levels of blood. From these investigations I established a set of basic conditions for binding both bacteria and fungi in saline of blood with general opsonin beads, which is then exploited in later chapters to concentrate pathogens out of blood for direct detection and identification. This work formed the laid the groundwork for experiments that other researchers at the Wyss have used to show FcMBL beads can capture a wide range of species in blood.

## **2.2 Materials and Methods**

### **2.2.1 Functionalizing Magnetic Beads**

One  $\mu\text{m}$  or 128 nm superparamagnetic streptavidin beads were washed with 1% BSA in PBS and incubated with 25  $\mu\text{g}$  protein/mg beads (MyOne Dynabeads streptavidin T1, Invitrogen or Bio-Adembeads, Ademtech). Either used WtMBL (Sino Biological Inc) or recombinant FcMBL produced in house at the Wyss Institute on the beads was used. After the MBL was conjugated to the beads, the remaining streptavidin was blocked with 50  $\mu\text{l}$  of biotin solution (Endogenous biotin blocking kit, Invitrogen). After the blocking was complete the beads were resuspended and diluted to 5 mg beads/ml in 1% BSA in PBS with 10 mM EDTA and stored at 4°C for up to four weeks.

### **2.2.2 Pathogen Stocks**

Liquid cultures of *C. albicans* (donated by Brown et al [123]), *C. parapsilosis*, *S. cerevisiae*, *P. pastoris*, *E. Coli* (ATCC 8739), *S. aureus* (clinical isolate) and *Klebsiella pneumoniae* (clinical isolate) where grown overnight in an Innova 42 incubator (New Brunswick Scientific) with 100 ml of media in an erlenmeyer flask, circulating at 250 rpm. Bacteria were grown at 37°C in LB broth and fungi were grown at 30°C in YPD media. Samples of all pathogens were centrifuged and resuspended in PBS with 20% glycerol and aliquoted into PCR tubes for long term storage at -80°C. The average pathogen concentration in each aliquot

was determined by performing quantitative microbiological plating on serial dilutions of five aliquots chosen randomly from each batch.

### 2.2.3 Binding Quantification (Depletion Assay)

Binding quantification was carried out in micro centrifuge tubes containing 500 or 1,000  $\mu\text{l}$  of sample containing the pathogens of interest. For flow cytometer quantification, the pathogen load in the sample was  $\sim 10,000$  to  $1,000$  cfu/ml while for the plate based quantification the concentration was  $\sim 1,000$  cfu/ml. Three samples were made for each condition, one experimental with MBL beads, one with non-functionalized beads to assess non-specific adhesion and one with no beads to check for growth during the experiment. All three samples received the same treatment during mixing and analysis steps of the experiment.

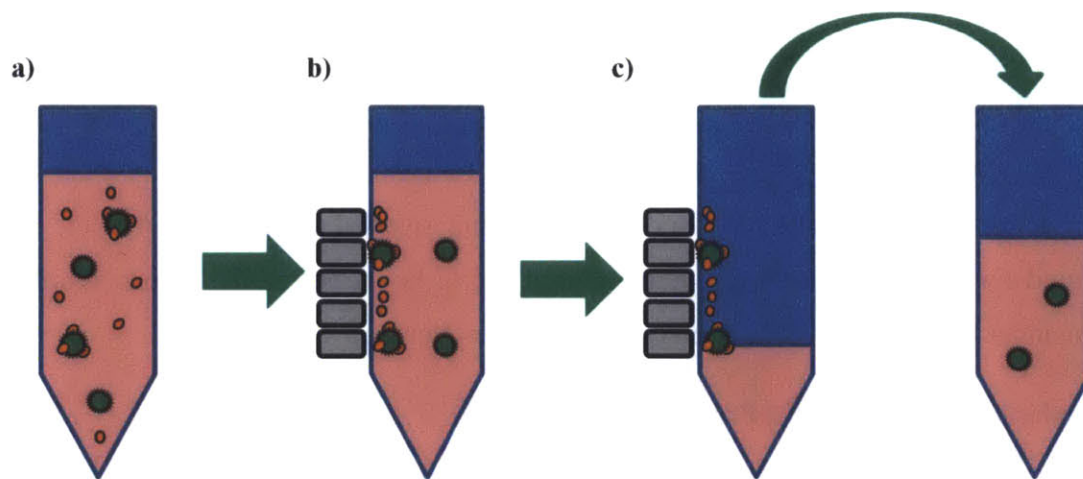


*Figure 2.1 Procedure for Depletion assay to measure bead binding*

*(a) Sample containing bound and unbound pathogen after MBL bead binding is complete (b) Sample is placed in magnetic separator rack, pulling the beads and bound pathogens out of solution (c) A portion of the sample fluid is removed and the concentration of unbound pathogens analyzed using the flow cytometer or plating.*

The samples were maintained at  $4^{\circ}\text{C}$  and placed in a Hula shaker (Invitrogen) for 20 minutes, then transferred into a DynaMag<sup>TM</sup>-2 Magnet separator rack (Invitrogen), unless otherwise specified, for 10 minutes. At the end of this time, the tubes were left in the rack and  $100\ \mu\text{l}$  of the depleted fluid (containing any pathogens not captured by the MBL beads) was removed for analysis on the flow cytometer or plate based methods (**figure 2.1 a-c**). Binding was quantified by taking a ratio of the pathogen concentration in the experimental and no bead tubes for each sample. Non-specific adhesion of the pathogens was calculated by comparing the depletion between the blank bead sample and the no bead sample.

For flow cytometer measurements (used for fungi in initial experiments), a known amount of CountBright™ absolute counting beads (Invitrogen) and 25 µM of calcofluor white stain (Sigma) to stain the fungi was added to the depleted and positive control samples and then processed through a LSR II Fortessa flow cytometer (BD). Flow cytometer quantification was only used for fungal species because the smaller bacteria were more difficult to reliably detect with the instrument while plate based analysis was used for both bacteria and fungi. The counting beads were used to determine the volume of fluid processed and derive the concentration of the fluorescently stained fungi in the starting sample.

Quantitative microbiological plating was employed to determine the concentration of both bacteria and fungi at concentrations at or below 1,000 cfu/ml. One hundred millimeter Petri dishes (BD) were pre-warmed in the incubator for 30 minutes before use (LB agar plates at 37°C for bacteria, Potato Dextrose Agar plates at 30°C for fungi). For quantification, 100 µl of the depleted fluid was spread on the plate using EZ-Spread plating beads (Genlantis), then transferred upright into an Innova 42 incubator (New Brunswick Scientific), at 37°C for bacteria or 30°C for fungi, and given one hour to dry before being inverted and stacked. Aerobic bacteria were cultured for 24 hours and fungi were cultured for 48 hours before the colony number was analyzed using a Flash and Grow system colony counter (Neutec).

#### **2.2.4 Recombinant MBL (FcMBL) Production**

FcMBL was designed as a homodimeric fusion protein with the hinge, CH2 and CH3 sequences of human IgG1 fused to the neck and CRD regions of human MBL. Then the FcMBL plasmid was transiently transfected into Hect 293F cells. The secreted FcMBL was isolated from the culture medium using FpLC purification. The protein was then biotinylated using aminoxybiotin (Biotium). For full details see Super et al [124].

#### **2.2.5 Calcium Dependence**

These tests were a variation of the standard depletion assay with flow cytometer analysis. In this case, *C. albicans* were stained with 25 µM calcofluor white and added to buffer TBS-Tween 20 buffer containing 0, 1, 2, 3, 4, 5, and 10 mM of calcium chloride in microcentrifuge tubes. Fifty µg 1 µM WtMBL beads/ml were added to the sample and mixed in the Hula Shaker (Invitrogen) for 20 minutes before being transferred to the magnetic separation rack for 10 minutes. Then flow cytometer analysis was carried out on 100 µl of the depleted fluid. After this, 0.25 M Ethylenediaminetetraacetic acid (EDTA) was added to the sample tubes to chelate the free calcium from the buffer and the tubes

were mixed in the shaker for an additional five minutes before magnetically separating the samples again and analyzing the depleted fluid again for fungi released by the EDTA chelation process.

## **2.2.6 Binding in Blood**

### ***2.2.6.1 Blood Collection and Separation into Different Components***

Fresh blood samples were collected from healthy adult volunteers by a trained phlebotomist at the Wyss Institute into a range of vacutainers (blank discards, serum, sodium heparin, EDTA) depending on the assay being performed. Serum tubes were placed in a 37°C incubator for 1 hour, after which the liquid portion of the sample was removed, centrifuged at 200xg for 20 minutes and the serum transferred into a new tube, ready for the experiment.

Plasma was generated from sodium heparin treated vacutainers by centrifuging the blood at 200xg for 20 minutes. The plasma was first transferred to a new tube, and then the white blood cell buffy coat was aspirated and discarded from the sedimented red blood cells, which were then resuspended in PBS. The plasma was spun again at 500xg for 10 minutes. The platelet poor plasma was transferred to a new tube and the platelet pellet resuspended in the same volume of PBS as the plasma (preserving their physiological concentrations). These components were then used for different binding tests. This gave serum, platelet poor plasma, platelets and red blood cell solutions that could be used for different experiments

### ***2.2.6.2 Dilution Experiments***

Blood was collected from healthy volunteer donors into a 10 ml sodium heparin vacutainer and maintained at 4°C during the experiment. Samples of undiluted blood, blood diluted 1:1 with TBS-Tween 20 buffer and blood diluted with 1:9 with TBS-Tween buffer were compared, each containing 1,000 cfu/ml of *C. albicans*. Both lysed (containing 1% Triton X-100) and unlysed samples were run at each condition. Ten µg of 1 µm FcMBL beads per milliliter were added to the sample and mixed for 20 minutes in the hula shaker (Invitrogen). A standard plate-based depletion assay (see 2.2.3) was used to analyze the binding results. After the plating for the depletion was completed, the captured beads and pathogens were washed and examined under phase contrast on an inverted microscope (Leica).

### ***2.2.6.3 Phagocytosis Assay***

Fresh heparinized donor blood was split into two halves, with one half being held at 4°C for the duration of the experiment and the other half being held at 25°C. WtMBL beads (25 µg of 1 µm/ml) were added to the samples and before they were placed in the Hula Shaker for 0, 30, 60 and 90 minutes, after which time the samples were placed in a magnetic separation rack for 10 minutes. The blood was then aspirated from the tube and magnetic beads and any retained human cells were resuspended in 200 µl of TBS-Tween 20 buffer and analyzed on the microscope. The relative number of white blood cells that had bound or phagocytosed the magnetic beads at each time and temperature were compared to ascertain how effectively cooling could slow the phagocytosis process.

#### **2.2.6.4 Anticoagulant Experiments**

To determine the effectiveness of adding additional anticoagulants to blood at increasing binding, different concentrations of salicylic acid (active ingredient in aspirin) in blood were investigated. Initially 0, 100 and 1,000 µg salicylic acid/ml were added to heparinized blood and checked on the microscope if it could prevent clot formation on the beads after magnetic pull down (because it was difficult to image the beads in blood before magnetic pulldown). The effect of adding 1,000 µg salicylic acid/ml on binding of *C.albicans* with 20 µg 1 µm FcMBL beads/ml in undiluted blood was then investigated. Both lysed (with 1% Triton X-100) and unlysed bloods were run using a standard depletion plate-based assay.

Binding was compared in heparinized and recalcified EDTA blood. Blood from healthy human donors was collected into both heparin (control) and EDTA vacutainers. Both types of blood were diluted 1:1 with TBS-Tween 20 and had 1,000 cfu/ml *C. albicans* added. FcMBL beads (20 µg 1 µm beads/ml sample) and 0, 5, or 10 mM calcium were added to the samples, which were then immediately placed in the Hula Shaker for 20 minutes. Next the samples were transferred to the magnetic rack for the depletion plating assay (see 2.2.3) to measure fungi binding in the different samples.

#### **2.2.6.5 Binding Time**

To ascertain the required binding time for magnetic beads in blood, FcMBL beads and *C. albicans* were added to blood to measure the percent of pathogens bound over 20 minutes of mixing time. Five micrograms of beads per milliliter sample were added into 10 ml diluted (1:1 with TBS-Tween 20) and undiluted blood samples before the tubes were placed in a Hula Shaker

for mixing. The mixing was paused periodically and 500  $\mu$ l samples removed at specific time points. The 500  $\mu$ l samples were immediately placed into a magnetic rack to pull down the beads and stop the binding reaction. The concentration of unbound pathogens in the depleted fluid from the different time points was assayed using depletion plating.

#### **2.2.6.6 Bead Concentration**

To determine the optimal bead concentration for 1  $\mu$ m FcMBL beads to bind to *C. albicans* in blood, a binding depletion assay was carried out in fresh donor blood (both undiluted and diluted 1:1 with TBS-Tween 20) with a bead concentrations ranging from 10 to 50  $\mu$ g/ml sample.

#### **2.2.6.7 Magnetic Separation Different Beads**

The binding of bacteria was tested with the different bead types. *S. aureus*, *E. coli* and *K. pneumoniae* in diluted, recalcified EDTA blood with 25  $\mu$ g of 1  $\mu$ m, 128nm or both beads types per ml sample. The samples were given 20 minutes to bind before being placed in a magnetic rack for 10 minutes for separation.

Separation of *C. albicans* from diluted heparin blood was assayed by adding *C. albicans* to the blood and 33.3  $\mu$ g of 1  $\mu$ m or 128 nm beads/ ml sample. The beads were given 20 minutes to bind in the inverting shaker before the tubes were placed in the magnetic rack for 10 minutes. Over the course of the ten minute separation, 100  $\mu$ l aliquots were removed and plated to determine the percent of pathogens that had been separated out over time.

To get a better idea of how well 128 nm beads worked for removing bound bacteria from blood, the binding and separation of the *S. aureus* was tested with 50  $\mu$ g 128 nm beads/ml sample. Different amounts of mixing time were investigated. Samples for each time point were prepared in separate microcentrifuge tubes, mixed for a set amount of time (0, 10, 20, 30, 60 minutes) and then placed in the magnetic rack to stop the binding reaction. The samples were in the rack for 10 minutes before being plated to measure the pathogen depletion. Two controls were run; one in saline and the second with pre-bound *S. aureus* added into the blood (this checked to make sure that the bound pathogens were being separated with the rack) and mixed the pathogens with the beads for up to one hour. To study the effect of the cellular fraction of blood on binding, the same experiment was run using heparinized plasma instead of blood.

## 2.3 Results

### 2.3.1 Binding in Saline

#### 2.3.1.1 MBL vs. Antibody beads

After functionalizing 1  $\mu\text{m}$  superparamagnetic beads (Dynabeads, Invitrogen) with WtMBL, I compared them with antibody functionalized beads for binding two different species, *C. albicans* and closely related *C. parapsilosis*. Anti-*Candida albicans* antibody beads were able to capture the majority of *C. albicans* out of buffer, but capture dropped to less than 20% for the closely related *C. parapsilosis* species in buffer (**figure 2.2a**). The WtMBL beads were tested with a range of bead concentrations (**figure 2.2b**). Capture increased with increasing bead concentration, starting at 20% for both species at 10  $\mu\text{g}$  beads/ml sample and plateauing at 95% capture at 100  $\mu\text{g}$  beads/ml.

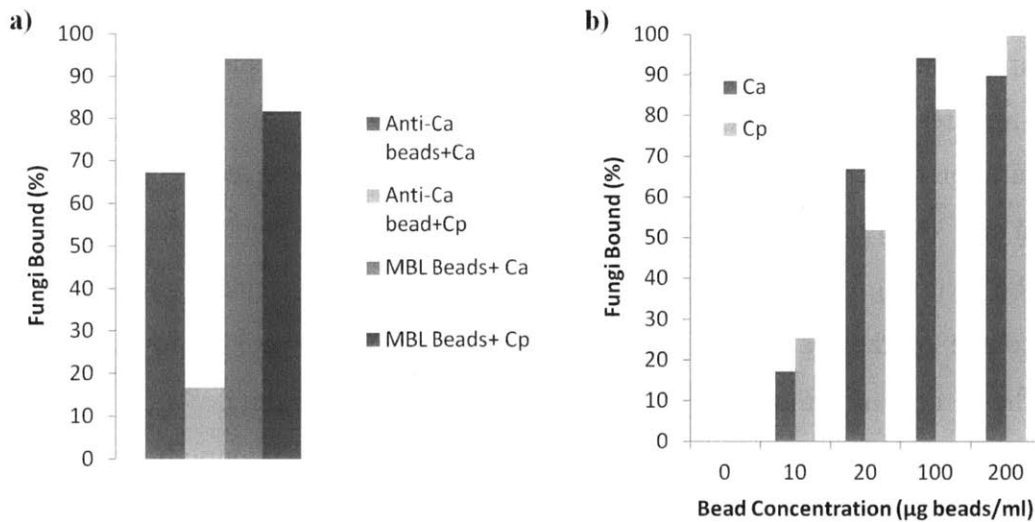


Figure 2.2 Antibody vs. MBL beads

(a) Binding of *C. albicans* (Ca) and *C. parapsilosis* (Cp) with Anti-*C. albicans* and WtMBL 1  $\mu\text{m}$  Beads: 100  $\mu\text{g}$  1  $\mu\text{m}$  beads/ml. Poor binding of Anti-*C. albicans* beads to closely related *C. parapsilosis* while WtMBL beads to both is good (b) Binding of *C. albicans* (Ca) and *C. parapsilosis* (Cp) with different concentrations of WtMBL 1  $\mu\text{m}$  Beads: Binding is similar with both species and increases with increasing bead concentration, saturating around 95% binding with 100  $\mu\text{g}$  beads/ml sample.

The surface area of 100  $\mu\text{g}$  of the 1  $\mu\text{m}$  beads is 0.16  $\text{m}^2$ , meaning that if the beads are uniformly suspended in one milliliter of fluid, nothing in the fluid will be more than  $\sim 6$   $\mu\text{m}$  away from the surface of a bead, greatly limiting the distance over which the beads need to diffuse or



convect for binding to occur. The Stokes-Einstein equation can be used to estimate the diffusion coefficient for a spherical bead: [125].

$$D = \frac{K_B T}{6\pi\eta r} \quad (2.1)$$

Where  $D$  is the diffusivity of the particle,  $K_B$  is Boltzmann's constant,  $T$  is the absolute temperature,  $\eta$  is the viscosity of the fluid and  $r$  is the radius of the bead. The amount of time ( $t$ ) required for a bead to randomly diffuse a set distance  $x$  can be estimated with the following equation [125]:

$$t \propto \frac{x^2}{2D} \quad (2.2)$$

The diffusivity on a 1  $\mu\text{m}$  bead is on the order of  $4.3 \times 10^{-13} \text{ m}^2/\text{s}$ , meaning it will diffuse across 6  $\mu\text{m}$  in approximately 60 seconds, allowing the bead surfaces to rapidly probe the entire fluid volume in a matter of minutes, giving us the binding ability of liquid chromatography with a great deal more flexibility since the beads and tagged pathogens can be easily manipulated, while a high pressure liquid chromatography columns cannot. Given these estimates and the ability of MBL to bind a range of different pathogens, these general opsonin magnetic beads could form the basis of a robust sepsis diagnostic system and were further characterized.

### ***2.3.1.2 Calcium Dependence***

Calcium ions play a key role in stabilizing the tertiary structure of the carbohydrate recognition domain (CRD) of MBL, which is the part of the MBL protein responsible for actually binding to exposed sugar groups [111]. Therefore, the effect of calcium concentration on binding of pathogens with the WtMBL beads was investigated (**figure 2.3**). I tested calcium chloride concentrations from 1-10 mM and found that binding saturated at  $95\% \pm 5\%$  capture for *C. albicans* under all concentrations. Less than 10% binding of the fungi was observed when no calcium was added to the buffer. This result offered a relatively simple way to differentiate between MBL and non-specific binding: MBL binding activity of the beads should be calcium dependent (without calcium the carbohydrate recognition domains in MBL cannot establish stable binding) while non-specific binding should be constant even with no calcium in the buffer.

From this point on saline experiments were carried out in Tris Buffered Saline with 1% Tween 20 and 5 mM calcium chloride to ensure that there was always sufficient calcium in the buffer.

Calcium dependence could offer a simple way to reverse the binding and release the pathogens from the beads on demand since the stability of the binding pocket in the CRD is reduced once the calcium is removed. However, I found that the binding of WtMBL beads to *C. albicans* was very stable with less than 30%  $\pm$  16% of the pathogens being released even when 0.25M EDTA was added to the buffer to remove all free calcium ions (**figure 2.3**). Chemically denaturing the MBL on the beads with high pH could effectively release the bound pathogens, but this was not compatible with the majority of the analysis techniques (such as immunofluorescence staining) I wanted to use to detect magnetically tagged pathogens. Porter et al. found that adding a large amount of competing sugars could release bacteria bound to lectin functionalized beads [126] and other members of the Wyss Institute found that a large proportion of *E. coli* could be released with EDTA chelation of calcium [124], suggesting that this elution method is dependent on the affinity of MBL for a specific species or strains, making it unreliable for use in a diagnostic system to detect an unknown pathogen.

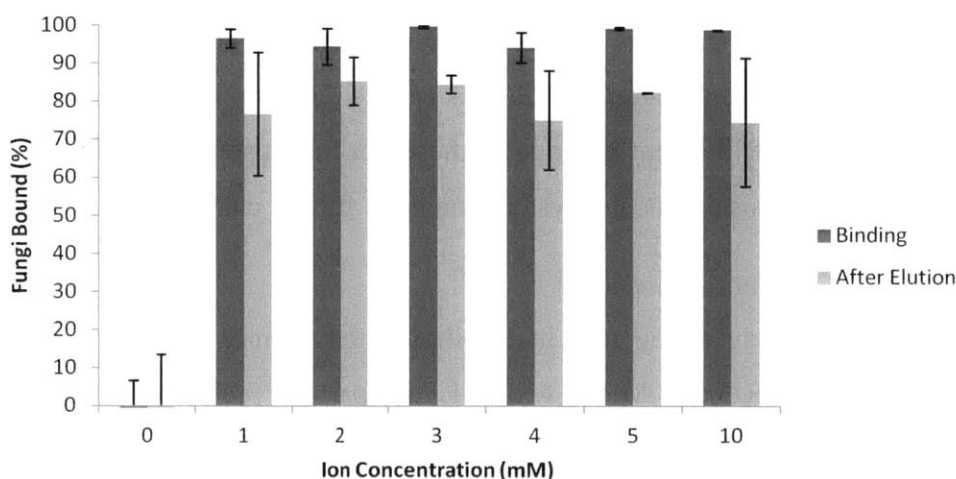


**Figure 2.3 Calcium Dependence of MBL Binding**

Binding of *C. albicans* with 50  $\mu$ g 1  $\mu$ m WtMBL beads/ml sample. Binding requires 1 mM of calcium be present in the buffer. Addition of 0.25 M EDTA depletes the ionic calcium from the buffer but fails to elute the pathogens off of the beads, causing less than 25% to detach.  $n=2$ , error bars: SEM

### 2.3.1.3 MBL Bead Binding to Other Pathogens

I carried out further investigations with a wider range of fungi and bacteria to characterize the diversity of the MBL bead binding in buffer. The 1  $\mu$ m WtMBL beads could

bind well to all the fungal species tested (*Candida albicans*, *Candida parapsilosis*, *Saccharomyces cerevisiae* and *Pichia pastoris*) with binding observed between 90-95% ± 3% for the fungi in buffer with 10 µg bead/ml sample (**figure 2.4a**). Three species of bacteria were tested: *S. aureus* as a representative Gram positive bacteria implicated in sepsis and *Escherichia coli* and *Klebsiella pneumoniae* as two gram negative species commonly implicated in sepsis. However, the 1 µm WtMBL beads performed poorly for capturing bacteria species under the same conditions. Capture for the bacteria ranged from 35% ± 8% for *Klebsiella pneumoniae* to as low as 18% ± 7% for *Escherichia coli*. Based on previous work done in the lab with *E. coli* and antibody beads [90], it seemed likely that this was a problem with the bead size and collision interactions rather than an actual issue with the binding affinity of MBL for the bacteria, particularly when MBL is known to bind *S. aureus* and *E. coli* well in serum [109].

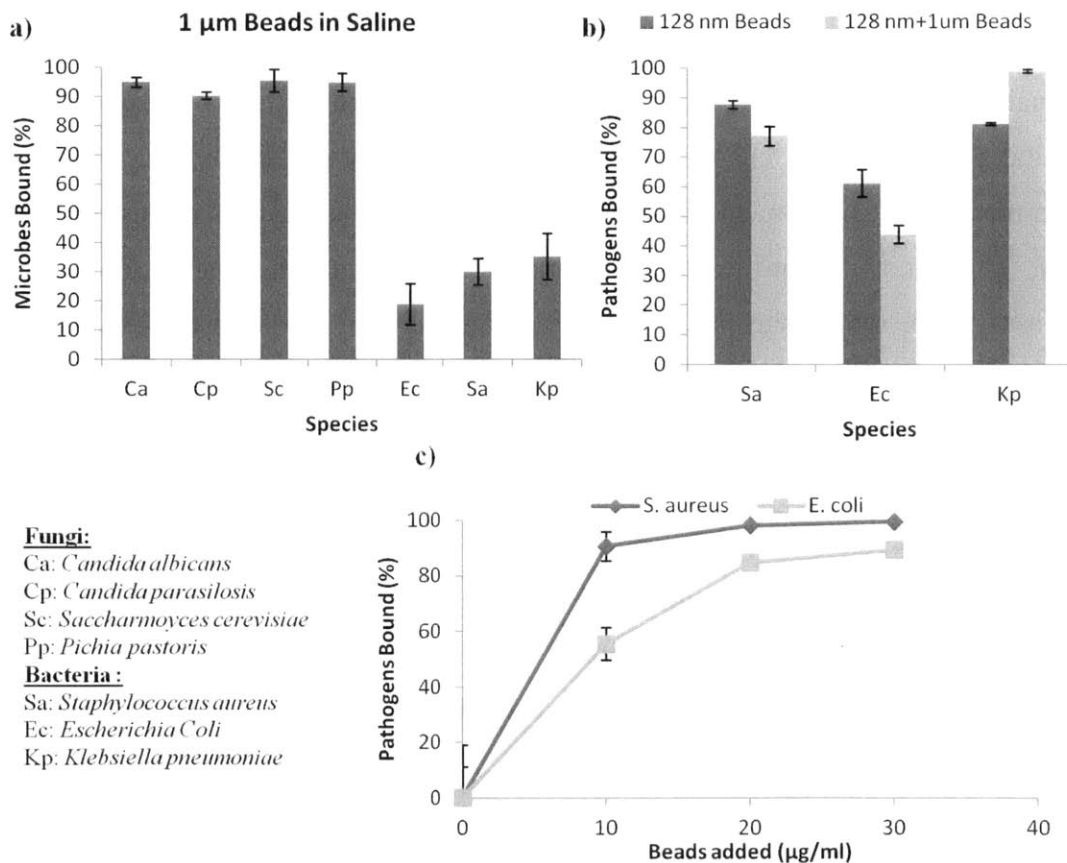


Figure 2.4 WtMBL Bead Binding in Saline (both 1 µm and 128 nm beads)  
 (a) Binding of 1 µm beads to different species of fungi and bacteria: Excellent binding to fungi but poor binding to the three bacterial species tested (Ec, Sa, Kp). n=3, error bars: SEM (b) Binding of bacteria with 128 nm beads or a combination of both beads types: Much better binding of bacteria with 128 nm beads. Adding both bead types in together did not alter the

binding significantly from that seen with the 128 nm WtMBL beads alone.  $n=3$ , error bar: SEM  
(c) Binding of *E. coli* and *S. aureus* with different concentrations of 128 nm beads: Able to capture over 90% of bacteria with higher bead concentrations.  $n=3$ , error bar: SEM

To test this hypothesis, the binding experiment with bacteria was repeated using 128 nm beads (Ademtech) with the same 25  $\mu\text{g}$  WtMBL/mg beads added as was used for making the 1  $\mu\text{m}$  beads (this translated to a higher number of smaller beads with a lower density of MBL on their surface relative to their 1  $\mu\text{m}$  counterparts). Bacteria capture with these smaller beads was much better; more than doubling the binding rate for all three species tested (**figure 2.4 b**). Further investigations with *S. aureus* and *E. coli* showed that the binding could be increased to 100% with a higher concentration of 128 nm beads (40  $\mu\text{g}/\text{ml}$ ) (**figure 2.4 c**). See section 2.4 for a detailed discussion on theoretical factors affecting bead binding.

#### 2.3.1.4 Comparing WtMBL to FcMBL

In blood, the ability of MBL to attach to pathogens and necrotic or mutated human cells is only a small part of its activity. It is also linked to serine proteases (MASP 1 and MASP2) that can sense the conformational change in the MBL protein caused by binding, activating the proteases to recruit the complement cascade, coagulation and phagocytosis to destroy the tagged cells [106]. These downstream cascades would be detrimental for most of our proposed diagnostic assays. Therefore, the Wyss Institute created several recombinant versions of MBL designed to minimize their activation by producing a truncated version of MBL that retained the CRD binding sites but lacked the binding sites for the serine proteases [124]. I compared the binding affinity of beads functionalized with the first two versions of the recombinant protein to beads with WtMBL. I found that these versions of the protein had poorer binding than WtMBL at all the bead concentrations tested with *C. albicans*. However, the third recombinant version of the protein, named FcMBL because it contains two CRD binding pockets attached to the Fc portion of an antibody (**figure 2.5 a-b**), actually had slightly higher and more consistent binding activity than WtMBL coated onto beads when tested. The two MBL beads types were tested with four different species of fungi, *Candida albicans*, *Candida parapsilosis*, *Saccharomyces cerevisiae* and *Pichia pastoris*. The FcMBL bound better to all of them, binding an average of  $99\% \pm 0.3\%$  of the pathogens versus  $95\% \pm 2.5\%$  binding for the WtMBL beads (**figure 2.5 d**). These results showed that the activity of the FcMBL on the beads was comparable to or slightly better than WtMBL and it was much more convenient to work with a protein that could be produced on demand at the Wyss Institute, therefore, FcMBL conjugated beads were used for

subsequent testing. Further evaluation of the new protein by other group members showed that it did indeed have decreased complement and coagulation activity [124].

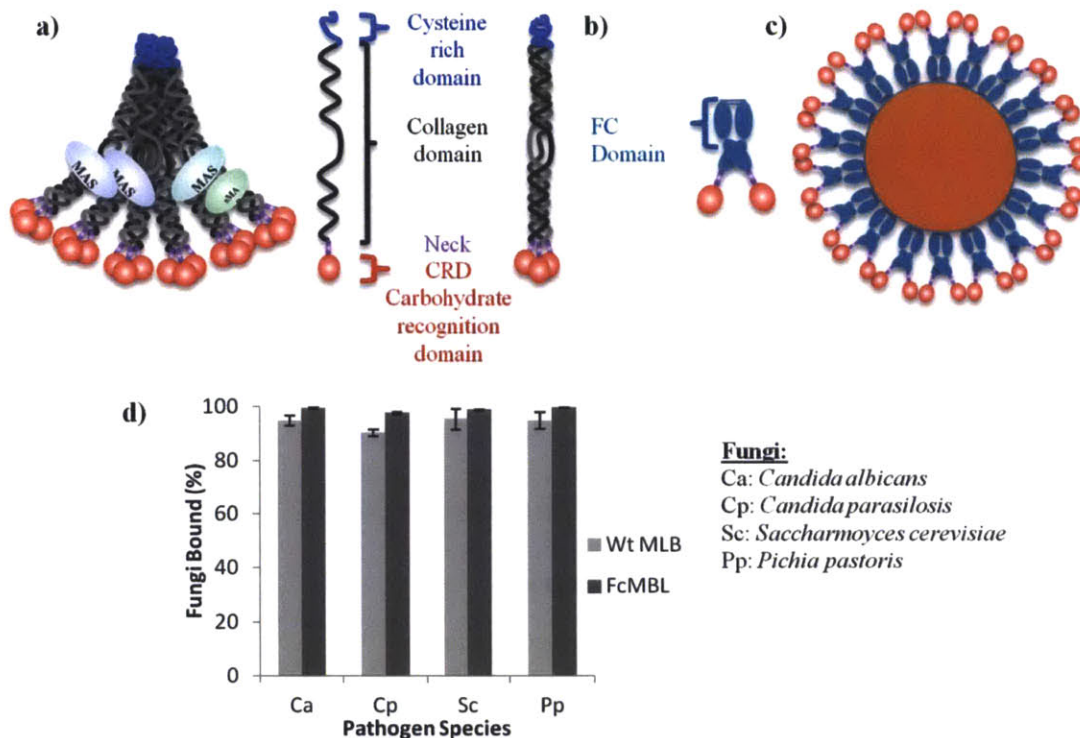


**Figure 2.5 Recombinant MBL (FcMBL)**

(a) Structure of WtMBL showing full polymeric form and composition of each monomer (b) Recombinant FcMBL produced at the Wyss Institute, with two CRD domains grafted onto Fc domain derived from a human antibody (c) FcMBL coated on superparamagnetic bead with CRD heads oriented outward (d) Binding of fungi with WtMBL and FcMBL 1  $\mu\text{m}$  beads: Binding with both the bead types was good but FcMBL beads has slightly a slightly higher binding percentage than the WtMBL beads for the four of the fungal species tested.  $n=3$ , error bar: SEM

### 2.3.1.5 Dependence of Bead Size, Concentration, MBL Density and Binding Time

The majority of work up to this point had been performed using 1  $\mu\text{m}$  MBL beads targeted to fungal pathogens, based on extensions with our previous work with antibody beads and *C. albicans* [91]. Therefore, a systematic approach to characterize the binding to bacteria with FcMBL beads was needed. I had already established that 128 nm beads were more effective for binding the bacteria and wanted to determine the relative importance of other factors on binding, including bead concentration and FcMBL density on the beads. *E. coli* was chosen as a typical bacterium to work with, mainly because *S. aureus* is known to express Protein A in its cell wall. This protein allows binds the Fc portion of FcMBL independently of the MBL binding to the *S. aureus*, which is beneficial in terms of pathogen capture to this species but does not

reflect the actual MBL affinity., Therefore *E. coli* (the other major bacterial species implicated in sepsis) would give a much more accurate reflection of MBL binding [127].

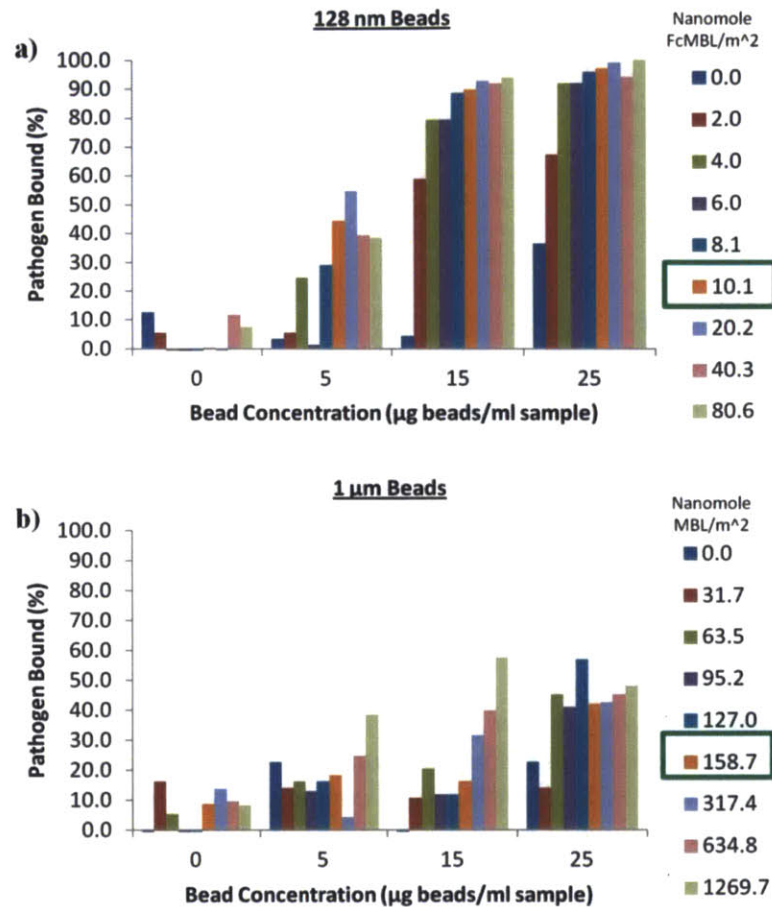


Figure 2.6 Role of bead size, concentration and FcMBL density in binding of *E. coli* in saline (a) 128 nm beads: Binding of 128 nm beads was > 90% with more than 15 µg beads/ml sample and more than 10.1 mM FcMBL/ m<sup>2</sup> on the bead surfaces (b) 1 µm beads: Binding of the 1 µm beads lower at <60% regardless of bead concentration or MBL density on the bead, never reaching more than ~50%. The green box indicates the MBL concentration typically used to manufacture the beads (25 µg FcMBL/ mg beads), which appears optimal for both bead types despite the sixteen fold differences in the surface density on the bead.

The relative effects of different bead concentrations and FcMBL densities with both 1 µm and 128 nm beads on the binding of the *E. coli* were compared. As with previous experiments, the largest factor affecting the binding was the bead size. The 128 nm FcMBL beads were able to bind over 95% ± 1.4% of the *E. coli* while the best binding with the 1 µm beads was 50% ± 1.4% (figure 2.6 a-b). Bead concentration appeared to have the next greatest effect; bacteria binding

increased for both bead sizes with increasing bead concentration, plateauing for the 128 nm beads at 15  $\mu\text{g}$  beads/ml sample while the binding with the 1  $\mu\text{m}$  appeared to saturate at about 25  $\mu\text{g}$  beads/ml sample. The amount of FcMBL coated onto the beads had little impact on the binding, especially considering the surface density of the FcMBL on the 128 nm beads was much lower than for the 1  $\mu\text{m}$  because of their much higher surface area per milligram bead. One milligram of the 1  $\mu\text{m}$  beads contains  $5 \times 10^8$  beads with a total surface area of  $1.6 \text{ m}^2$ , while one milligram of the 128 nm beads contains  $4.8 \times 10^{11}$  beads with a total surface area of  $25 \text{ m}^2$  and both have the same amount of FcMBL per milligram, meaning that the surface concentration of the MBL on the smaller beads is much lower but the binding is actually better. So given that the FcMBL surface density of the smaller beads was sixteen times less than for the 1  $\mu\text{m}$  beads but the binding was better, it appears that bead size and bead concentration play a larger role than the FcMBL density for binding in saline. The binding for both bead sizes plateaued at 25  $\mu\text{g}$  FcMBL/mg (10.1 nanomoles FcMBL/ $\text{m}^2$  for 128 nm beads, 158.7 nanomoles FcMBL/ $\text{m}^2$  for 1  $\mu\text{m}$  beads). Therefore, both beads types were manufactured using 25  $\mu\text{g}$  FcMBL/mg beads for subsequent experiments.

### 2.3.2 Binding in Blood

Optimization up to this point had been carried out in saline, but I was primarily interested in binding pathogens in blood, which is a more difficult fluid to work with (**figure 2.7**). In terms of mechanics, blood is a non-Newtonian colloidal suspension of cells, with approximately 45% of the volume being made up of red blood cells and the remaining volume made up of plasma [128, 129]. Plasma itself is about six times as viscous as water and it contains high concentrations of antibodies, complement, glucose, metal ions and trace vitamins; all the things that need to be delivered or removed throughout the entire body. Blood has a coagulation cascade in place (mainly composed of plasma proteins and platelets) that will rapidly activate when the blood stops moving or escapes from a blood vessel. Fibrin monomers then combine to form a dense polymer network that holds a blood clot together. As a result, blood can transform from a liquid into a solid in a matter of minutes once removed from the body unless it is treated with anticoagulants (**figure 2.7 b**). This process is highly effective at closing cuts in the body to prevent a patient from bleeding to death but highly inconvenient for most *in vitro* assays [129]. In addition to these minor complications, one milliliter of blood also contains over a million white blood cells that will engulf (phagocytose) foreign particles, such as magnetic beads,

usually in a matter of minutes [63]. All of these factors explain why historically it has been difficult to directly detect pathogens out of blood. We believed that constructing FcMBL from proteins normally found in human blood (MBL and IgG) should allow it to bind pathogens but not mammalian cells, which is not the case for other plant and invertebrate lectins [102, 103]. Removing the MASP binding sites in the recombinant protein should also have the effect of minimizing activation of clotting and phagocytosis in the blood samples as well [109].

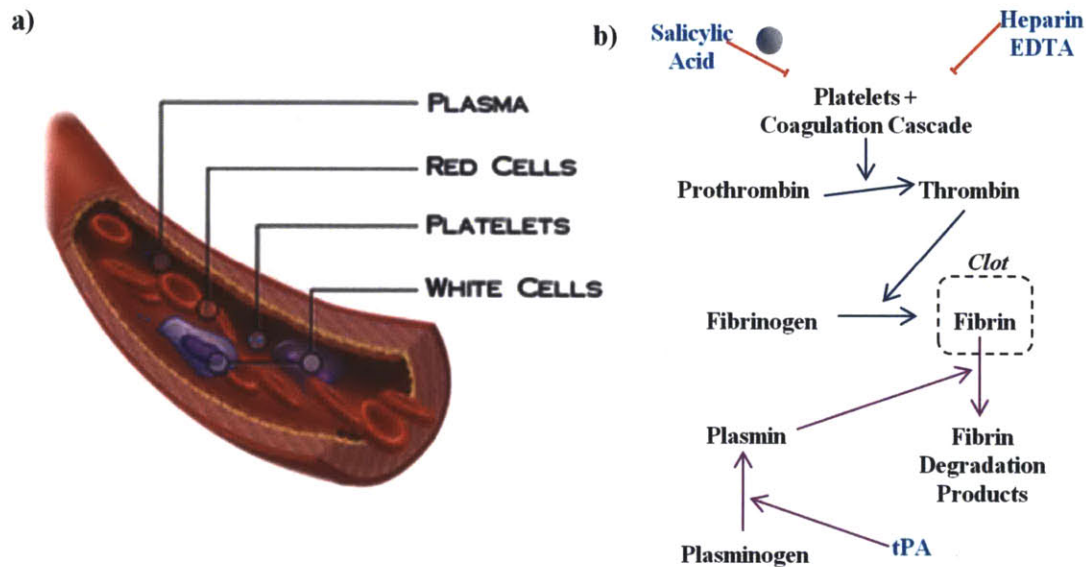


*Figure 2.7 Complexity of Blood*  
 (a) The various components of blood. Image reprinted from [130] (b) Coagulation cascade and different anticoagulants that can inhibit it. Image adapted from [131].

### 2.3.2.1 Initial Experiments

The initial tests of binding pathogens spiked into human blood were problematic. Tests with *C. albicans* indicated less than  $19\% \pm 5.5\%$  binding of the fungi spiked into blood samples even with  $40 \mu\text{g}$   $1 \mu\text{m}$  beads/ml sample. Given that MBL evolved to work in blood; I believed there should be conditions under which the beads should function. Groups using immunomagnetic beads to isolate circulating tumor cells from blood rely on enriching the nucleated cells out of blood using a Ficoll density gradients first [73, 87, 88], which would not be effective for pathogens since their size is on par or smaller than red blood cells. Wills et al. found that diluting blood was enough to boost the binding so that they could recover circulating endothelial progenitor cells [75], an approach that I adapted for our assay. Diluting the blood 1:1 with Tris buffered saline with 1% Tween 20 dramatically improved the binding results, increasing binding of spiked fungi in the blood by as much as 80% (figure 2.8). Gomez et al.



hypothesized that a small amount of dilution can reduce the hydrodynamic shielding effect in colloidal suspensions such as blood, improving bead binding [132]. When a sphere moves through fluid at low Reynolds number (which is the case for the beads), its influence extends out several radii from its surface, making it interact with nearby objects, which reduces its velocity [133]. Diluting the blood increased the average gap between adjacent red blood cells from 3  $\mu\text{m}$  to 4.6  $\mu\text{m}$ , giving the magnetic beads more space to circulate through the volume with less drag from adjacent cells to slow their movements. I found that further increasing the dilution factor did not significantly improve the binding, so the minimal possible dilution (1 part saline: 1 part blood) was used in future experiments. Since then, other researchers at the Wyss have determined that a 1:4 dilution factor improves the binding further [124], which I used in some later experiments in chapter 4.

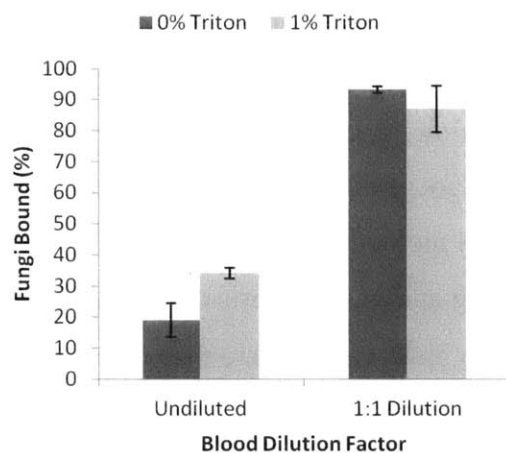


*Figure 2.8 Effect of Dilution on binding of *C. albicans* with 1  $\mu\text{m}$  beads in heparinized blood. Diluting the blood 1:1 with saline greatly increases the capture of the fungi. Lysis with Triton X-100 does not appear helpful in diluted blood and only slightly improved binding in undiluted blood.  $n=3$ , error bar: SEM*

Phagocytosis of coated beads was also a major concern (**figure 2.9 a**). Other members of the Sepsis group at the Wyss Institute found that using FcMBL rather than WtMBL reduced the immune activation caused by the MBL on the beads (because the binding sites for the MASP's had been removed), but it was not enough to completely eliminate phagocytosis [124]. Phagocytosis of the magnetic beads meant that the white blood cells would be collected along with the magnetically tagged pathogens, which could be a serious problem, particularly for PCR assays where the leukocyte DNA can inhibit the amplification of the pathogenic DNA [69].

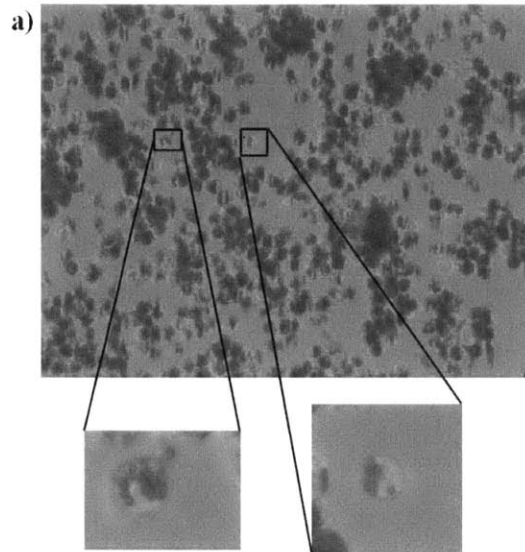
Several groups investigating using superparamagnetic nanoparticles as intravenous MRI contrast agents have found that the surface coating and bead size play key roles in the bead

phagocytosis rate in blood [134, 135]. Particles larger than 150 nm in diameter tend to be phagocytosed quickly, having a half life of 10-15 minutes in blood [136, 137]. Further reduction bead size was impractical for us since beads smaller than 100 nm generate much less of an induced force when magnetized, which would make it difficult to recover tagged pathogens. The 128 nm beads were already proving more difficult to recover from blood using conventional magnetic racks than their larger 1  $\mu\text{m}$  counterparts, so we did not want to reduce bead size any further. Therefore, a solution to the phagocytosis problem needed to be found. Both the beads types we employed were large enough to be phagocytosed quickly, so different methods for preventing or at least slowing phagocytosis of the beads in the blood samples were investigated. Unlike the groups using these beads for MRI contrast, I could alter the composition of the blood, so I focused on different sample treatments to reduce the phagocytosis rates. Other members of the Wyss Institute have been investigating altering the bead size and surface composition. The simplest method, also employed by other groups working with immunomagnetic beads [73, 75], is to keep the blood at 4°C, slowing the metabolic machinery driving receptor mediated phagocytosis. Comparison of phagocytosis rates of 1  $\mu\text{m}$  beads in cooled and room temperature blood samples confirmed that this method effectively reduced the phagocytosis rate for up to 90 minutes so that little or no binding and phagocytosis of the 1  $\mu\text{m}$  beads was observed (**figure 2.9 b-c**). This gave us enough time to bind and separate the pathogens out of blood with the FcMBL beads before phagocytosis became problematic.

One percent Triton X-100 can be used to permeabilize and kill white blood cells, preventing them from engulfing anything. Triton X-100 at this concentration also dissolves the red blood cell membranes, causing them to lyse. It most likely damages the platelets as well. The problem with this lysis is that it releases a large amount of pro-coagulant debris, which surprisingly did not have a significant effect on the binding of *C. albicans* with the 1  $\mu\text{m}$  beads (**figure 2.8**), but accelerated clot formation. Another destructive method to prevent phagocytosis is to poison cellular metabolism with a substance such as cyanide or arsenic. However, this was less attractive due to safety concerns.

In summary, diluting the blood 1:1 with saline buffer and holding the sample at 4°C during the binding and concentration process was sufficient to increase the binding above the  $19\% \pm 5.5\%$  observed in initial experiments and reduce the phagocytosis rate. The roles of anticoagulants, bead concentration and binding time in blood were then investigated to further

improve pathogen binding. The phagocytosis study should be repeated in patient blood at in various stages of sepsis to determine if the systemic inflammation and subsequent immune suppression has any major effect of FcMBL bead phagocytosis



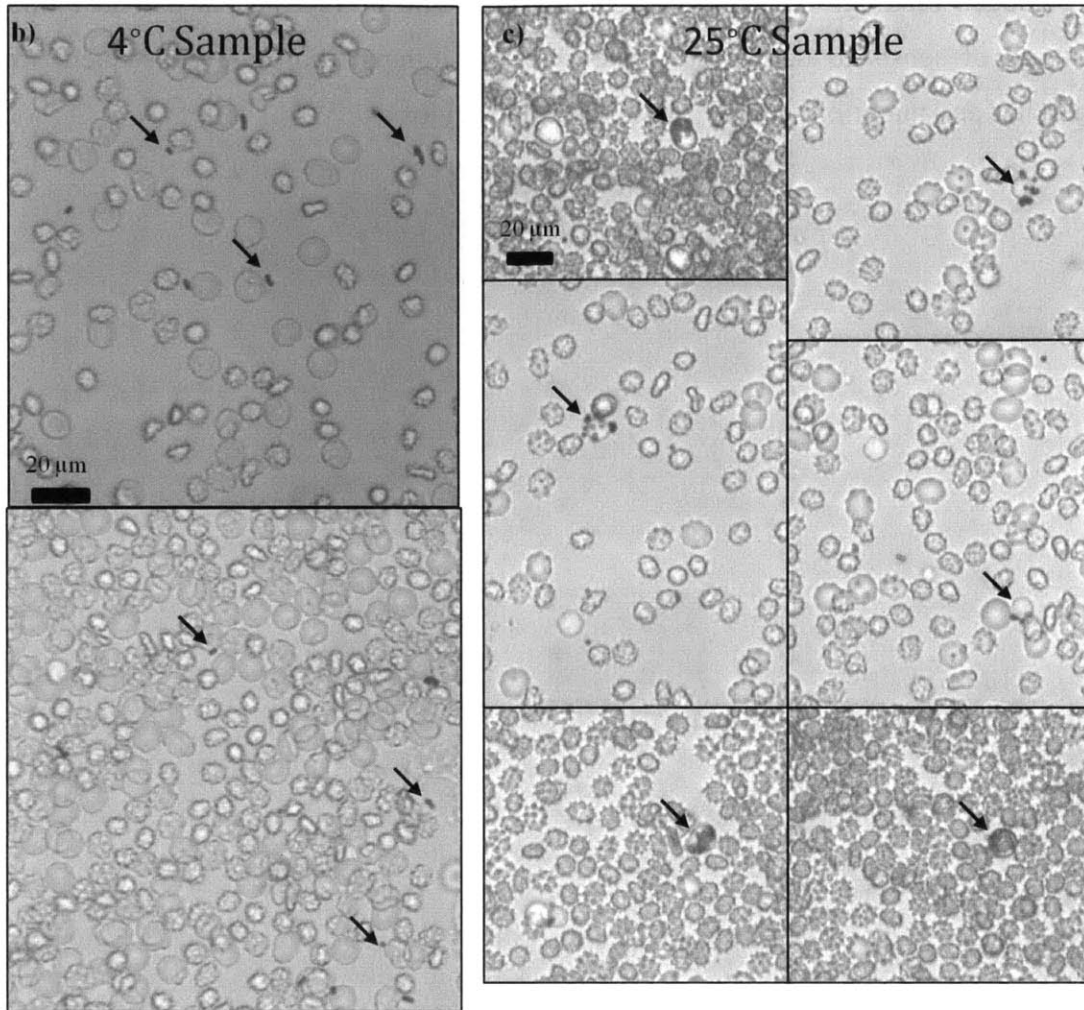


**Figure 2.9** Effect of Temperature on phagocytosis

(a) Phagocytosis of 1  $\mu\text{m}$  WtMBL beads (small, darker spheres) in a blood sample with some phagocytes engulfing more than 10 beads each (b) Isolated beads, indicated with black arrows, from blood maintained at 4°C during 90 minute incubation showing virtually no phagocytosis of the beads (c) Isolated beads from blood maintained at 25°C during 90 minute incubation showing both adhesion (first step of phagocytosis) and phagocytosis of beads. Cells phagocytosing beads are indicated with a black arrow

### 2.3.2.2 Anticoagulants

Heparin is a highly negatively charged molecule normally produced in blood vessels to help prevent coagulation. Purified forms have been widely used *in vitro* as an anticoagulant in vacutainers to prevent sample clotting and *in vivo* for prevention of deep vein thrombosis [138]. Heparin is responsible bringing thrombin in close proximity with its inhibitor, antithrombin III, preventing activation and clot formation [139]. For these reasons we chose to use it as our

baseline anticoagulant for all blood-based tests. Donor blood collected into standard 10 ml sodium heparin vacutainers was stable for over 24 hours at room temperature, suiting our needs.

The fresh donor samples were collected in sodium heparin vacutainers (BD), but it was not clear if this was enough anticoagulation to allow the FcMBL beads to function optimally. In blood, I found that resuspending the aggregated beads after magnetic concentration was difficult due to the deposition of clotted material on the beads, fusing the majority of them together. If the clotting was initiating during the binding process, it could have been blocking the surface of the FcMBL beads so that the protein could not access the pathogen surfaces. I experimented with different anticoagulants to see if this was the case.

Salicylic acid, as the active ingredient in aspirin, is a commonly used platelet inhibitor that permanently inactivates the COX 1 enzyme in platelets, making it difficult for them to degranulate and release their pro-coagulant molecules [131]. Adding increasing doses of salicylic acid to heparinized blood samples did not have any significant effect on the binding. However, it did prevent clot formation on the beads aggregated by the magnetic field, making it possible to resuspend beads and tagged pathogens after the field had been removed. One hundred  $\mu\text{g/ml}$  of salicylic acid greatly reduced the amount of clot on the aggregated beads and 1000  $\mu\text{g/ml}$  of salicylic acid almost completely eliminated it on the 1  $\mu\text{m}$  FcMBL beads (**figure 2.10 a-d**). These results indicated that the clot formation was not playing a major role in blocking the pathogen binding in these tests but only making it difficult to resuspend the magnetically aggregated beads and pathogens.

The calcium levels of blood are tightly regulated to stay around 2.1- 2.8 mM in the body because calcium is required for muscle contraction, nerve conduction, but it is also a key cofactor for several of the enzymes in the coagulation cascade [140]. Many common anticoagulants, such as ethylenediaminetetraacetic acid (EDTA), work by depleting blood calcium levels to slow sample clotting [141]. EDTA works by chelating calcium (and other metal ions), which is a required cofactor for several of the enzymes in the coagulation cascade. Therefore, removing ionic calcium from the plasma can effectively slow clot formation and give clinicians time to perform tests on the blood. However, the calcium depletion is a problem for MBL as well, since it also requires calcium as a cofactor to stabilize the CRD binding pocket. I had determined in saline that little or no binding would occur without calcium in the buffer (**figure 2.3**). However, many clinical samples are treated with EDTA, so we needed to see if it

was possible to bind pathogens in them. To accomplish this, blood was recalcified immediately before adding the FcMBL beads and mixing the sample for binding. This provided approximately 40 minutes to bind and concentrate the pathogens out of the sample before clotting began in earnest. Using this approach I found no significant difference in binding between the recalcified blood and heparinized blood except when no calcium was added, in which case binding in EDTA blood was lower than in the heparin samples (**figure 2.10 d**). Adding a therapeutic dose of heparin before recalcifying the blood prevented reactivating the coagulation cascade and made the blood stable over several hours [124].

Heparin was preferred for these assays due to its simplicity, however, but it was possible to get comparable binding in EDTA treated blood samples with the correct treatment, giving the FcMBL beads much more flexibility when working with clinical samples.

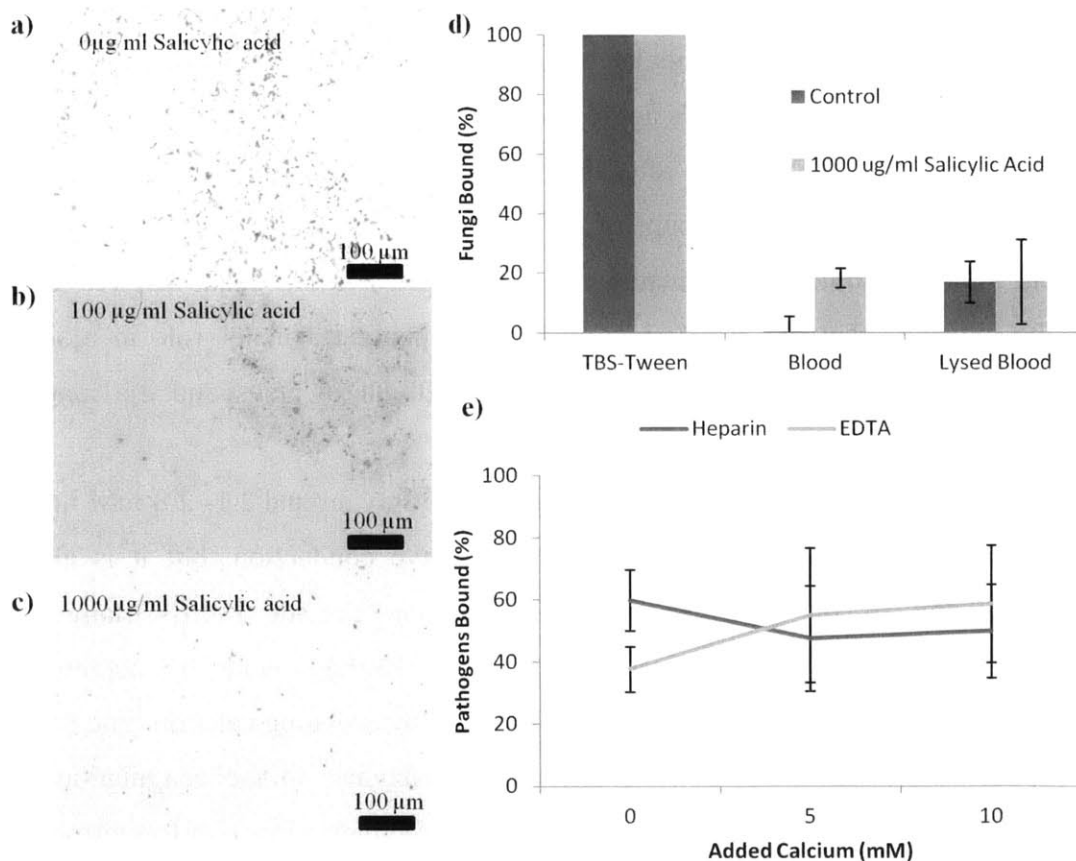


**Figure 2.10** Effect of Salicylic Acid on Coagulation and binding in blood  
 (a) Aggregated 1 µm beads with no Salicylic acid added, faint outlines of fibrin clots can be seen holding the clumps of beads together (b) Aggregated 1 µm beads from blood sample treated with 100 µg/ml salicylic acid, much less fibrin formation and some free beads visible (c) Aggregated 1 µm beads from a blood sample with 1,000 µg/ml Salicylic acid added, virtually no fibrin clots visible, mainly free beads. Any aggregates are composed of less than 5 beads (d) Effect of Salicylic Acid at 1,000 µg/ml on the binding of *C. albicans* in undiluted blood : no major effect

on the binding of fungi in blood in lysed (1% Triton X-100) or unlysed blood.  $n=3$ , error bar: SEM (e) Binding of *C. albicans* with  $1\ \mu\text{m}$  FcMBL beads in diluted blood in Heparin vs. EDTA treated blood (diluted 1:1 with buffer): EDTA blood with no calcium added has lower binding than heparinized blood although still higher than expected. With calcium added to the samples, the binding performance of both was comparable.  $n=4$ , error bar: SEM

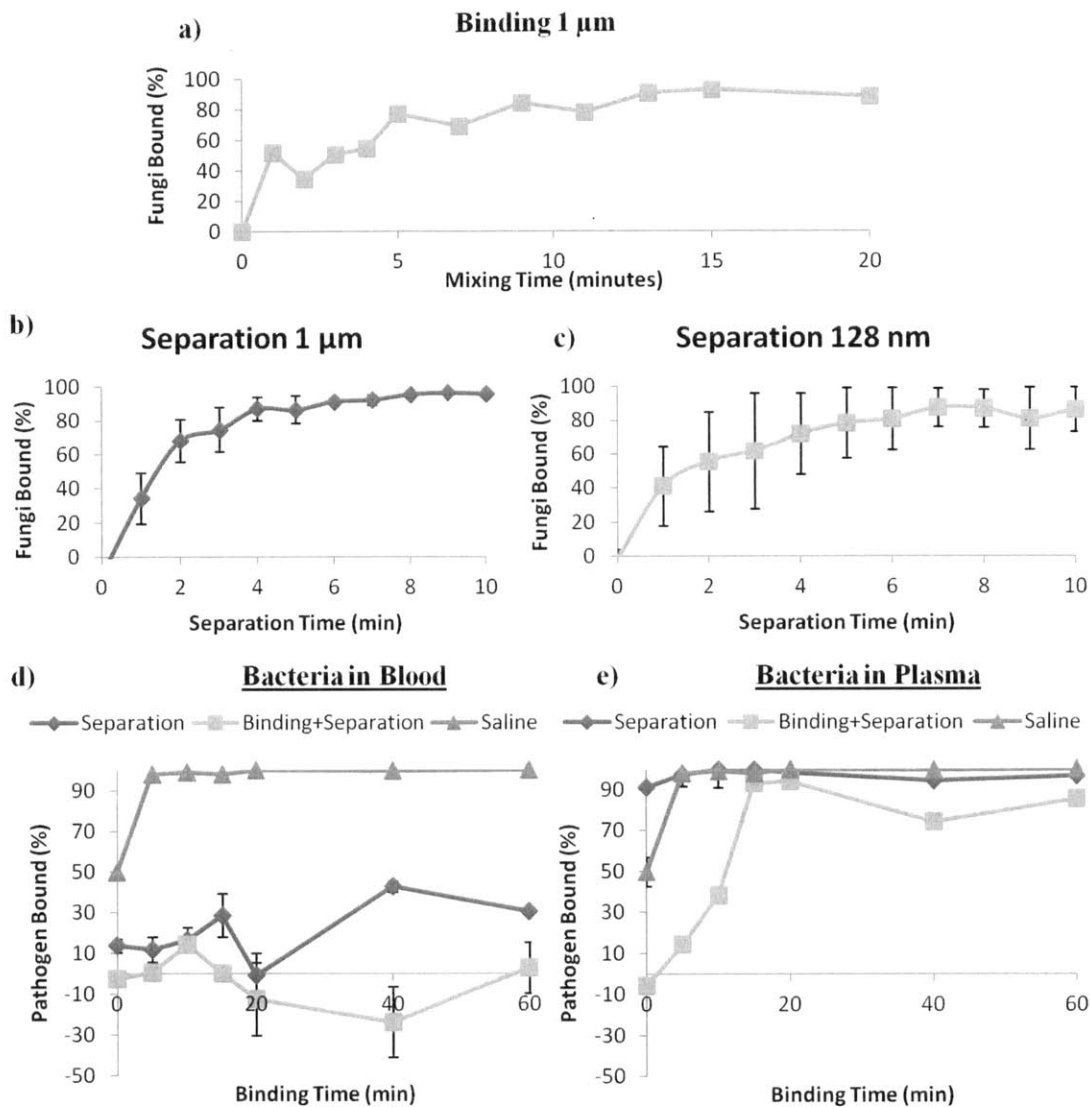


Figure 2.11 Binding and separation of magnetically tagged fungi and bacteria from diluted blood

(a) Binding of *C. albicans* with  $1\ \mu\text{m}$  beads with different mixing times (b) Binding and separation of *C. albicans* from diluted blood with  $33.3\ \mu\text{g}\ 1\ \mu\text{m}$  beads/ml sample: binding and magnetic pulldown of *C. albicans* with the larger beads looks good  $n=2$  error bar: SEM (c) Binding and separation of *C. albicans* from diluted blood with  $50\ \mu\text{g}\ 128\ \text{nm}$  beads/ml sample: Magnetic separation of fungi with the smaller beads is more variable, taking longer but saturating after about 7 minutes in the magnetic rack  $n=2$ , error bar: SEM (d) Check of binding and separation of *S. aureus* with  $50\ \mu\text{g}\ 128\ \text{nm}$  beads/ml sample in diluted blood: Bacteria were pre-tagged with beads before being added to diluted blood (separation) and bacteria were mixed with beads for different amounts of time (binding and separation) in diluted blood. Not able to pull out magnetically tagged bacteria with the DynaMag 2 rack. Poor recovery of pre-bound bacteria indicates that the DynaMag 2 rack is failing to pull out the  $128\ \text{nm}$  beads due to

their having a smaller induced magnetic dipole. rack  $n=3$  error bar: SEM (e) Check of binding and separation of *S. aureus* with 50  $\mu\text{g}$  128 nm beads/ml sample in plasma: Bacteria were pre-tagged with beads before being added to diluted plasma (separation) and bacteria were mixed with beads for different amounts of time (binding and separation). Much better separation out of plasma, DynaMag 2 rack works alright when blood cells are not present.  $n=3$  error bar: SEM

### 2.3.2.1 Reevaluating Bead Concentration, Bead Size and Binding Time

Reevaluation of bead binding parameters was important at this stage due to the complexity of blood as a multi-component fluid. Its higher viscosity and colloidal nature slows movement of beads and pathogens, both during the binding and separation phases. For these reasons, I suspected that many of the guidelines for good binding found previously in buffer would have to be reevaluated. A systematic investigation into the optimal binding time, separation time, bead size and bead concentration for binding in the diluted blood samples should increase the binding further.

For *C. albicans* with 1  $\mu\text{m}$  FcMBL beads at 10  $\mu\text{g}$  beads/ml in blood, I found the binding plateaued at  $91\% \pm 1.2\%$  after approximately 12 minutes of mixing time in an inverting shaker (**figure 2.11 a**). For *S. aureus* with 128 nm beads at 50  $\mu\text{g}$  beads/ml, I found the binding in blood saturated after 15 minutes of mixing time at  $18.4\% \pm 7\%$  (**figure 2.11 d-e**). The poor separation of *S. aureus* in blood indicated that the commercial magnetic rack used to recover them was not sufficiently powerful enough to pull out the smaller 128 nm beads. Both binding and separation of the bacteria worked fine in plasma (**figure 2.11 e**), so it appears that the poor depletion is mainly caused by the cellular fraction of blood. The most likely explanation is that the red blood cells impede the motion of the magnetic beads and tagged bacteria. From these experiments, it was concluded that 20 minutes of mixing time was sufficient for the binding to reach completion in blood for both fungi and bacteria, which was double the 10 minute time employed in saline.

Binding of bacteria in diluted blood produced variable results, prompting examination of the pitfalls of using the smaller beads (**figure 2.12**). The 128 nm beads were more difficult to use in blood because they are much more difficult to pull out onto the magnetic than the 1  $\mu\text{m}$  beads. This is due to their volume being  $1/470^{\text{th}}$  that of the 1  $\mu\text{m}$  beads. The volume of the beads controls the number of magnetic nanoparticles crystals inside, which determines the magnetic force on the bead when it is placed in the magnetic rack, so the 128 nm beads have a smaller net magnetic force on them than the 1  $\mu\text{m}$  beads [142]. Difficulty in pulling out the beads and tagged



pathogens affected the results of the depletion assay because it was also picking up magnetically tagged pathogens that had not finished being pulled out of the blood.

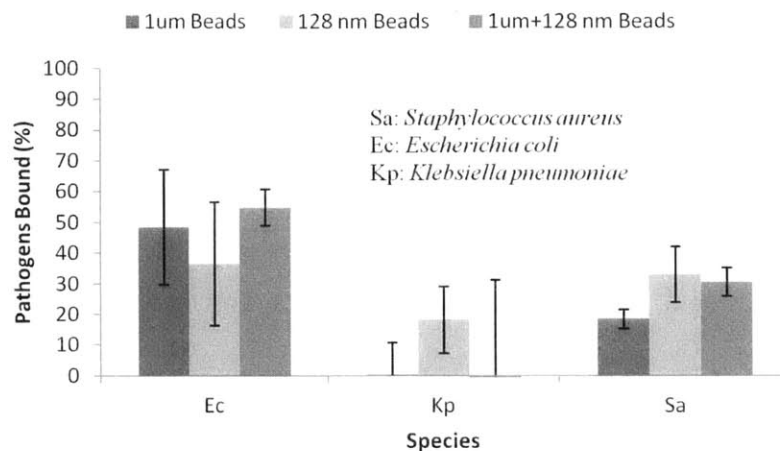


*Figure 2.12 Binding of Bacteria in blood with 1µm and/or 128 nm beads*  
*Twenty five micrograms of each bead type per ml diluted blood added. Binding to the bacteria is variable, possibly due to poor magnetic separation with the 128 nm beads. Adding both bead types together seems to reduce the variability of the binding to a small degree. n=3, error bar: SEM*

For fungi, it made a great deal more sense to use the larger 1 µm beads, since we knew they bound well to the larger pathogens and they created a large force when magnetized by the DynaMag 2 rack (Invitrogen), although magnetic separation of the fungi with 128 nm beads was also satisfactory, most likely due to the larger surface area of the fungi allowing up to fourteen thousand 128 nm beads to attach. This would give force comparable to about thirty 1 µm beads. Considering we can pack up to two hundred thirty 1 µm beads on a typical *C. albicans* cell, it made much more sense, in terms of magnetic separation, to use them. This difference may also explain why the separation of the fungi was more variable with the smaller beads, since the net force on the pathogens most likely lower (**figure 2.11 b-c**). The 128 nm beads bound better to the bacteria but were much more difficult to pull out of blood. Even when the 128 nm beads were prebound to bacteria before adding them into the diluted blood sample, only able to recover 40% of them were recovered (**figure 2.11 d**) and the separation was much more variable than with the 1 µm beads and fungi. It appears that a lot of the problem was the cell-based component of blood, since I ran the same test in plasma and was not only able to separate out only 95% of the prebound pathogens, but also bind and separate up to 90% of *S. aureus* spiked the plasma sample with 50 µg beads/ml (**figure 2.11 e**). Based on the hypothesis that the DynaMag 2 rack

was poorly optimized for recovering nanometer scale beads from blood, I developed two new separation strategies to recover bound bacteria from blood in Chapter 4 which boosted bacteria separation up to over 85% out of diluted blood.

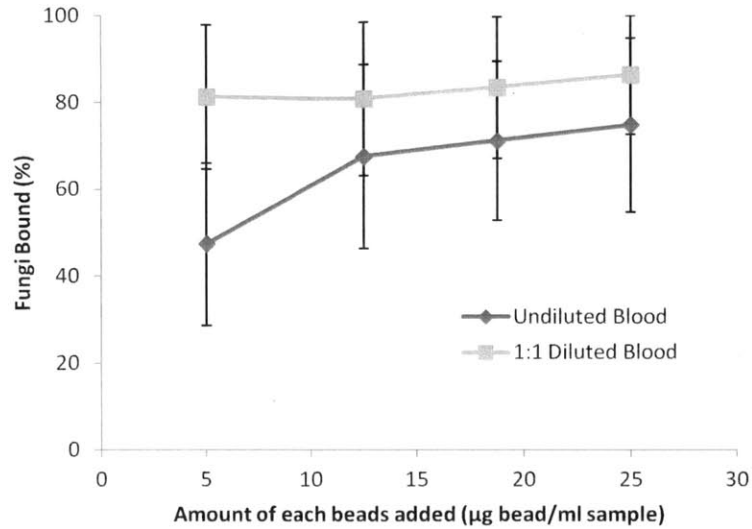


*Figure 2.13 Binding of *C. albicans* in diluted and undiluted blood with different concentrations of 1 µm FcMBL beads*

*Binding in diluted blood is better, although relatively high capture rates in undiluted blood are possible at high enough bead concentration*

The binding of *C. albicans* in both diluted and undiluted blood was tested with a range of different bead concentrations and showed that I could obtain an average of 86% ±14% fungi capture in diluted blood with 25 µg beads/ml sample in diluted blood and up to 75% ±20% binding in undiluted blood (**figure 2.13**). The standard deviation between different donors was relatively high (over 20% in some cases). Other members of the sepsis group at the Wyss Institute have been studying causes of this inter-donor variability. The impact of different fractions of on binding was examined and revealed the most consistent factor that decreased the binding was the red blood cells. Adding red blood cells to a saline sample lowered the capture rate of the pathogen more than plasma, serum or platelets from blood. In a small fraction of the donors tested, there were components in their serum that inhibited binding as well, which we hypothesize was IgG antibodies and other endogenous opsonization proteins against the pathogens which blocked the binding sites for our FcMBL beads. However, no correlation between endogenous MBL levels in our donors and *C. albicans* binding in diluted blood was found.

Since these investigations were carried out, other members of the Wyss Institute have developed binding and separation systems that can recover over 80% of *S. aureus* and *E. coli* from blood [143]. Working with these initial guidelines, Mark Cartwright, Martin Rottman, Nazita Gamini and others have developed a high throughput method to test FcMBL bead binding to a wide range of pathogens (**figure 2.14**) [124]. From their investigations, they have found that binding in EDTA blood could be improved further by diluting 1:4 with TBS-Tween 20 with 5 mM calcium and treating it with ten mM of glucose and 0.8 mg heparin per ml (JT Backer Inc.) [124]. I made use of these improvements to help characterize new methods for separation of bound bacteria out of blood in chapter 4.

Species	Type	Capture( as determined by plating)
<i>S. aureus</i>	gram+	Yes
<i>Clinical S. aureus</i>	gram+	Yes
<i>MRSA01-clinical</i>	gram+	Yes
<i>MRSA03-clinical</i>	gram+	Yes
<i>MRSA04-clinical</i>	gram+	Yes
<i>MRSA05-clinical</i>	gram+	Yes
<i>IRE</i>	gram+	Yes
<i>Strep. Group B</i>	gram+	Yes
<i>S. pyogenes</i>	gram+	Yes
<i>Bacillus Thuringiensis</i>	gram+	Yes
<i>Streptococcus pneumonia</i>	gram+	No
<i>Streptococcus pneumonia</i>	gram+	No
<i>Streptococcus bovis</i>	gram+	No
<i>Salmonella Paratyphi A</i>	gram-	Yes
<i>Salmonella Enteriditis</i>	gram-	Yes
<i>Salmonella Typhi CT18</i>	gram-	Yes
<i>Salmonella Typhymurium LT2</i>	gram-	Yes
<i>Salmonella Typhimurium 14028</i>	gram-	Yes
<i>P. aeruginosa</i>	gram-	Yes
<i>E. coli</i>	gram-	Yes
<i>N. meningitidis</i>	gram-	Yes
<i>K. pneumoniae</i>	gram-	No
<i>K. oxytoca</i>	gram-	No
<i>B. cepacia</i>	gram-	Yes
<i>Haemophilus influenzae (b)</i>	gram-	No
<i>Candida albicans</i>	fungi	Yes
<i>Candida parapsilosis</i>	fungi	Yes
<i>Saccharomyces cerevisiae</i>	fungi	Yes
<i>Pichia pastoris</i>	fungi	Yes
<i>Aspergillus fumigatus</i>	fungi	Yes

**Figure 2.14** Testing multiple species of pathogens with FcMBL beads  
 Testing of FcMBL bead capture of bacterial species performed by other members of the Wyss Institute. This expanded study shows that FcMBL beads can bind to many pathogenic bacteria,

*although they have the same difficulty with encapsulated pathogens that serum MBL does. Image adapted from [124]*

## 2.4 Bead Binding Theory

The binding of pathogens with the magnetic beads is affected by several factors, including diffusion, convection and the binding reaction itself. The binding reaction is dependent on both the collision rate between the beads and the target pathogens and the actual binding chemistry of MBL to the pathogen. For a diagnostic system where the concentration of pathogens ( $C_c$ ) is unknown, certain parameters can be used to improve the binding. The first is bead concentration ( $C_b$ ) added to the sample. For binding rare pathogens in a timely manner, a large excess of beads is required to maximize the odds of the beads coming in contact with the pathogens [144]. To a small extent, diffusion can be controlled by changing the size of the beads. For increasingly small beads, the importance of diffusion in the binding rate becomes increasingly important as their diffusion coefficient increases [84]. The fluid convection that is responsible for dispersing the beads throughout the sample can be controlled by the mixing parameters employed in the system.

The actual collision rate and the binding rate given pathogen-bead contact are the most complex parts of the problem, dependent on both collision theory and the binding chemistry of FcMBL itself. The collision rate between the beads and pathogens ( $R_{cb}$ ) is a function of their concentrations, their relative velocity ( $v_{cb}$ ) and their radii ( $r_c$  for the pathogens and  $r_b$  for the beads) [84] :

$$R_{cb} = \pi(r_c + r_b)^2 C_b C_c v_{cb} \quad (2.3)$$

The actual binding rate is typically lower than the collision rate since not every contact event results in binding [86]. The probability of binding given contact depends on the chemistry of the MBL, the constituents in of the fluid (like calcium), the shear rate between the pathogen and the bead and the surface density of antigens on the surface of the pathogen [145]. This subject is highly complex and warrants a detailed investigation of its own, particularly since relatively little quantitative data on the density of mannose and fucose residues on the surfaces of different pathogens is available. For these analyses, I will focus primarily on the mechanics of binding interaction. Other members of the sepsis group at the Wyss are working to optimize the binding chemistry (such as adding glucose to lessen non-specific FcMBL binding [124]).

The collision rate is proportional to the mean free path of the beads in the fluid, which is why the radii of each and their concentrations must factor into the analysis. The relative velocity between the beads and pathogen at the time of collision depends both of the difference in velocities between the streamlines containing the bead and the pathogen and the diffusion velocity of both species across different streamlines [84, 146]. The Peclet (Pe) number gives an estimate of the relative importance of convection over diffusion for both beads sizes and not surprisingly diffusion is more than ten times as important for the smaller 128 nm beads [125].

$$Pe = \frac{ru}{D} \quad (2.4)$$

Where  $r$  is the characteristic length of the system (assumed to be on the order the bead diameter here),  $u$  is the characteristic velocity (assumed identical for both bead types and on the order of 1 cm/s in the (given the rotation rate of the inverting mixer), and  $D$  is the diffusivity of each bead type (calculated with equation 2.1).

To try and understand why the 1  $\mu\text{m}$  beads did not work nearly as well for bacteria, a closer examination was taken of the binding kinetics and the maximum number of beads that can attach to each pathogen type. The relative velocity induced by diffusion ( $v_{diff}$ ) is [84]:

$$v_{diff} = \frac{4(D_c + D_b)}{(r_c + r_b)} \quad (2.5)$$

This full form of the equation must be used when the bead and pathogen are of similar size (assumed to be the case for the 1  $\mu\text{m}$  beads binding to 1  $\mu\text{m}$  bacteria) because the relative Brownian motion of each is of similar importance and must be taken into account. However, if the bead is much smaller than the pathogen (assumed to be the case for the 1  $\mu\text{m}$  beads binding to 10  $\mu\text{m}$  fungi and the 128 nm beads binding to the 1  $\mu\text{m}$  bacteria), the relation simplifies to

$$v_{diff} = \frac{4D_b}{r_c} \quad (2.6)$$

because diffusivity of the smaller bead dominates the motion and the larger pathogen can be approximated as stationary. This results in faster diffusion of the bead to the pathogen surface, increasing the binding rate. Increasing the mixing speed can increase the convective relative velocity, but it also increases the shear rate between the bead and pathogen, which is believed to

reduce the probability of binding given contact because there is not sufficient time for avidity binding to occur before the bond is stressed; only a few CRD's attach before the bead is torqued by the fluidic shear. If the bead diffuses to the surface of the pathogen, there will be more time for many CRD's to attach, creating a strong bond through avidity that is unlikely to be broken by shear. The larger beads on the surface of a bacteria would also be subject to more shear than the smaller beads, making them more likely to be ripped off while beads much smaller than the pathogen will be more protected by the boundary layer flow on the surface of the pathogen and should be submitted to lower shear rates, making them more likely to stay in place [133].

A second reason that can explain why the 1  $\mu\text{m}$  beads do not effectively bind to bacteria is the maximum number of beads that can attach to the pathogen. The surface density of spheres on a planar surface ( $\rho_{2d}$ ) is [84]:

$$\rho_{2d} = \frac{\pi}{\sqrt{12}} \sim 90.7\% \quad (2.7)$$

If the bead is much smaller than the pathogen, the pathogen surface can be treated as roughly planar, so the total number of beads that can attach to the surface ( $N_{max}$ ) is [84]

$$N_{max} = 4\rho_{2d} \left( \frac{r_c}{r_b} \right)^2 \quad (2.8)$$

Using this relation, approximately two hundred thirty 1  $\mu\text{m}$  beads can attach to one fungal cell and about two hundred twenty 128 nm beads can attach to one bacteria; very similar for both of them. This approximation is not valid for 1  $\mu\text{m}$  beads, where trying to pack beads onto the surface of something with nearly equal size is much more complicated. The larger beads will wind up having to competing with each other if enough bind to begin covering the pathogen surface.

Judging from these calculations and empirical observations with the different bead sizes, the binding of pathogens with beads appears more effective if the beads are much smaller than the pathogen (at least 1/10<sup>th</sup> the size). This allows the relative diffusive velocity to increase slightly because the movement of the pathogen is no longer significant. The smaller beads should also be more sheltered from fluidic shear during the initial binding instant when avidity is being established and more of them can be easily packed onto the surface of the pathogen. Reinforcing

this concept is that the 128 nm beads can effectively bind to the larger fungi as well, packing roughly up to 14,000 beads onto the surface. The main disadvantage of this approach is that the smaller beads exert a much smaller magnetic pull on the pathogen, making it more difficult to pull them out in a given magnetic field, a problem that I address in detail in later chapters.

## **2.5 Discussion**

Our objective was to create a single set of magnetic beads that could bind a wide range of pathogens in blood by coating the beads with a general opsonin derived from the human primitive immune system called MBL. In serum this protein is capable of binding to a wide range of bacteria and fungi and I have shown that this magnetic beads coated with this protein can bind a wide range of pathogens in saline and blood [109].

I decided to move away from using the flow cytometer for quantification and employ plate based quantification instead for several reasons. The first was that the cytometer worked fine for picking up the larger fungal cells used for most my initial evaluations, but it had much more difficulty detecting the fluorescence signature of an individual bacterium in the millisecond it was illuminated. The other reason was that flow cytometry had difficulty detecting less than 1,000 cells per ml, and that number went up to 10,000 cfu/ml if I was trying to detect pathogens in blood samples (due to the increased complexity of the sample). Microbiological plating could operate at pathogen concentrations much closer to the physiological range in sepsis (1000 to 100 cfu/ml) and was not affected by the complexity of the sample. With proper controls and technique, we found that plating was an accurate way to assess pathogen concentration in a sample. It had the added advantage that all the analysis could be done in the BL2 facility, rather than having to risk bringing blood and pathogen samples out of containment to the flow cytometer at the Wyss Institute core facility. In addition to the plating depletion assay, several other group members at the Wyss Institute have recently developed ELISA and Bactiter Glo assays to quantify FcMBL binding to pathogens and the viability of the captured pathogens [124].

I chose to use the depletion assay to measure binding because we had determined that the MBL beads can cause pathogens to aggregate, so that what looked like a single colony during plate analysis may in fact have originally contained several bacteria welded together by the beads. The unbound bacteria remaining in the sample fluid did not normally aggregate, so

comparing the positive control to the unbound pathogens proved a more reliable way to quantify the binding.

The development of a single set of magnetic beads that can bind to many pathogens, including *S. aureus*, *E. coli* and *C. albicans* (three important species in sepsis), but not mammalian cells has huge implications for the diagnosis of sepsis because it offers a novel method to bind and separate unknown pathogenic cells out of blood. In our previous work with magnetic beads in blood, we could only pick up one known species at a time [91]. Most other work immunomagnetic beads in blood has focused on capturing nucleated cells such as tumor or progenitor cells, which allows them to use size-exclusion centrifugation [73, 75, 87, 88]. The similar size of pathogens to red blood cells means that this approach is not viable for binding pathogens, but I have shown that we can obtain good binding without this sample preparation technique. MBL has the advantage relative to other plant or invertebrate lectins in that it evolved to function in blood and typically does not bind to human cells. Plant and invertebrate lectins also have the ability to bind a wide range of bacteria, but they bind to blood cells as well, severely limiting their utility in human samples [102, 103, 126] while MBL has no such problem. Magnetic bead and rack systems are robust, inexpensive and easy to use. The ability to bind and concentrate pathogens directly out of blood makes direct detection of an infection possible, without the need for a time consuming and unreliable culture step first [27]. These two abilities mean that these general opsonin beads could form the basis of a rapid sepsis diagnostic technology that would not require an expensive, culture-based central laboratory to operate. Other members of the Wyss Institute are also actively investigating the use of these beads in a dialysis-like therapeutic system to continuously remove pathogens from the blood of septic patients to help stop the spread of the infection. Blood is arguably one of the most complex fluids in the world [147], so the fact that these MBL beads can operate in it suggests that they may function in a wide range of other complex samples, so they may have applications in the testing food for bacterial contamination as well.

For working with blood, I was looking for the simplest effective sample treatment methods because we were developing these beads to be used a general method to recover pathogens from blood for a wide range of applications, both diagnostic to therapeutic. Dilution, cooling and heparin were sufficient to give good binding without significantly increasing the sample volume or damaging the pathogens. Radiation or chemical treatments could have also inactivated the



phagocytes in the sample, but this would then interfere with potential downstream PCR or AST testing by degrading the pathogen DNA and viability [21]. Dilution of blood 1:1 with saline greatly improved pathogen binding, boosting it as much as 80% in the blood of some donors and addition of extra anticoagulants (EDTA, salicylic acid), had no significant effect on the binding. These treatments were typically withheld unless they were needed for something after bead capture (like using the salicylic acid treatment to make the beads easier to resuspend after concentration). Work is ongoing to improve binding in blood further using various blood treatments (anticoagulants, sugars), bead size, bead concentration and bead surface chemistry in the sepsis group at the Wyss Institute, improving on the groundwork laid here.

Despite these relatively simple treatments, we were able to show that FcMBL beads can effectively bind more than 20 different pathogen species in both saline and blood, including gram positive and negative bacteria and fungi. The recombinant form of MBL (FcMBL) conjugated to magnetic beads appeared to be able to reproduce the binding abilities of the native serum protein. My experimental measurements found that bead size and bead concentration were the two biggest factors affecting binding in saline. Collision theory confirmed that binding to pathogens is most effective when there is a large excess of magnetic beads that are much smaller [84], roughly  $1/10^{\text{th}}$  the diameter or less. For this reason, we chose to use 1  $\mu\text{m}$  beads to bind the larger fungi and 128 nm beads to bind to the smaller bacteria. Blood is a much more complex fluid, so I had to increase the bead concentration, binding time and separation time relative to that used in saline in order to achieve a similar amount of fungi binding. I also found that the disadvantage of the smaller 128 nm beads is that the bacteria tagged with them are much more difficult to magnetically separate of blood with a commercial magnetic rack, even though the actual binding to bacteria seemed fine. This led me to develop several strategies to boost the magnetic field that boosted separation of magnetically tagged bacteria to more than 85% (see chapter 4). These experiments should be repeated in the blood from septic patients when available to determine immune up regulation or suppression (depending on the stage of sepsis) significantly alters the behavior we have observed in blood from healthy donors.

I have laid out the groundwork for using the FcMBL beads in blood which other members of the sepsis group at the Wyss Institute are actively expanding to further maximize pathogen binding and determine the full range of pathogen species and strains that these beads can be used

to capture. To date they have confirmed that FcMBL beads can bind over twenty different pathogens in blood, including MRSA, VRE and *Salmonella* species [124].

## **Chapter 3 Optical Detection of Fungi**

### **3.1 Introduction**

Fungemia is becoming increasingly problematic in intensive care units (ICU). It was once a rare infection but now represents 6-11% of sepsis cases thanks to an increasing number of immunocompromised patients who have difficulty clearing fungal infections, usually a *Candida* species [19]. Patients have a higher probability of survival if effective therapy is started in the first 48 hours, but it usually takes 3-7 days to detect fungi with traditional blood culture and AST techniques [19]. We have shown that magnetic beads coated with recombinant mannose binding lectin (FcMBL), can bind to a wide range of pathogen species in blood, particularly fungi. Here, I have used these beads as the basis of a diagnostic system to rapidly detect the presence of fungi in blood. Concentrating fungi out of blood using magnetic beads is a relatively simple matter, but visualizing them for rapid, optical detection is much more difficult due to them being buried among the excess beads. The one of the major limitations for rapid detection was that the large excess of opaque, magnetic beads required for optimal binding obscured the fungi we were trying to optically detect. To overcome the difficulty of visualizing rare pathogens captured with magnetic beads, I have developed a microdevice that can efficiently concentrate magnetically tagged pathogens from a blood sample for optical detection by balancing the fluidic shear and magnetic field so that the beads and bound pathogens from the sample are spread into a thin layer suitable for automated detection with an epifluorescence microscope. Using this system, I have detected the presence of *C. albicans* in fresh human blood samples at concentrations down to 1 fungus/ml in less than three hours.

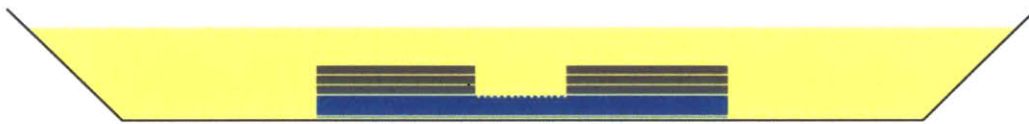
### **3.2 Materials and Methods**

#### **3.2.1 Microdevice Fabrication**

All devices and prototypes were made from polydimethylsiloxane (PDMS), also called Sylgard 184 (Dow Corning). The base and curing agent were mixed in a 10:1 ratio by weight according to the manufacturer's instructions. Device fabrication employed standard microfabrication techniques [148], but we employed a variety of different methods to produce the molds from which PDMS devices were cast.

The molds for the early devices (before micropatterning was introduced) were fabricated using a rapid prototyping method developed by Chong Yung in the Ingber lab. The layout of the device was created using Corel Draw and then a CE5000-60 cutter-plotter (Graphtec) cut the pattern of the channels out of 80  $\mu\text{m}$  thick mirror chrome Mylar (Supplies Unlimited Inc, Wakefield, MA). The excess Mylar could then be picked out of the design using the tip of a scalpel blade and the sticker of the channels could then be moved into the bottom of a flat Petri dish using transfer tape (Clear Choice, South Plainfield, NJ). Multilayer patterns could be constructed by stacking layers of the Mylar stickers on top of each other, allowing us to create devices with heights of 80  $\mu\text{m}$ , 160  $\mu\text{m}$ , 240  $\mu\text{m}$  and so on. The cutter plotter could not reliably create patterns smaller than 500  $\mu\text{m}$ , so this technique was largely used to create millimeter scale features. By using this approach, a sketch could become a useable PDMS device in less than one day.

**a) Cast Epoxy**



**b) Remove Mold**



**c) Cast PDMS**



**d) Bond to glass**



*Figure 3.1 Fabrication of microdevice mold*

*(a) A sacrificial master device (made of Mylar (grey) and micropatterned PDMS (blue)) is duplicated using casting epoxy (yellow/orange) (b) After the casting epoxy has set, the sacrificial master is removed and the mold prepared for use (c) uncured PDMS is poured into the mold and a glass slide laid across the top to create a microdevice with a defined thickness (d) The*

*microdevice with a combination of millimeter scale fluid channels and micron scale patterns on the channel ceiling is removed from the mold and bonded to a glass slide, ready for use.*

To combine millimeter scale channels with micron scale features, I developed a method to combine the large scale Mylar-patterned channels with micropatterned features created using standard SU-8 photolithography methods (**figure 3.1 a-d**). To do so, I combined Mylar channels created with the cutter plotter with micropatterned PDMS to make a sacrificial master device that was then cast in epoxy to produce the final mold. I designed various types of micropatterned features for the magnetic beads to settle into using AutoCAD and Output City (Boston, MA) produced a transparency mask that was used to cast several SU-8 wafers with various feature heights (10, 20, 40, 80  $\mu\text{m}$ ) onto silicon wafers at the Harvard CNS facility. To fabricate the micropatterned PDMS that would form the ceiling of the microdevice, I placed 280  $\mu\text{m}$  spacers on edges of the wafer to define the thickness of the PDMS. Then a glass plate was clamped across them. Once cured, I removed the PDMS from the wafer and attached it to several stacked Mylar stickers that formed the shape of the channel to make a sacrificial master device (**figure 3.1 a**). This was what the final device would look like. A negative of this device was cast with EasyCast Clear Casting Epoxy (Castin'Craft), after which the sacrificial master was peeled out of the epoxy and the epoxy was then used to cast PDMS devices of a defined height by clamping down a glass slide across the top of the epoxy while curing (**figure 3.1 b-c**).

Once the PDMS device had been removed from the epoxy mold, I punched inlet and outlet ports in the device using a 3 mm biopsy punch. Next it and a glass coverslip were treated with oxygen plasma for thirty seconds and sealed together. Tygon tubing (1/8" OD 1/16" ID, Saint-Gobain Performance Plastics) was then inserted into the ports in the device and glued in place using 9-1363 Industrial Assembly Adhesive (Dow-Corning), after which the devices were ready for use.

The final prototype consisted of a single long channel (3mm wide, 35 mm long, 280  $\mu\text{m}$  high) with a repeating array of wells (50  $\mu\text{m}$  in diameter, 20  $\mu\text{m}$  deep) micropatterned into the ceiling of the middle 25-mm section of the channel. In each row, the circles were spaced 100  $\mu\text{m}$  apart with each subsequent row 50  $\mu\text{m}$  below the previous row and shifted 50  $\mu\text{m}$  relative to it. The ceiling of the channel separating the MFC from the liquid in the channel was made as thin as possible (300  $\mu\text{m}$  thick) to minimize the dissipation of the magnetic field.

### **3.2.2 Testing Early Prototypes**

The early version of the diagnostic device was constructed using the Mylar cutter plotter to create the molds (section 3.2.1). It contained a low shear capture chamber 4 mm wide by 20 mm long by 240  $\mu\text{m}$  high over which were positioned five stacked neodymium magnets (2" x 1/4" x 1/8," K&J magnetic) as shown (**figure 3.2**). Concentration and detection was tested in this device using either 10 ml of saline or packed red blood cells obtained from the Children's Hospital Blood Bank, diluted to 40% hematocrit with saline. Different concentrations of *C. albicans* were added along with 25  $\mu\text{M}$  Calcofluor to stain their cell walls and 50  $\mu\text{g}$  1  $\mu\text{m}$  WtMBL beads/ml sample. The beads were mixed for 30 minutes and then run through the device at 10 ml/hour, followed by a 3 ml saline wash to flush out the blood out of device for imaging.

For imaging, the magnet was removed from the top of the device and used to manually manipulate the beads in the capture chamber to spread them out on the bottom of the device (the glass slide). The device was then scanned with an epifluorescence microscope looking for fluorescent yeast cells, using their fluorescence, size and morphology to differentiate them from background.

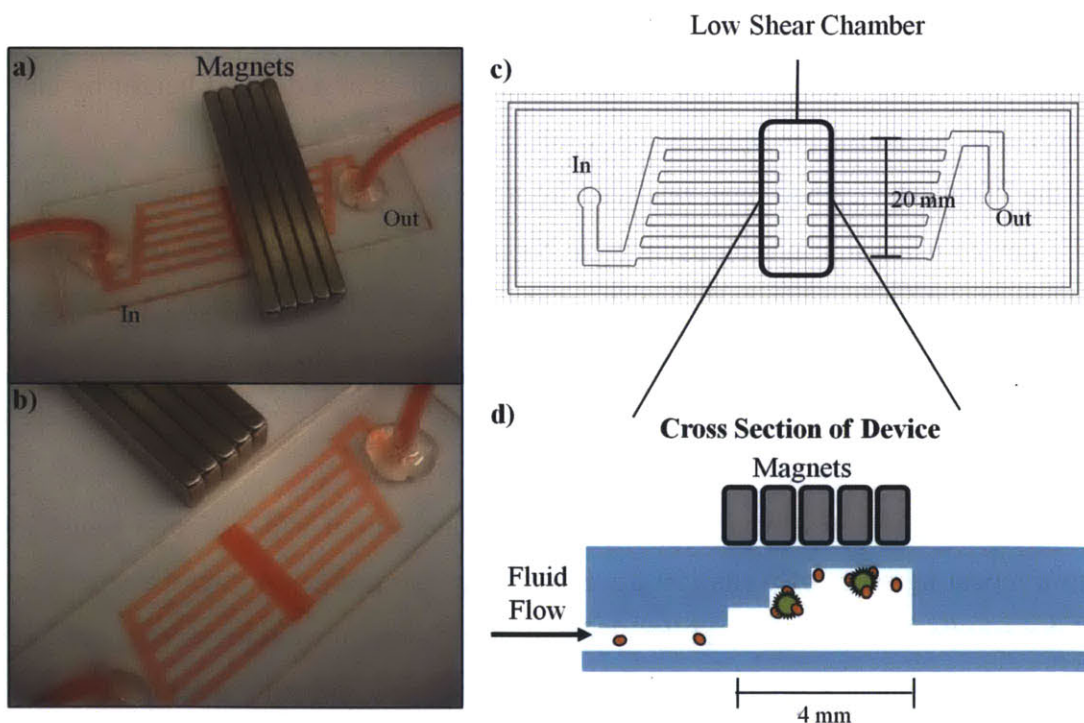


**Figure 3.2 Initial Diagnostic Prototype**

(a) Blood with magnetically bound pathogens enters the inlet port on the left, flows through the device where the magnets pull out magnetically tagged pathogens in a low shear chamber and the blood is then removed through the outlet. (b) Device with the magnet removed (c) Schematic

of device showing location of the low shear chamber (d) Cross-section of low shear chamber: beads and tagged pathogens enter the chamber and are pulled up the ceiling of the chamber where they are retained

### 3.2.3 Mass Balance Study

To determine where the pathogens were going in the device, I performed a set of mass balance experiments to check for non-specific adhesion, pathogen capture and optical detection of pathogens. This testing was done using 850 cell aliquots of GFP transfected *C. albicans*, donated by Brown et al [123], metered out using a FACS Aria cytometer (BD) to obtain very accurate pathogen counts in each aliquot.

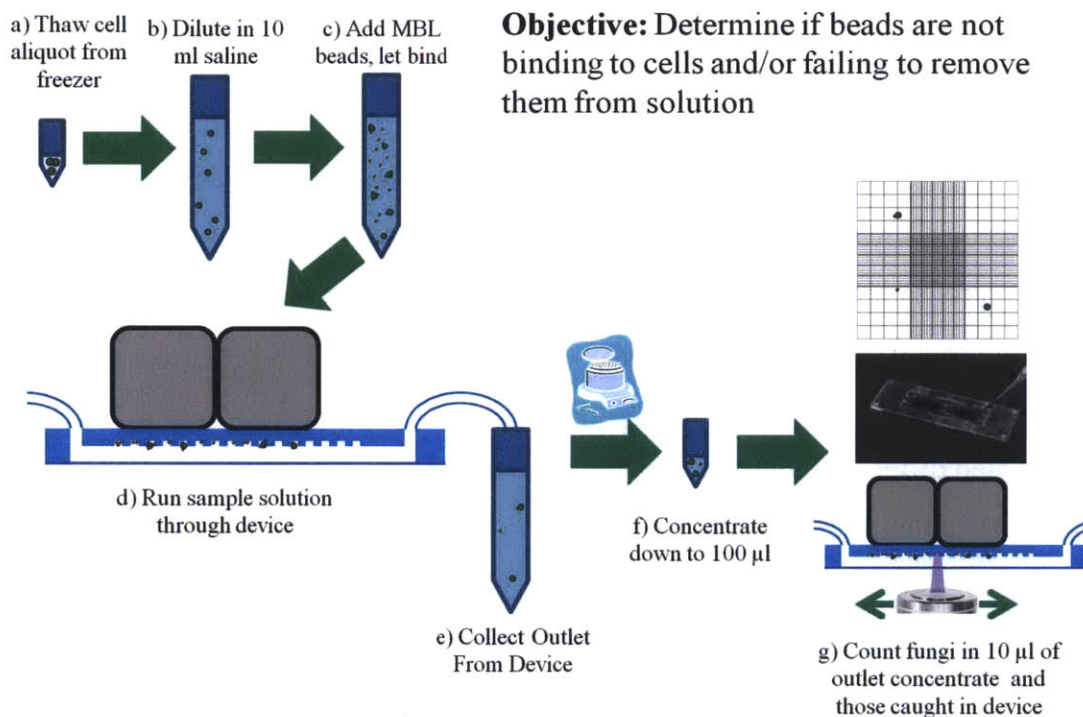


Figure 3.3 Initial Diagnostic Prototype

(a) 850 fungi aliquot is removed from cryostorage (b) Fungi are diluted in 10 ml of saline (c) WtMBL beads are added and given time to bind (d) fluid sample is run through the device and the number of detected pathogens determined by scanning over the low shear chamber using epifluorescence microscope. The positive control sample bypasses this step (e) Outlet fluid from the device is collected (f) Outlet fluid is centrifuged and aspirated down to 100 µl (g) The number of pathogens not captured in the device is determined using hemocytometer to count number of fungi in the outlet fluid and comparing that to the positive control. Non-specific adhesion to the device surfaces was assessed using this same system except that WtMBL beads were not added, so any fungi binding was due to attachment to the surfaces. Countess chip image reprinted from [149].

These tests were performed in saline. To determine the concentration in samples after testing, each sample was spun for 10 minutes at maximum speed in the centrifuge and then the liquid was aspirated so that only 100  $\mu$ l remained, in which all the fungi were resuspended and their concentration determined by manually counting the number of fluorescent fungi in 10  $\mu$ l of that fluid using a hemocytometer chip (from the Countess Machine, Invitrogen). This method allowed us to accurately quantify a physiologically relevant number of pathogens in the system for these tests.

I ran the entire system without magnetic beads to check for adhesion of the pathogens to the surfaces of the tubing or device and compared the count to control samples not passed through the device. For evaluating pathogen capture vs. detection, I ran the system with magnetic beads this time (40  $\mu$ g 1  $\mu$ m WtMBL beads/ml). I then used a microscope to scan over the device and determine the number of pathogens optically detected and evaluated the number of pathogens not captured in the device by checking the outlet fluid for fungi. Both of these counts were compared to a positive control sample that was not passed through the device to determine what fraction of the fungi were detected and what fraction were lost in the waste (**figure 3.3**).

#### **3.2.4 Magnetic Flux Concentration Characterization**

I evaluated different geometries for the MFC with Dan Leslie and Karel Domansky using finite element modeling in COMSOL to analyze the magnitude of the magnetic gradient created by each magnet and Permalloy configuration. The magnetic flux concentrator was designed in SolidWorks and CNC-machined from EFI alloy 79 (Ed Fagan, Inc.) The alloy has maximum relative permeability of 230,000 and saturation induction of 8700 Gauss. The MFC was employed to alter the field generated by a 3/4" neodymium cube magnet (K&J Magnetics) and a non-magnetic polysulfone holder was used to keep the MFC and the magnet correctly positioned relative to each other. The MFC is composed of a single bar of the EFI permalloy 5 mm wide, 1.55 mm thick and 25 mm long. The front end is tapered to a wedge in order to decrease the initial magnetic field gradient spike produced by the magnet. The remaining area of the MFC has 400  $\mu$ m deep and wide grooves with 800  $\mu$ m center-to-center spacing. These grooves create places where the magnetic field lines diverge outwards periodically, resulting in the high magnetic field gradient zones required for bead capture. Finite element modeling results were validated by securing a Hall magnetic probe to a motorized xyz positioning system and scanning



it 500  $\mu\text{m}$  above the MFC surface to measure the magnetic field produced by the MFC and magnet.

### 3.2.5 Bead Isolation

The efficiency of magnetic bead isolation with the MFC and microfluidic flow cell was tested by running a 10 ml water sample through the device containing 5  $\mu\text{g}$  1  $\mu\text{m}$  beads/ml. The sample solution was agitated with a thermomixer (Eppendorf) to prevent bead settling while a peristaltic pump (Ismatec) pulled liquid through the device at 10 ml/hr. Photographs of the bead distribution in the micropatterned device were obtained on a trans-illumination microscope after the magnet and MFC had been removed and the bead concentration in the outlet was analyzed with a BD Fortessa flow cytometer to determine the fraction of magnetic beads removed by the device.

### 3.2.6 Running the Diagnostic Device

The efficiency of the combined MFC and microfluidic device was determined by detecting 850 GFP positive *C. albicans* (counted out using FACS) added to either 10 ml of saline (TBS-Tween 20 with 5 mM calcium) or in 5ml of human blood diluted with 5 ml of TBS-Tween (maintained at 4°C during assay). For experiments using pre-bound fungi, the fungi were resuspended in 1 ml of TBS-Tween 20 with 5 mM calcium chloride and 50  $\mu\text{g}$  FcMBL beads then mixed for 20 minutes before adding to 5 ml of blood and 4 ml of TBS-Tween to create the 10 ml sample. For direct capture in blood, we added the fungi and beads directly to a mix of 5ml of blood and 5 ml of TBS-Tween 20, without any pre-binding time, and gave 20 minutes of mixing to bind the pathogens in the diluted blood.

Calcofluor white (25  $\mu\text{M}$ ) was added to the sample to stain the fungal cell walls. Blood was collected from healthy human volunteers into heparin vacutainers (BD). The fungi were bound using 1  $\mu\text{g}$  of 1  $\mu\text{m}$  beads/ $\mu\text{l}$  in saline or 5  $\mu\text{g}$  of 1  $\mu\text{m}$  beads/ $\mu\text{l}$  in blood. After binding the sample was placed in thermomixer (Eppendorf) and pulled through the device at 10 ml/hr using a syringe pump (Harvard Apparatus) equipped with a 20 ml syringe (**figure 3.4**). After the 10 ml sample had been run, a 3 ml wash for saline. For blood, I added a 2 ml wash (for blood) of TBS-Tween 20, followed by a 1 ml wash containing 1% Triton X-100 and a final 2 ml TBS-Tween 20 wash through the device. The Triton X-100 lysed any residual red blood cells trapped in the device. Detection efficiency was determined by manually scanning over the device at 200x with

an epifluorescence microscope (Leica) looking for cells with an overlapping calcofluor and GFP signature.

Tests in saline with several different bead concentrations were done to study the relation between pathogen detection and bead concentration. Samples were run with 560  $\mu\text{m}$  high channel without micropatterning (performed before bead isolation studies to optimize channel design) with bead concentrations ranging from 1 to 2.5  $\mu\text{g}$  1  $\mu\text{m}$  WtMBL beads/ ml in 10 ml of calcium buffer with one 850 *C. albicans* aliquot added.

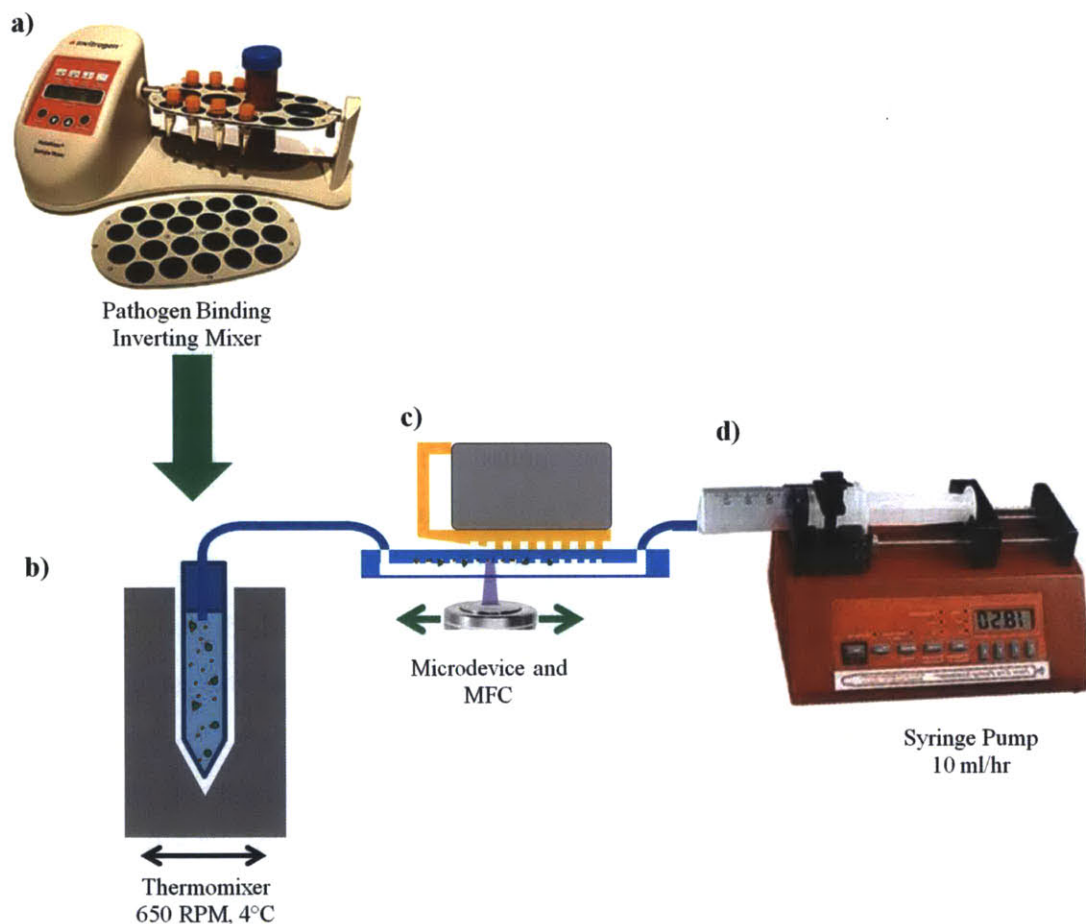


**Figure 3.4 Experimental Layout of Optical Diagnostic System**

(a) MBL beads were added to the samples and mixed for 20 minutes in an inverting Hula Mixer (Invitrogen). Hula Mixer image reprinted from [150] (b) Then the fluid sample is placed in the thermomixer, which agitates it to keep the beads and pathogens suspended and cools the sample to minimize phagocytosis. A sip tube takes fluid from the sample tube and pulls it through the microdevice with the magnet and MFC in place (c) where the magnetic beads and magnetically tagged pathogens are retained. A syringe pump (d) with a 20 ml syringe withdraws at 10 ml/hr, pulling fluid through the system. When the sample has finished running, 5 ml of wash buffer is added to the sample tube in the thermomixer (b) and pulled through the device, washing any

remaining pathogens into the microdevice and clearing the blood out of the tubing for imaging. Syringe pump image reprinted from.[151]

### 3.2.7 Automated Detection

A biotinylated anti-*Candida albicans* antibody (Abcam) was labeled with Cy3 streptavidin (Invitrogen) and diluted to 1/200 in TBS-Tween 20 with 1% bovine serum albumin for staining of fungi in the device after the washes were complete. Two milliliters of the stain was loaded into the device and then allowed to incubate for 30 minutes with the pump stopped before the excess dye was washed out with TBS-Tween 20 and 1% BSA, giving a simple and effective method to immunofluorescently label pathogens captured in the device.

Working with Abhishek Jain, we placed the device with the magnet on an Axio Observer Z1 microscope (Zeiss) and employed the 10X objective to photograph the entire capture region of the device. Metamorphosis image acquisition software controlled the scanning and prepared a composite of all the acquired images. We then used the MATLAB Image Processing Tool commands to binarize the image after background removal for automated cell counting. Sensitivity analysis was done with pathogen numbers in the sample ranging from 0-850 fungi and compared with manual counting of the same sample.

## 3.3 Results

### 3.3.1 Initial Prototypes and Mass Balance Experiment

The initial diagnostic prototype was relatively simple, mainly consisting of channels to split flow into a central low shear chamber over which the magnets were placed (**figure 3.2**). The beads were collected in this low shear chamber from a 10 ml fluid sample. The beads were then spread along the bottom of the chamber using the magnet and imaged. This system was able to efficiently concentrate pathogens out of the sample, with less than 2% of the fungi added escaping into the outlet fluid. But, the detection with this system was very low; detecting less than 15% of the fungi in the device from saline (**figure 3.5 a-b**) and less than 3% in bank blood (**figure 3.5 c-d**). The primary problem was that the device could not efficiently visualize the pathogens because they were being buried and obscured by the excess opaque beads required for timely binding of the rare pathogens. This resulted in low detection rates in both saline and a blood equivalent (red blood cells at 40% hematocrit) (**figure 3.5**). I could see the beads forming a dense pile under the upstream edge of the magnet inside the device that light from the epifluorescence microscope could not penetrate (**figure 3.6**). We concluded that to improve

pathogen detection, the beads and magnetically tagged pathogens needed to be spread thinly enough so that I could image fluorescent cells through them. This would require us to balance the magnetic and convective forces on the particles in the microdevice to maximize the bead spread while still removing all the tagged pathogens.

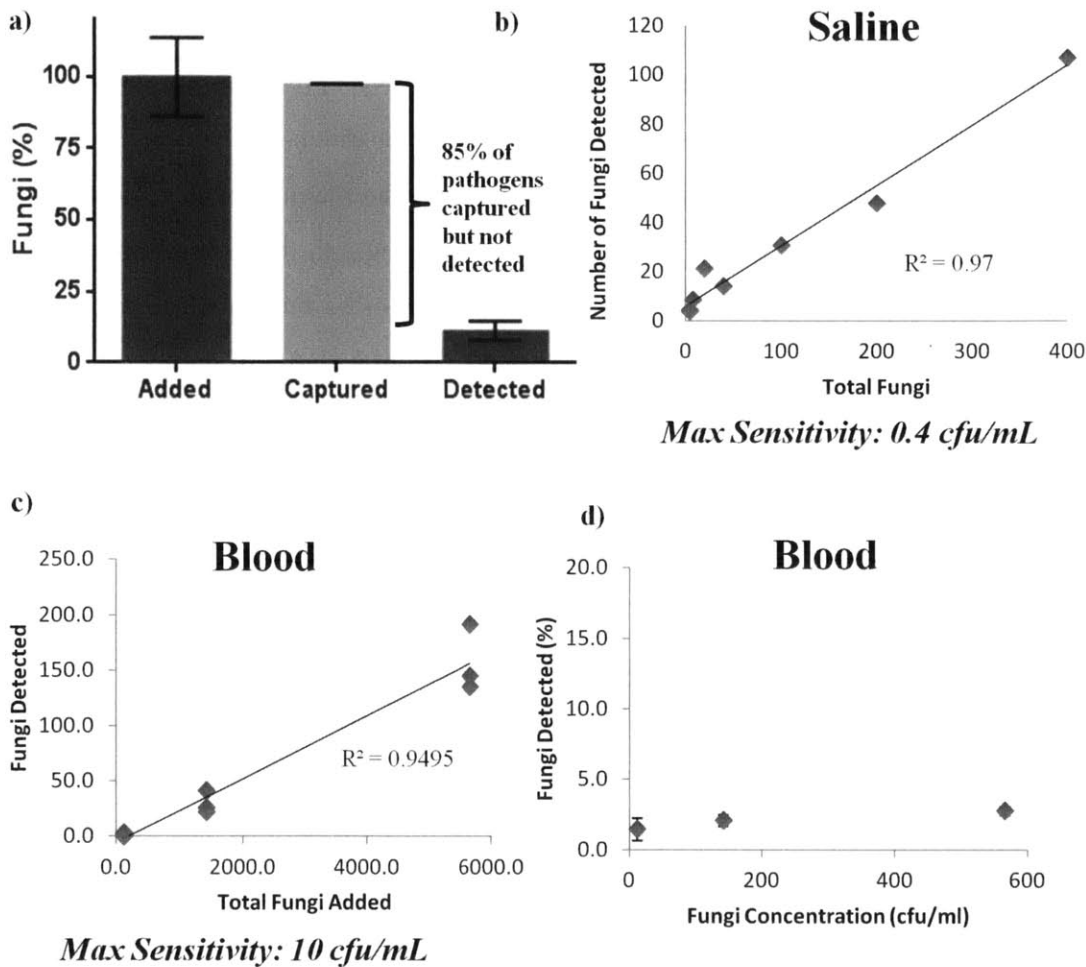
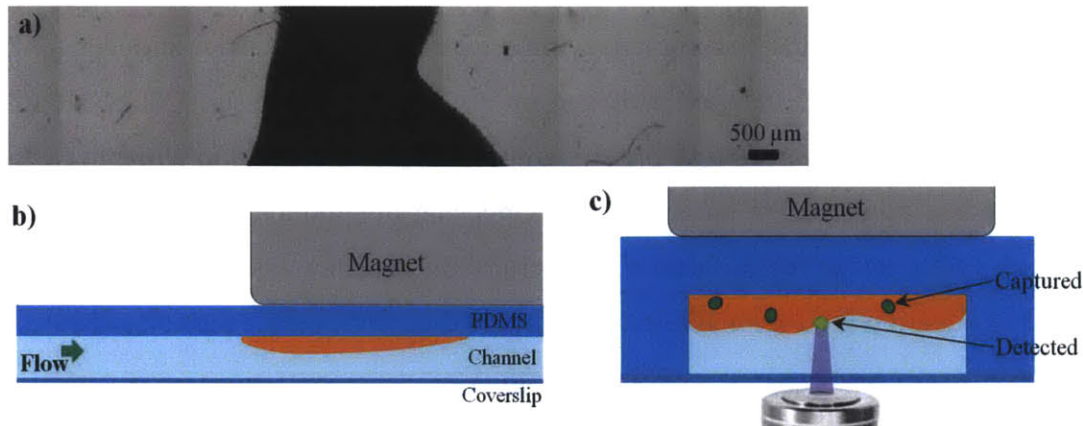


Figure 3.5 Results from early device prototypes

(a) Data from initial prototype: This device could capture 98% of the pathogens from the saline but out only optically detect 13%, leaving 85% of the pathogens captured in the device but impossible to visualize because they were buried under a dense pile of opaque beads (b) Detection of *C. albicans* in saline using early device with WtMBL beads: Despite only being able to detect a small fraction of the cells, there was a good correlation between total pathogen count and detected pathogen count, suggesting this could be used for a quantitative readout. (c,d) Detection of *C. albicans* in Blood Bank blood using early device with WtMBL beads: detection of fungi in the blood bank blood was even lower, typically only detecting between 2-3% of the

pathogens added to the sample, although the correlation between total number and the number detected still appeared consistent



*Figure 3.6 Problem with magnetic beads and optical detection (a) Stacked Image of bead pileup in channel: In most systems, the beads pile up at the edge of the magnet, forming the dense pile seen in the channel of one of our early prototypes, burying most of the captured pathogens and make optical detection difficult. (b) Device cross section parallel to flow showing bead pile relative to magnet. The preferentially pile under the edge of the magnet where there is a high magnetic field gradient (c) Device cross section perpendicular to flow showing pathogens buried in the bead pack. Many are captured but only those near the surface can be detected with epifluorescence microscopy*

### 3.3.2 Separation Theory

Manipulating magnetic beads in fluid to obtain a desired distribution is a complex problem with several different factors that must be taken into account, including convection, fluidic drag, magnetic forces and aggregation behavior. The superparamagnetic beads employed in our system contain nanometer-sized, single-domain  $\text{Fe}_3\text{O}_4$  crystals embedded in a polymer matrix [142]. These  $\text{Fe}_3\text{O}_4$  particles become strongly magnetized in the presence of an applied magnetic field but no remnant magnetization remains once the field is removed [152].

The magnetic force on magnetic bead (where  $\mu$  is a point-like magnetic dipole) simplifies down to equation 3.1 where  $\mathbf{F}_m$  is the magnetic force vector,  $N$  is the number of beads attached and  $\mathbf{B}$  is the applied magnetic field [152]. In one dimension this relation simplifies down to equation 3.2 with the force directed parallel to the local magnetic field lines.

$$\vec{\mathbf{F}}_m = N(\mu \cdot \nabla)\vec{\mathbf{B}} \quad (3.1)$$

$$F_m \propto N\mu \frac{\partial B}{\partial x}$$

(3.2)

As the magnetically tagged pathogen enters and flows along the length of the microdevice, it comes into close proximity with the external magnet, which induces a magnetic force in the bead that pulls the tagged pathogen up to the ceiling. The strength of the magnetic dipole induced in the beads varies with the strength of the magnetic field in a manner which can be approximated as a hyperbolic tangent [142]. Opposing this motion is the fluidic drag force (**figure 3.7 a**). In the microdevice, like other microfluidic systems, viscous forces dominate, so the Stokes drag equation is a reasonable estimate of the drag force on the particles [133]:

$$F_d = 6\pi\eta r v_s \quad (3.3)$$

Where  $F_d$  is the drag force,  $\eta$  is the fluid viscosity,  $r$  is the particle radius and  $v_s$  is the magnetically-induced settling velocity at which the particle is moving toward the ceiling. If we assume that the channel height is much greater than  $r$  and that the magnetic movement of the dilute beads and pathogens does not affect the bulk fluid flow, we can neglect the shear induced lift forces on the particle and assume that the forces caused by convection are directed parallel to the streamlines. This means the settling of the bead in the chamber can be treated as roughly one dimensional, moving the magnetic particle from the channel up to the ceiling of the chamber. The horizontal flow towards the outlet sets a time limit on how long this settling has to occur before the tagged pathogens are carried away from the magnet and the magnetic force drops to zero (meaning the pathogen was not removed and is lost in the waste fluid). We can equate 3.2 and 3.3 to estimate that vertical separation velocity ( $v_s$ ):

$$v_s \propto \frac{N\mu \frac{\partial B}{\partial x}}{6\pi\eta r} \quad (3.4)$$

Exactly determining the settling velocity is actually somewhat more complicated, because of the complexity of the magnetic field, the variation of the magnetic dipole ( $\mu$ ) with the magnetic field and the tendency of the beads to stochastically start aggregating when they are magnetized, but the equation above represents the basic behavior.

But getting the magnetically tagged pathogen up to the ceiling of the channel is only part of the problem, once it's there it must be held in place to control the final spread of the beads and tagged pathogens for imaging (**figure 3.7 b**). The main difficulty here is that the magnetic force

is primarily vertical while the shear induced drag force trying to push the pathogen downstream is primarily horizontal. The diverging magnetic field lines at the edge of a bar magnet have some horizontal components, which can help hold the beads in these places. The main problem is that the majority of magnetic particles are pushed to these points, forming the dense piles that lower the detection rate of the pathogen.

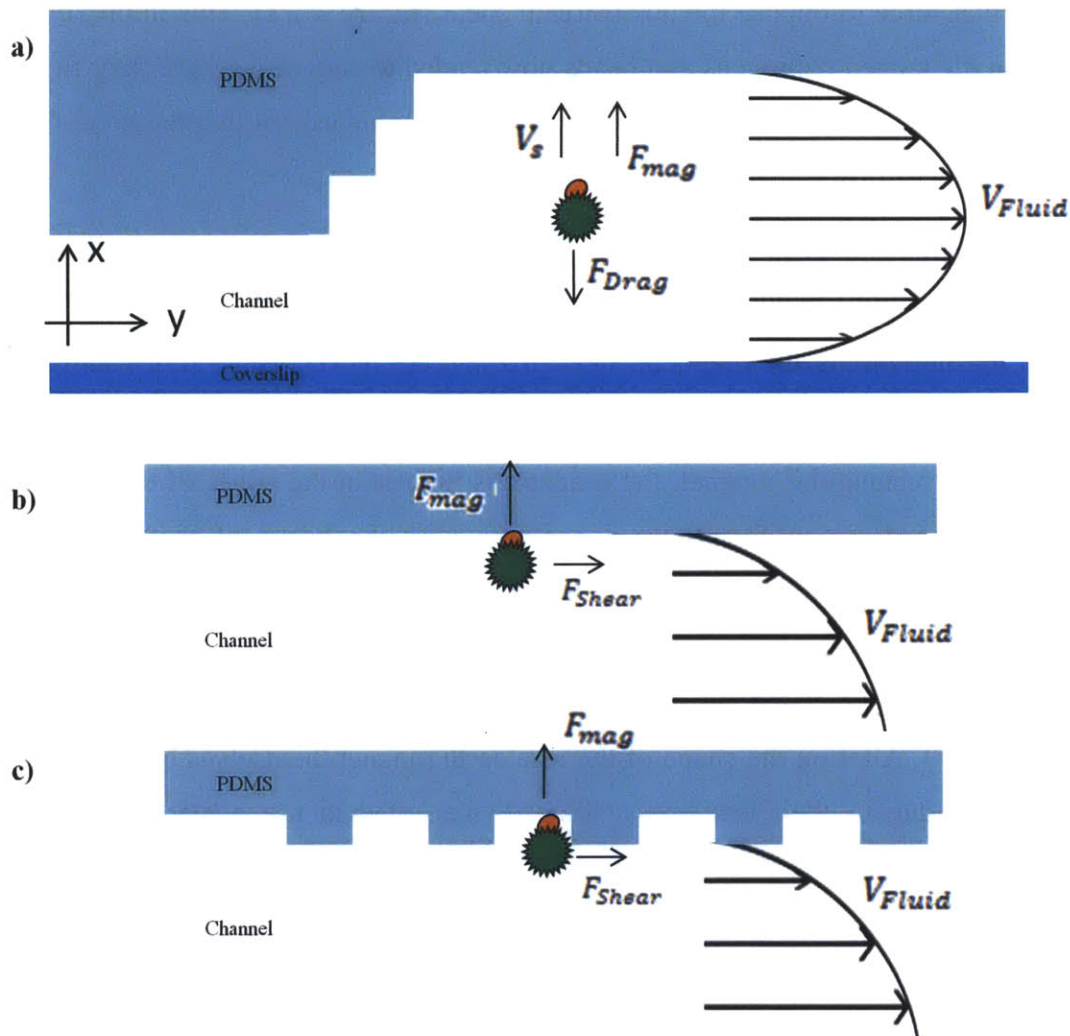


Figure 3.7 Forces at work during the separation process

(a) Pulling magnetically tagged pathogen up to the ceiling of the chamber: The magnetic force pulls the pathogen up towards the ceiling and the permanent magnet as fluid convection pushes the pathogen parallel to the ceiling. Opposing the magnetic force is the Stokes drag on the particle. The balance of these two forces results in a settling velocity ( $v_s$ ) towards the ceiling of the capture chamber. The pathogen must move upward quickly enough to reach the ceiling of the channel before it swept out of the device by the bulk fluid flow (b) Forces at work on the chamber ceiling: The primarily vertical magnetic force can do little to oppose the fluidic drag trying to move the pathogen downstream, either pushing it to a point where there is enough

*horizontal magnetic force (usually at the edge of the magnet, or pushing the tagged pathogen all the way to the outlet and into the waste. Normal force not shown. (c) Solution to horizontal drag: introducing micro features such as wells into the channel ceiling provides a normal force that can oppose the downstream drag, preventing the beads from being pushed into dense piles at the magnet edge or lost in the waste. Normal force not shown.*

Micropatterning the channel ceiling with wells provided a simple way to create a horizontal normal force to oppose the downstream shear (**figure 3.7 c**). This improved the bead spread because the tagged pathogens and beads now tended to stay near where they first reached the ceiling of the channel, but this did little to solve the problem with the magnetic field being poorly suited for a uniform spread of the magnetic particles.

### 3.3.3 Altering the Magnetic Field

Based on these empirical and theoretical results, an efficient way of manipulating the tagged pathogens is by modulating the magnetic field gradient ( $\frac{\partial B}{\partial x}$  in 1D,  $\nabla B$  in 3D). I chose to work with permanent neodymium magnets rather than electromagnets to avoid problems with overheating. For a rectangular magnet, the gradient is highest at the edges of the magnet which causes magnetic beads to preferentially congregate near the edges of the magnet, making detection of tagged cells difficult. Spreading the beads over a larger area required a more appropriate distribution of high magnetic field gradient zones. The shape and strength of a field created by a magnet is dictated by its shape, material and the presence of nearby magnetic materials (like iron). Altering the shape of the rare earth magnet themselves by CNC machining was not practical due to their brittleness. Instead, we opted to use a piece of ferromagnetic material in close proximity to the magnet to alter the field (**figure 3.8**), in much the same way that a ferromagnetic core alters the shape of field from an electromagnet [72]. The advantage of this approach is that ferromagnetic materials are readily machinable, so shaping them is much simpler. This magnetic flux concentrator can then be placed between the permanent magnet and microdevice to control  $\nabla B$ .



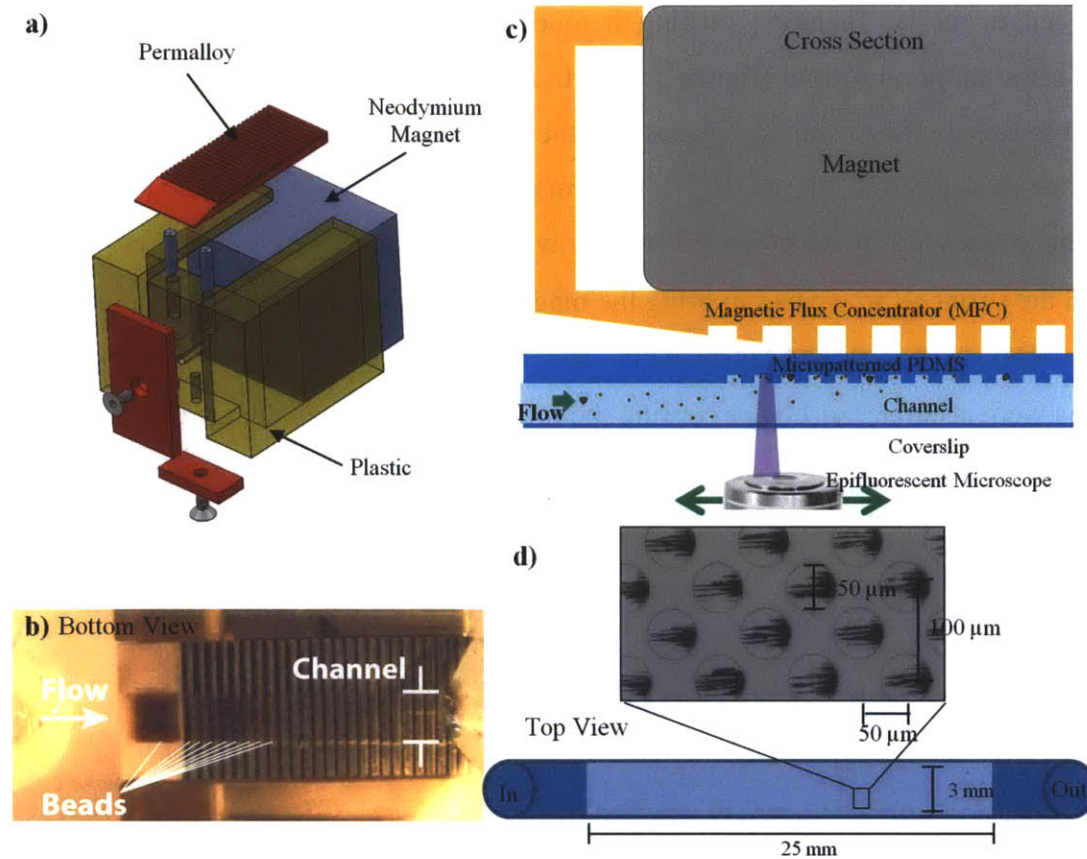


*Figure 3.8 Layout of MFC and microfluidic device*

(a) Magnetic flux concentrator made out of permalloy (red), Neodymium Magnet (grey) and plastic casing (yellow), forming a single, simple to use unit for capturing and displaying magnetic beads and tagged pathogens (b) Image of beads captured in the system, spread into a thin layer by the presence of the MFC (c) Cross section of the entire system, showing orientation of the magnet, MFC and channel relative to each other (not to scale). (d) Top view of the microfluidic channel layout with close up shot of magnetic beads captured in the microwells molded into the channel ceiling. The dimensions and spacing of the microwells is indicated on the diagram.

To determine the optimal shape for this magnetic flux concentrator (MFC), I worked with Dan Leslie and Karel Domansky to create a finite element model in COMSOL that accounted for the magnetic saturation of the concentrator material and evaluated a range of geometrical features machined into the MFC and the magnetic gradient each produced. Tapering the leading edge of the MFC reduced the number of field lines passing through this area, which had the net effect of decreasing the gradient spike at the edge of the magnet so that the beads no longer formed a dense pile in this area. Machining a washboard-like structure into the MFC created many high gradient zones above the microfluidic channel, which boosted the net field gradient

along the length of the chamber, making it much more uniform and helping the beads and pathogens settle more uniformly (**figure 3.9 a**). In addition, we have also linked the two poles of the magnet to reduce the forwards projection of the field and decrease possible inference with the beads before they reached the device. The primary limitation the MFC is that the beneficial effect of the washboard in the drops off rapidly with distance (having little effect over 700  $\mu\text{m}$  away from the surface), so we had to bring the magnet as close to the capture channel as possible (300  $\mu\text{m}$ ). Dan and Karel's experimental measurement of the field confirmed that our simulations were accurate, so I began testing the most promising magnet and MFC combinations with the microfluidic device.

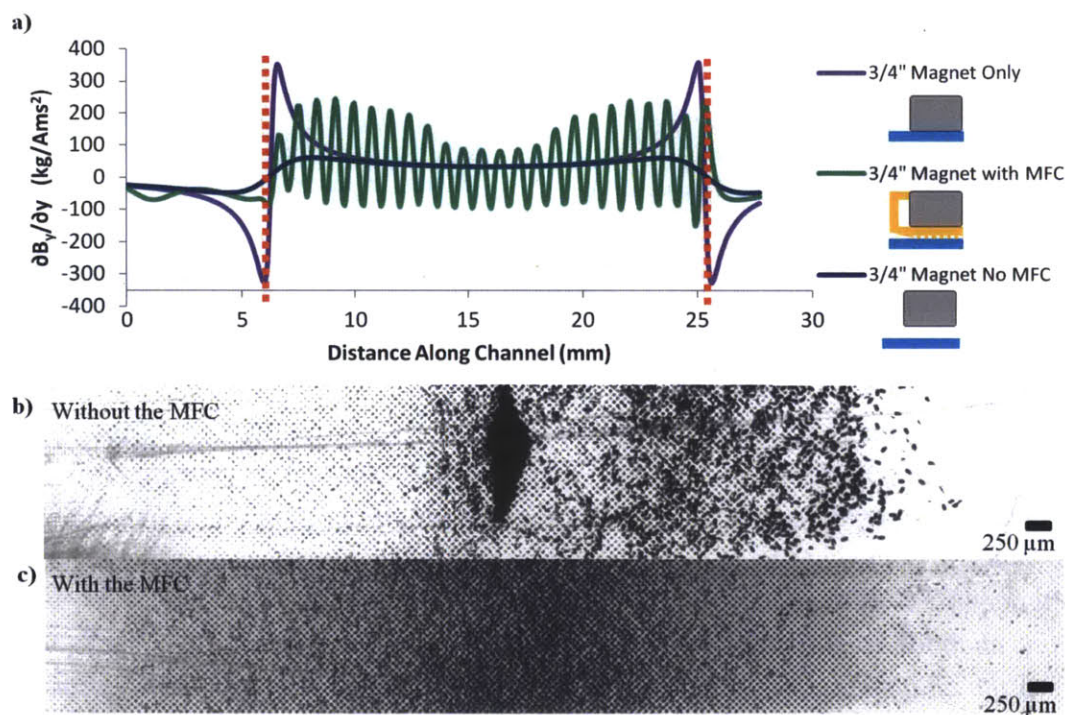


**Figure 3.9** Characterization of the MFC

(a) Magnetic gradient in the channel for different magnetic configurations: Purple represents the magnet alone, showing the large gradient spike that causes the beads to pile up at the upstream edge of the magnet (dotted red line marks the edges of the magnet). Green line shows the improved gradient created by the MFC, resulting in much more even distribution of gradient. The peaks of the sinusoidal pattern correspond to the teeth of washboard in the MFC. Blue shows the gradient produced by the negative control (magnet positioned above the PDMS but without MFC). Cartoons under each label show the orientation of the magnet and MFC relative to the PDMS. (b) Spread of beads produced by the magnet alone, with large number of beads piling up at the forward edge of the edge regardless of the micropatterned wells (c) Spread of

*beads with the MFC in place, much better distribution, making it possible to directly image fluorescent cells among the beads*

### **3.3.4 MFC Characterization**

Altering the magnetic field with the MFC allowed me to spread the beads in the channel much more effectively than was possible with the magnet and channel dimensions alone. I experimented with different channel dimensions to optimize spreading the 1  $\mu\text{m}$  magnetic beads into a thin layer so that I could image the fluorescently labeled pathogens among them while still ensuring removal of more than 99% of the magnetic particles from the flow (**figure 3.9 b-c**). Overall I found that a 280  $\mu\text{m}$  high by 3 mm wide channel gave the best results, which gave a wide enough cross section to operate at 10 ml/hr while minimizing bead capture variation across the width of the channel, which was a problem with taller channels. With these dimensions, I could pull reliably pull the magnetic beads up to the ceiling of the channel and had tuned the magnetic and drag forces so that the beads only stopped moving if they settled into one of the microwells, producing a much more uniform, planar pathogen distribution that could be easily scanned over with a microscope.

The bead spread was best with the MFC in place, although the spread was also acceptable if the MFC was removed from the plastic holder (preserving the spacing of the magnet above the device), but the strength of the magnetic gradient in the channel was much weaker with this configuration. These initial experiments were conducted with 1  $\mu\text{m}$  beads only, so I suspected that that without the MFC to focus the field, the magnet in the plastic holder would not exert enough force on the beads to capture the larger magnetically tagged pathogens. The magnetically tagged pathogens would experience a similar amount of magnetic force to the beads but a higher Stokes drag due to their larger size and would therefore need either a stronger magnetic field gradient or a longer channel for effective capture [133]. To see if this was the case, I began testing the system with both beads and pathogens.

### **3.3.5 Detection of Pathogens**

In the microdevice, there is a trade off between ensuring complete binding of the pathogens and optical detection. With too many FcMBL beads in the sample, the captured pathogens are much more likely to be buried. With too few beads added to the sample, pathogen capture is incomplete, so there are unbound pathogens that are not retained in the device. In saline I found the best balance between these two opposing factors as 2  $\mu\text{g}$  1 $\mu\text{m}$  beads/ml (**figure 3.10**), using

more or less beads caused the detection rate to decrease. However, I had to increase the bead concentration up to 10  $\mu\text{g}$  1  $\mu\text{m}$  beads/ml for adequate capture in the blood.

Binding and detection of fungi directly in blood proved variable because we were still optimizing pathogen capture. With the MFC, I could detect up to 34%  $\pm$  8% fungi spiked into the blood. Using the magnet alone, I detected 25%  $\pm$  8% of the pathogens in blood, but could not show a significant difference between the two due to the variability of pathogen binding in blood, leading to large error bars for both configurations (**figure 3.11 a**).

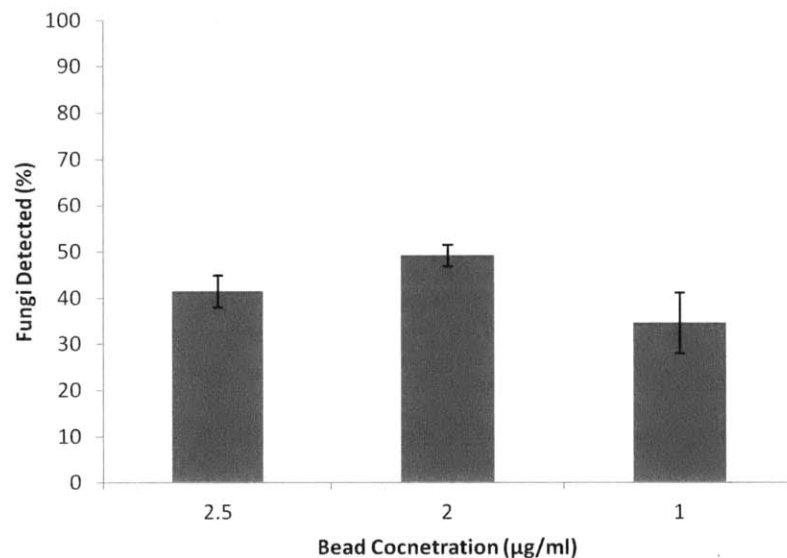


*Figure 3.10 Detection of *C. albicans* in microdevice vs. bead concentration*

*Because the opaque microbeads can obscure the pathogens in the sample, I tried to minimize the amount of beads used. At too high of a bead concentration, the excess beads tend to bury more of the pathogens, but if the bead concentration in the sample is too low, not all of the pathogens were bound, resulting in lower capture and detection.*

To get a better look at pathogen detection with the device, I removed the initial binding as a factor in the system by attaching magnetic beads to the pathogens before they were spiked into donor blood. I found that I could detect significantly more fungi in saline with the MFC ( $\alpha=0.05$ ) compared to the magnet only or the magnet in the plastic MFC holder. With the magnet directly on the PDMS, the beads still formed a pile under the upstream edge that buried a large fraction of the fungi so that I could only detect 47%  $\pm$  1% of the *C. albicans* seeded into a 10 ml saline volume (**figure 3.11 b**). With the magnet in the MFC plastic holder (negative control), detection was slightly better at 52%  $\pm$  4% of the fungi. With this configuration, tagged fungi were captured right up to the downstream edge of the magnet, consistent with my hypothesis that the weaker magnetic field gradient produced by this configuration was insufficient to capture all the tagged

fungi from the flowing sample. Adding the magnetic flux concentrator boosted the detection up to 68% ± 4% of the 850 fungi added to a 10 ml volume of saline, significantly better than the magnet only configuration.

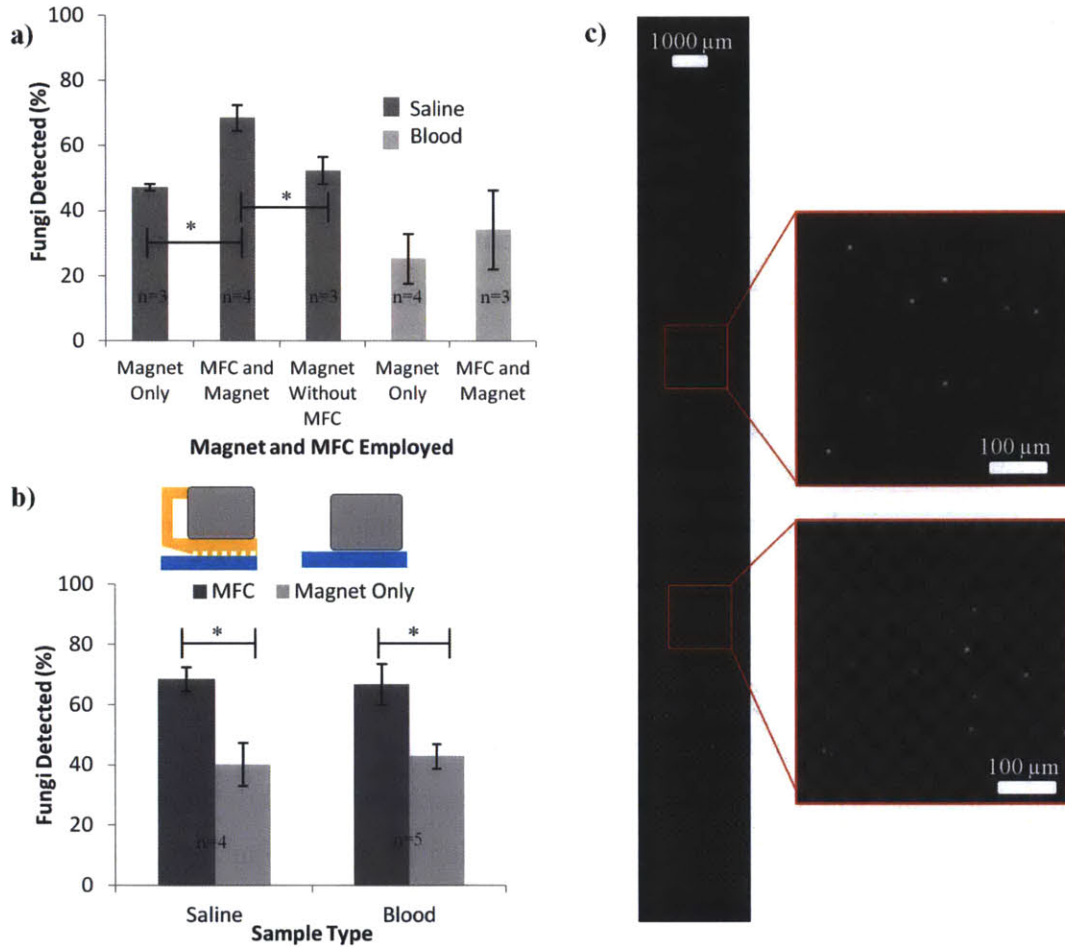


**Figure 3.11 Detection of *C. albicans* in Saline and Blood**  
 (a) Binding and Detection of *C. albicans* in Saline and Blood in simulated septic sample. Magnet with MFC performs significantly better ( $\alpha=0.05$ ) than either magnet only configuration, detecting 68% of the fungi added to a 10 ml saline sample. The system can detect up to 34% of the fungi in blood. Large error bars in blood result from binding variability in blood from different donors. (b) Comparison of detection with and without MFC in both saline and blood. Significantly better detection of pathogens in both saline and blood with MFC when the initial binding is ignored ( $\alpha=0.05$ , error bars exp. Error). Detection levels in blood and saline are almost equivalent with pre-bound pathogens, showing that this system can significantly boost optical detection of magnetically tagged pathogens. (c) Image of immunofluorescent stained *C. albicans* assembled from automated scan of microdevice: In the enlarged pictures, individual pathogens in the microwells can be seen.

In the blood (diluted 1:1 with saline) with pre-bound fungi, I confirmed that combining the

magnet with and MFC significantly improved detection of captured fungi in the device ( $\alpha=0.05$ ). I could detect up to  $67\% \pm 7\%$  of the pathogens added to the sample, nearly equivalent to the detection rate in saline. Using the magnet alone to pull out tagged fungi, I could only detect  $43\% \pm 4\%$  of the pathogens added to the sample. The spread of the beads in blood was similar to that seen in saline, with the magnet only causing a pile of beads at the leading edge of the magnet which could have definitely buried some of the tagged fungi while the spread with the MFC was much more even, with beads and cells captured almost exclusively in the micropatterned wells. The high detection rate in blood means that the system could pick up fungal concentrations down to 1 cfu/ml, which would translate to visualizing 3 out of the 5 total pathogens in the 5 ml blood sample (10 ml after dilution).

### **3.3.6 Automated Counting**

By using the MFC to spread the beads out more evenly in the channel, I was able to place all the pathogens in a single focal plane, greatly facilitating automated scanning of the captured pathogens. These fluorescent images obtained from this scanning were stitched back together and fed into an automated counting program that Abhishek Jain designed (**figure 3.11 c**). By manually and automatically counting the same microdevice, we found that once the thresholding values on the program had been set correctly, the automatic program was able to correctly quantify the pathogens within  $\pm 10\%$  of the manual count and correctly detect when no fungi were present in the device. The only downside to using an fluorescent detection method was getting a specific stain bright enough for detection, given our current image processing program. Calcofluor worked well in both blood and saline, but the immunofluorescent staining had a much weaker signal intensity in blood. More advanced image processing techniques would increase the flexibility of automated counting system by analyzing the pathogen shape and size as well.

## **3.4 Discussion**

I have developed a simple microfluidic system using the general magnetic opsonins and shown that it can magnetically opsonize and visualize up to  $67\%$  of the fungi from blood in less than three hours, more than 20 times better than my initial prototype. This system can detect down to 1 fungus/ml in human blood, making it potentially useful as a rapid sepsis diagnostic for fungemia. The tagged pathogens can then be concentrated in a microdevice, increasing the pathogen density to the point where they can be directly detected.

Fabrication of the device proved difficult because I was trying to combine millimeter scale channels with micropatterned features on the ceiling of the channel. The SU-8 photoresist used to create most soft lithography molds can usually only create tall 100  $\mu\text{m}$  features while the channel employed in my device was 280  $\mu\text{m}$  tall. Deep reactive ion etching (DRIE) could be used to create such a mold, but it is an expensive process, requiring special photolithography masks and fabrication equipment, making it unsuitable for rapid device prototyping [153]. Instead I used Mylar channels (created with the plotter cutter) and then combined these with micropatterned PDMS (made with traditional soft lithography methods) to produce a hybrid device that I cast in epoxy to make the actual device mold [154]. This gave me a rapid, inexpensive way to produce the devices with the proper combination of dimensions that the system required.

The typical magnetic field created by a block magnet has a strong gradient spike near its edges, which caused the excess magnetic beads in the channel to form a dense pile that obscured the captured fungi. Introducing a MFC made of a ferromagnetic material allowed us to redirect the magnetic field lines and alter the gradient creating the magnetic force on the FcMBL beads. Various other groups have employed electromagnets with custom pole pieces or microfabricated electromagnets inside of the device to achieve a similar purpose [72, 155]. These approaches work well, but I calculated the power draw required for an electromagnet to maintain a field comparable to the permanent magnets I was employing would rapidly overheat, so we opted for a simpler, more reusable approach. Simulations of different MFC shapes allowed us to find a suitable design and experimental measurements confirmed that the simulations matched well with reality. I found that the MFC did greatly improve the spread of the magnetic beads in the microdevice, although the fluid convection in the channel needed to be optimized as well to correctly balance the drag and magnetic pull on the particles.

I employed the conditions I had previously found to give good pathogen binding in blood, although there was a tradeoff between pathogen detection and higher beads concentrations, so I compromised and used 5  $\mu\text{g}$  of 1  $\mu\text{m}$  FcMBL/ml sample. Despite this, the variability of pathogen binding in blood was still making it difficult to confirm what effect the MFC was having on pathogen detection, so I switched to attaching the beads to fungi before they were added to the blood to focus only on the detection. This allowed me to confirm that adding

the MFC into the system significantly improved detection over a device without a MFC to modulate the magnetic field gradient created by the block magnet.

There are several methods for continuous size based separation of particles in microfluidic devices, potentially letting us use a larger bead concentration for binding and then remove the majority of excess beads before they enter the detection device. However, very few of these separation methods are capable of operating at flow rates of 10 ml/hr and their use is complicated by the non-Newtonian characteristics of blood, which makes the precise fluid behavior difficult to predict accurately enough for the separation to work [156]. Mach et al had to dilute blood to 1/10x before they could use inertial focusing for sized based separation in blood, which would increase our sample volume from 10 ml up to 50ml, greatly increasing the time required for detection [157]. Immunofluorescent staining of pathogens after they had come in contact with blood also proved difficult although it worked well in saline. Our belief is that the endogenous antibodies in the blood were blocking all the antigens on the pathogens before our staining process occurred. In future versions, we would most likely switch to using Fluorescent In Situ Hybridization (FISH) to fluorescently label the pathogens in addition to the calcofluor dye, which would not suffer from this surface blocking problem and can be used for general or species-specific identification of the pathogens [28].

The microdevice system works well for concentrating and detecting fungi bound with 1  $\mu\text{m}$  beads. But, I found it was poorly suited for the optical detection of bacteria, due to the fact the binding of 1  $\mu\text{m}$  beads to bacteria is low and the system is not optimized for capturing the smaller 128 nm beads out a flowing sample, although it should be possible to redesign the device to work with these beads. Joo Kang at the Wyss Institute has designed a system that can continuously separate bacteria tagged with the 128 nm FcMBL beads out of blood which could be adapted for optically detecting bacteria [143]. The smaller bacteria are also much harder to visualize than the fungi. For these reason, I focused on using the FcMBL beads for PCR identification of bacteria out of blood in the next chapter instead of adapting this optical detection system.

Combining the MFC with the device I developed allowed us to create a system that could detect up to 67% of the magnetically tagged fungi in either a 10 ml saline or 5 ml blood sample in less than three hours. Even when I did not prebind the fungi with beads, I was still able to detect 34% of the pathogens out of blood. This proves that the FcMBL beads can be used to pick



out fewer than 850 fungi among more than five billion human cells and, with the proper fluid and magnetic manipulation, display them for detection. The system itself is simple to run and operate, with the most expensive part being the fluorescent microscope for detection, although Daniel Levner at the Wyss has produced a comparable microscope that can be assembled for less than \$5,000, putting the price of this diagnostic system well within the range of small clinics, not just large hospitals. A simple, rapid method for detecting fungal sepsis could greatly reduce the mortality rate for this type of infection. Currently, detecting fungi in the blood stream takes 3-7 days because the organisms grow much more slowly than bacteria [158]. The antifungal medications required to treat the infection are much more toxic than antibiotics, so many clinicians prefer to have a definitive diagnosis before administering them [10, 159]. These two factors mean that patients with fungal sepsis can go for days without effective treatment, so they can progress into the late stages of sepsis, resulting in a 60% mortality rate even with the state of the art medical care [19]. The FcMBL beads combined with this detection system could offer clinicians a way to confirm or deny the presence of fungi in the blood in a matter of hours and start antifungal treatment right way, greatly increasing the patient's chances of successful treatment and a full recovery.

## **Chapter 4 PCR Detection of Bacteria**

### **4.1 Introduction**

PCR has sufficient sensitivity to detect pathogens in septic blood directly and various groups have explored using PCR, nested PCR, qPCR and multiplex PCR in both conventional benchtop and microfluidic systems to rapidly detect the presence of pathogens in blood [61]. However, these groups have encountered difficulty in realizing the full potential of this amplification method because blood contains a large amount of PCR inhibitors that interfere with the reaction and greatly reduces the sensitivity of the assay [69]. Substances such as hemoglobin, leukocyte DNA, calcium, and most anticoagulants (including EDTA and heparin) abound in blood and can completely inhibit PCR amplification, which is the main reason why no PCR sepsis diagnostic is currently approved by the FDA for clinical use [69]. A few commercial kits are available for isolating bacterial DNA out of blood, but even the best of these has a maximum sensitivity of 50 cfu/ml [29, 160]. Meanwhile, the pathogen load in septic blood may be 1 cfu/ml or fewer [16]. In this chapter, I discuss using the FcMBL beads to isolate bacteria from blood in order to boost the reliability of PCR detection in blood. I previously found in chapter 2 that commercial magnetic systems (such as the DynaMag 2 rack) could not reliably separate bacteria tagged with 128 nm FcMBL beads out of blood (which is the bead size best for binding bacteria). To overcome these limitations, I designed a more effective magnetic separation system which significantly improved recovery of tagged bacteria out of blood and used this new system to create a simple method to separate and concentrate bacteria tagged with FcMBL magnetic beads out of blood while removing the vast majority of PCR inhibitors at that same time. I have shown that this method can separate bound bacteria from blood and purify them for PCR or qPCR identification. However, the FcMBL beads pull out enough white blood cells (containing human DNA) during the magnetic separation to partially inhibit the PCR reaction and reduce its sensitivity. After this contaminating DNA is enzymatically degraded (the Hybrid sample prep method), the FcMBL beads show comparable sensitivity to existing commercial methods. This FcMBL bead sample preparation method can also be easily adapted to detect bacterial contamination in other complex samples such as food, demonstrating the versatility of this technology as the basis for rapid pathogen detection systems.

### **4.2 Materials and Methods**

#### 4.2.1 Making a better magnetic rack

Several different magnet shapes and arrangements were modeled with finite element software in COMSOL to develop a better magnetic separation rack. The magnitude of the magnetic gradient at the inner wall of the sample tube and near its center were calculated and used to compare the different configurations. Several different permutations of rectangular and ring magnets, with different numbers, sizes and orientations, were investigated, looking for one that gave both a high maximum magnetic gradient and a high average gradient strength in the sample volume.

The Hex Rack was found to be the best of the configurations tested. It consisted of six magnets arranged in a hexagonal pattern around a BD FACS 12x75-mm tube (5 ml volume) (**figure 4.1 a-c**). Instead of positioning one magnet on one side of the tube (as is done in the DynaMag 2 rack), the Hex Rack was designed to completely surround a FACS tube (5 ml volume), minimizing the distance between the sample fluid and the magnets (which contact the outside of the tube directly). The 12x75 mm tubes fit well with the available 2 inch (50.8 mm) long magnets (neodymium N42 magnets, K & J magnetic, 2"x0.25"x0.25") and have the thinnest wall of a conventional test tube, making them well suited to this application. Through previous experimentation (chapter 3), I found that the gradient for a rectangular magnet is strongest at the corners where the field lines diverge outwards, so this rack places the edges of the six magnets directly against the tube surface to exploit this phenomena. Alternating the direction of the magnetic poles helps to create interlacing field lines through the entire volume of the tube (**figure 4.1 c**) rather than circling the rim (which is the case if they all had pointed the same direction), again boosting the magnetic gradient. The bottom of the magnets end 5 mm from the bottom of the tube, so any magnetic beads near the bottom are drawn to the particularly strong field at the bottom corner of the magnets, lowering the likelihood that they will be lost when fluid is aspirated out of the bottom of the tube. The 5 ml volume of the tubes also makes it possible to handle a much larger sample volume than was previously possible (DynaMag 2 has a maximum volume of 2 ml), increasing the sensitivity our assay. This technology can scale up for larger tube sizes as well.

Once the geometry had been optimized, an acrylic rack to hold the magnets and sample tube in the correct orientation relative to each other was designed in AutoCAD. The patterns were cut out of 1/4" and 1/8" acrylic sheets (McMaster) using an Epilog Legend 36EXT laser

cutter. The plastic holders were assembled, glued together with acrylic cement and then the magnets were inserted, at which point they were ready for use.

To estimate the gradient strength of the DynaMag 2 rack (Invitrogen), one of the racks was disassembled and calipers used to determine the dimensions of its magnets and their orientation relative to the sample tube in the device. These dimensions were used to create a 2D cross-sectional model of the rack in COMSOL. The magnets were assumed to be made of grade N42 neodymium (one the most powerful magnetic materials available). The finite element model was used to calculate the strength of the magnetic gradient in the commercial rack.

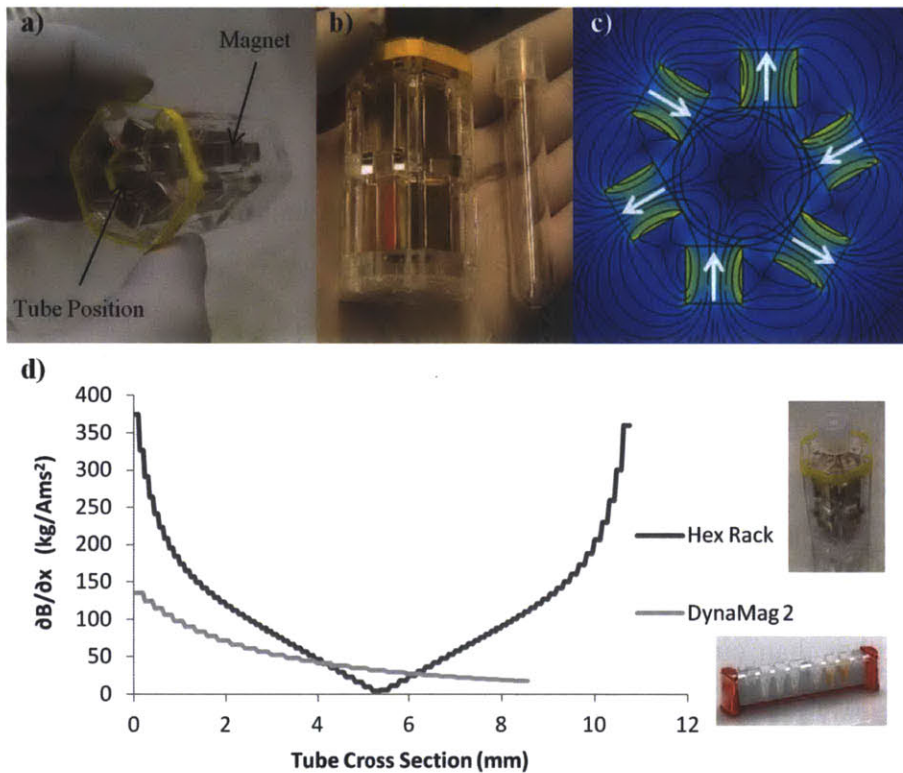


**Figure 4.1 The Hex Rack**

(a) The Hex Rack, constructed from six permanent magnets held together with a clear acrylic holder (b) Hex Rack with the 12x75 mm FACS tube it was designed to hold (c) Heat map of magnetic field in the cross section of the Hex Rack generated with finite element modeling in COMSOL. The black lines indicate the direction of the magnetic field lines and the white arrows indicate the direction of the pole in each magnet, showing the alternating pattern (d) Magnetic gradient strength in the Hex Rack and DynaMag 2 rack. Finite element modeling was used to predict the magnetic field gradient in each rack. The Hex rack has a higher average and maximum magnetic field gradient. DynaMag 2 image reprinted from [161]

#### 4.2.2 Magnetic Enhancement Beads (MEB)

Magnetic enhancement beads (MEB) were used as a second strategy to boost the separation and retention of 128 nm FcMBL bead tagged bacteria from of blood. To evaluate how much the MEB concept helped with magnetic separation, testing was conducted using the Kingfisher Flex Magnetic Particle Processor equipped with a 96 deep well magnetic head (Thermo Scientific). This machine is able to automatically perform magnetic separations in a very reproducible manner by inserting a magnetic head, sheathed in removable plastic, into either 24 or 96 well plates and has been used at the Wyss Institute for high throughput magnetic testing with 1  $\mu$ m FcMBL beads [124]. This machine has not been able to reliably remove 128 nm beads from diluted blood because the magnetic gradient it generates is not strong enough. The binding and separation of *E. coli* out of diluted blood was evaluated in this system using 128 FcMBL beads for binding and different concentrations of MEB to boost separation efficiency. A modified version of the depletion assay with 1 ml samples in a 96 well deep well plate was run. *E. coli* at 4,400 cfu/ml were added in triplicate to EDTA blood diluted 1:4 with TBS-Tween 20 with 5 mM calcium. Ten mM of glucose and 0.8 mg heparin per ml (JT Backer Inc.) were added (conditions which Nazita Gamini and Martin Rottman had determined gave optimal binding with this system [124]). Fifty micrograms of 128 nm FcMBL beads per milliliter sample were then added and the plate was placed in a thermomixer running at 950 rpm for 20 minutes for binding. After the binding was complete, 0, 5, 12.5 or 25  $\mu$ g of 1 or 2.7  $\mu$ m biotin and BSA blocked beads/ml were added to the 128 nm bead samples to act as aggregation aids. The plate was transferred onto the KingFisher and the magnetic head and protective plastic comb were lowered into the wells for a 7.5 minute magnetic separation. After the separation was complete, the beads and bound pathogens were withdrawn from the deep well plate along with magnetic comb when it was raised and moved to a new plate. Then the depleted sample was plated out using an Eddy Jet Spiral Plater. The colonies were counted the next day and the each of the samples was compared to a positive control to determine the amount of *E. coli* bound at each MEB concentration.

#### **4.2.3 FcMBL Sample Preparation Procedure**

The utility of the FcMBL beads and new separation systems for concentrating and purifying bacteria for PCR were tested in a range of fluids (donor blood diluted 1:1 with saline, 20% hematocrit red blood cells in saline from the blood bank or saline). A frozen *E. coli* aliquot was reconstituted in TBS-Tween 20 buffer with 5 mM calcium and serially diluted to create a

range of pathogen concentrations. For experiments using pre-bound bacteria (removing binding as an experimental factor), one hundred microliters of these concentrates were added into different 5 ml FACS tubes. Fifty  $\mu\text{g}$  of 128 nm FcMBL beads were added and given 10 minutes to bind to the concentrated *E. coli* before 2 ml of sample fluid (donor blood diluted 1:1 with saline, 20% hematocrit red blood cells in saline from the blood bank or saline) was added to the tube along with 25  $\mu\text{g}$  of blocked 1  $\mu\text{m}$  beads to act as MEB (section 4.2.2) and mixed by inversion. For direct binding in the sample, the *E. coli* were spiked into 2 ml of sample fluid and then the 128 nm FcMBL beads added. These were placed in an inverting mixer (Hula Shaker, Invitrogen) for 20 minutes, after which time the MEB were added and mixed briefly by inversion (**figure 4.2 a-b**).

At this point, the samples were placed in the Hex Rack for a 20 minute magnetic separation (**figure 4.2 c**). After the separation was complete, the blood was slowly aspirated from the tube using a 5 ml pipette and 3 ml of TBS-Tween 20 with 5 mM calcium buffer was added to wash the tubes (while they were still in place on the rack) (**figure 4.2 d**). After five minutes, the 3 ml wash buffer was aspirated out and replaced with 1 ml of fresh calcium buffer. Then, the tubes were capped and removed from the racks and gently agitated to resuspend the beads and tagged pathogens (**figure 4.2 e**). Then they were replaced in the rack and given 10 minutes to magnetically separate again (**figure 4.2 f**). This moved the beads and bacteria down the tube walls so that they were all resuspended in the 1 ml wash buffer. After the separation was complete, one more 1 ml wash was added and given five minutes to incubate before the final wash was aspirated (**figure 4.2 g**) and 50  $\mu\text{l}$  of distilled water was added. At this point, the tubes were removed from the rack and vortexed at maximum speed for 10 seconds to resuspend all the beads and tagged pathogens, which were then transferred to a DNA extraction tube (**figure 4.2 h**). The vortexing procedure was repeated with a second water wash (30  $\mu\text{l}$  for PrepGEM DNA extraction or 50  $\mu\text{l}$  for DNeasy kit) to collect any remaining pathogens from the FACS tube. At this point, the samples were ready for DNA extraction using either the PrepGEM or DNeasy extraction kits (see section 4.2.6).

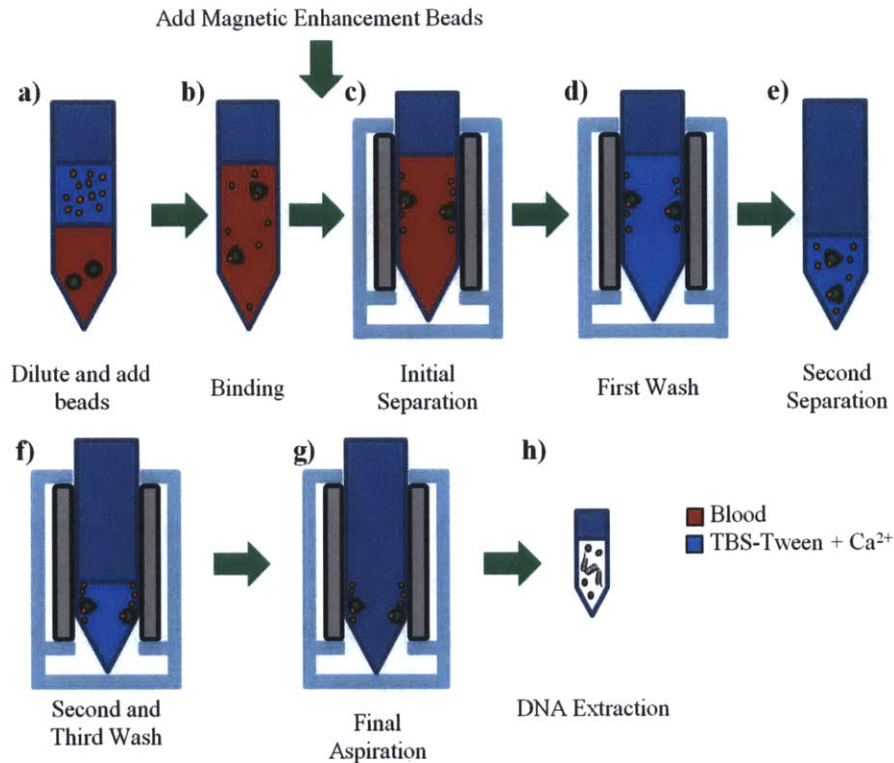
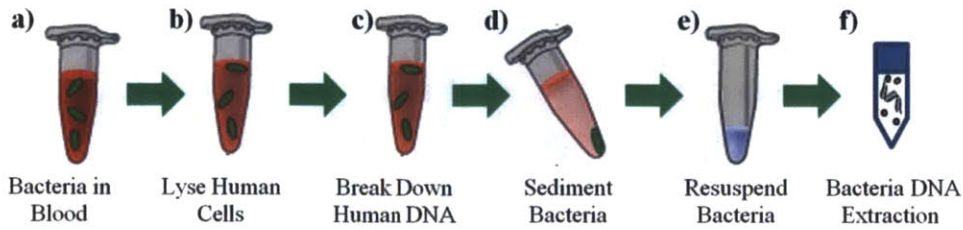


Figure 4.2 FcMBL sample preparation method

#### 4.2.4 MolYsis Sample Preparation Procedure

Preparation of *E. coli* spiked samples was the same as for the FcMBL method (section 4.2.3). These samples were in 2 ml microcentrifuge tubes instead of 5 ml FACS tubes without any FcMBL or MEB beads added. Pathogen recovery from the undiluted blood or saline samples was carried out with a MolYsis Basic 5 kit (Molzylm) according to the manufacturer's instructions. Briefly, CM buffer (250  $\mu$ l for 1 ml samples or 2 ml for 5 ml samples) was added to the samples (**figure 4.3 a-b**), vortexed and incubated at room temperature for 5 minutes to selectively lyse all the human cells in the sample. Then DB1 buffer (250  $\mu$ l for 1 ml samples or 2 ml for 5 ml samples) and 10  $\mu$ l of MolDNase B was added and incubated in the sample for 15 minutes, breaking down all of the human DNA in the sample (**figure 4.3 c**). Then the samples were centrifuged at maximum speed for 15 minutes. The pellet was resuspended in 1 ml of RS buffer and then centrifuged again at maximum speed for five minutes (**figure 4.3 d**). The pellet was then suspended in 80  $\mu$ l of PL buffer with 20  $\mu$ l of BugLysis solution (**figure 4.3 e**) and incubated in a thermomixer (Eppendorf) at 37°C, 1000 rpm for 30 minutes, after which the DNA was extracted from the sample using a DNeasy solid phase extraction kit for blood and tissue

(Qiagen) (**figure 4.3 f**). The MoLYsis kit required proteinase K digestion, so the PrepGEM DNA extraction method did not work (see section 4.2.6).



*Figure 4.3 MoLYsis sample preparation method  
Image adapted from [162]*

#### 4.2.5 Hybrid Sample Preparation Procedure

In order to see if pre-concentration with MBL beads could make the MoLYsis kit more effective, samples were run using the FcMBL procedure (section 4.2.3) until the beads and captured pathogens had been resuspended in the 1 ml of buffer (**figure 4.4 a-e**). At this point the samples were processed with the MoLYsis kit (section 4.2.4) using the procedure recommended for 1 ml samples according to the manufacturer’s instructions (e.g. 250 µl of CM and DB1 buffer were used, everything else stayed the same) (**figure 4.4 f-h**). DNA was then extracted from the concentrated bacteria using a DNeasy kit (Qiagen) (**figure 4.4 i**).

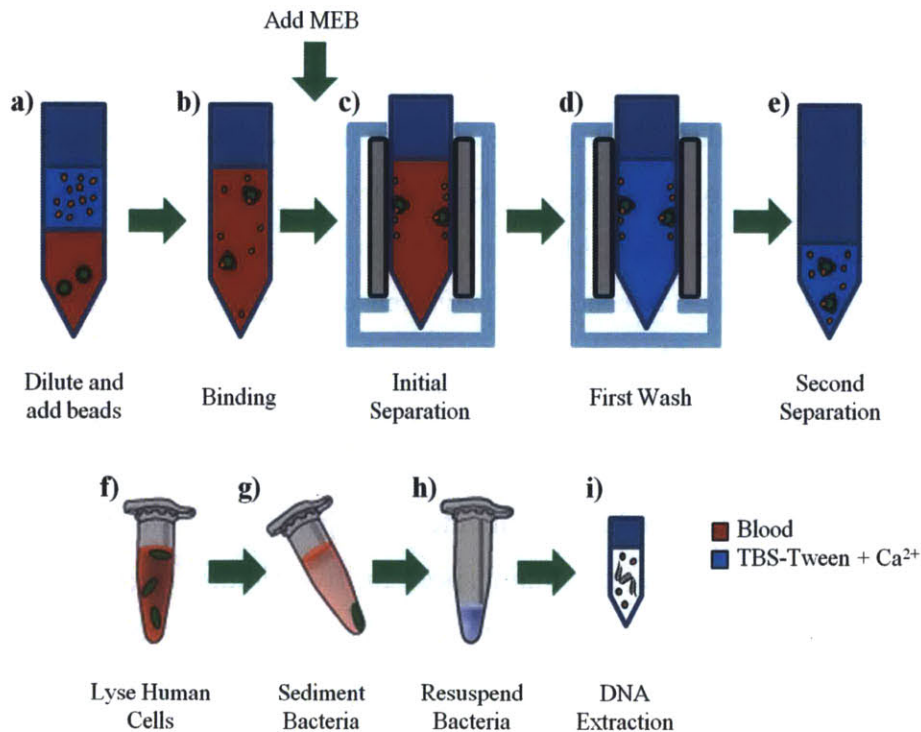


*Figure 4.4 Hybrid sample preparation method  
Image adapted from [162]*



#### 4.2.6 DNA Extraction

DNA for PCR was extracted from the recovered beads and pathogens using either the DNeasy Blood or Tissue Solid Phase Extraction (SPE) kit (Qiagen) or the PrepGEM Bacteria enzymatic kit (Zygem) according to the manufacturer's directions.

For the DNeasy kit, the samples were incubated with ATL buffer and proteinase K for 15 minutes at 56°C in the thermomixer (Eppendorf) at 1000 rpm to digest the cell walls of the bacteria and release their DNA. The digested bacteria were then diluted with equal parts AL buffer and pure ethanol before being added to the solid phase extraction spin column. The columns were spun at 8,000 rpm for 1 minute, with the DNA released from the bacteria being retained in the column matrix and the rest of the proteins and liquid passing through into the waste. The columns were washed twice more with the supplied buffers and then 100 µl of AE elution buffer was added to the column and allowed to incubate at room temperature for one minute to resolubilize the DNA in the column matrix. The eluted DNA was then collected in a fresh 1.5 ml microcentrifuge tube in a final centrifugation step.

The PrepGEM Bacteria kit took a similar amount of time to run as the DNeasy kit, however it had much less hands on time because it was a closed tube procedure that did not require centrifugation. This method used lysozyme enzymatic digestion to break down the cell walls. It also contained the PrepGEM enzyme, which is responsible for digesting intracellular proteins, particularly DNases that might break down the sample. Twenty microliters of buffer containing these enzymes were added to the 80 µl of purified beads and bacteria, then sealed into a PCR tube strip and placed in a Tetrad 2 Peltier Thermal Cycler (BioRad) for the temperature-dependent extraction. The samples were heated to 37°C for 15 minutes (giving the lysozyme maximal activity), then held at 75°C for 15 minutes (giving the PrepGEM enzyme maximal activity) and finally incubated at 95°C for 15 minutes (degrading both extraction enzymes so that they did not interfere with subsequent PCR reactions). This method had much less hands on time than the solid phase extraction method. This meant it had less potential for contamination or human error and was easier to automate, making it more favorable from a procedural prospective. Extracted DNA was either analyzed immediately or stored at -80°C for later analysis. Each PCR assay took less than 10 µl of the extracted DNA so many different tests were possible on a single sample. Concentration and purity of the extracted DNA was assayed using a Nanodrop 2000 Spectrophotometer (Thermo Scientific). The absorbance spectra of a sample

were measured using 2  $\mu$ l of liquid. The machine was calibrated using distilled water before each batch of samples. Concentration of double stranded DNA was calculated from the absorption of sample in the 260 nm wavelength and an estimate of the protein contamination determined from the absorption ratio at 260 nm and 280 nm.

#### **4.2.7 Bead interference with DNA extraction**

To determine if the FcMBL and aggregation aid beads interfered with DNA extraction, different concentrations of the beads (0, 10, 20, 30  $\mu$ g 128 nm FcMBL beads with half that mass of MEB) were added to 8,000 *E. coli* in 80  $\mu$ l TBS with Tween 20. DNA extraction with the PrepGEM kit (section 4.2.6) was then carried out and qPCR (section 4.2.9) was used to determine the relation between C<sub>q</sub> and bead concentration.

To check for pathogen losses during the binding and washing process, a similar experiment was carried out in a larger fluid volume. The same amount of bacteria and range of 128 nm FcMBL beads were added to 1 ml of TBS-Tween 20 with 5 mM calcium and given 20 minutes in the inverting mixer to bind. Then the MEB were added (one half the mass of the 128 nm FcMBL beads added) and the samples were placed in the magnetic rack and given 20 minutes to separate. The saline was then aspirated out and replaced twice before the beads and captured pathogens were resuspended in 80  $\mu$ l of water for PrepGEM DNA extraction and subsequent qPCR analysis (see section 4.2.10). The C<sub>q</sub> (threshold cycle) results from these bound and washed samples were compared to the first set of samples to determine if any *E. coli* were lost during the binding and washing procedure.

#### **4.2.8 PCR and qualitative analysis**

The initial phases of testing were carried out using normal PCR and known concentrations of bacteria to evaluate the approximate efficiency and sensitivity of the FcMBL preparation method and the behavior of the various primer sets selected. Four highly specific primers for *E. coli*, dubbed EcA, EcB, EcC and EcD were selected from a paper by Maheux et al. for testing [163] (**table 4.1**). These primers showed the best selectivity of the nine evaluated in that paper and had product lengths compatible with qPCR.

PCR was carried out using 8  $\mu$ l of the extracted DNA sample, 500 nM of the forward and reverse primers and Phusion High-Fidelity PCR Master Mix with HF buffer (New England Biolabs) in a 20  $\mu$ l volume. The samples were maintained at 4°C using a cold block inside of an Air Clean 600 PCR Workstation (USA Scientific) during preparation (in a separate location from

the sample preparation and DNA analysis areas to minimize the chances of cross contamination). The samples were placed in PCR tube strips and heated in a Tetrad 2 Peltier Thermal Cycler (BioRad), preheated to 98°C. The samples were treated at 98°C for thirty seconds to initially denature the double stranded DNA, then cycled through 98°C for 10 seconds, annealing for 30 seconds (temperature dependent on primer set, see table 4.1), and elongation for 40 seconds for a total of 35 cycles. After the cycles were complete, the samples were held at 72°C for 10 minutes to finalize any last elongations and then held at 4°C until ready for gel electrophoresis.

The results of the PCR were analyzed using gel electrophoresis. Ten microliters of each sample and 5 µl of water were added into each well of 1% agarose E-Gel (Invitrogen), with 56 ng of 100 BP ladder (Invitrogen Ca# 15628-050) for comparison. The gels were run for 9 minutes on an E-Gel Ibase (Invitrogen), 1-2% agarose setting, and then imaged using the SYBR-Green Safe setting on a FluorChem M Imager (Protein Simple). The band intensity was analyzed using ImageJ software and normalized relative to the band intensity of the DNA ladder (which was the same for all the gels). The PCR amplification was deemed positive if the resulting product band intensity was above the nonspecific background in the 0 cfu/ml sample (run in each experiment). In addition to this negative control, the fidelity of the DNA extraction and PCR was checked using a sample containing 48,000 *E. coli* in saline and no *E. coli* in saline (positive and negative controls).

#### **4.2.9 Primer Evaluations**

The four *E. coli* primers (table 4.1) were characterized using DNA extracted from a range of *E. coli* or *K. pneumoniae* concentrations (in triplicate) in saline to check for bacterial specificity. PCR and band analysis was conducted using the procedure outlined in section 4.2.8. The usefulness of each primer set was evaluated by checking for the formation of the intended product and presence of any non-specific amplification products in the *E. coli* samples of any amplification at all in the *K. pneumoniae* samples.

The specificity of the two best primer sets (EcA and EcD) was assayed in the presence of human DNA by amplifying DNA from *E. coli* purified from fresh human blood of ten different donors using FcMBL beads (see section 4.2.3). Each primer was then used to amplify *E. coli* extracted from donor blood and evaluated to see if there was non-specific amplification of human DNA, particularly in the 0 cfu/ml samples.

ID	Genetic Target	Annealing Temperature (°C)	Product Length (BP)	Primers	Sequence
EcA	tuf	58	258	TEco1553	5'- TGGGAAGCGAAAATCCTG -3'
				TEco1754	5'- CAGTACAGGTAGACTTCTG -3'
EcB	uidA	58	147	UAL754	5'- AAAACGGCAAGAAAAAGCAG -3'
				UAR900	5'- ACGCGTGGTTACAGTCTTGCG -3'
EcC	uidA	61	166	UAL1939b	5'- ATGGAATTCGCCGATTTTGC -3'
				UAL2105b	5'- ATTGTTGCCTCCCTGCTGC -3'
EcD	uidA	62	147	UAL	5'-TGGTAATTACCGACGAAAACGGC-3'
				UAR	5'- ACGCGTGGTTACAGTCTTGCG -3'

Table 4.1 *E. coli* specific primers tested for amplifying bacteria extracted using FcMBL Sample Prep

Table adapted from [163]

#### 4.2.10 qPCR analysis

From the primer characterizations, the EcD set was found to be the most reliable, forming a specific product with minimal non-specific amplification of human DNA, making it the most suitable for qPCR testing. SYBR® Green PCR Master Mix (Applied Biosystems) was used for the assay.

A genomic standard was chosen for qPCR quantification since the uidA gene (target of the EcD primers) has only one copy per bacteria [164] and size of the genome for the *E. coli* strain employed in the experiments (ATCC 8739) was known [165]. From this I calculated that 52.9 ng of extracted DNA should contain  $10^7$  copies of the target gene. To obtain purified DNA to make standard aliquots, *E. coli* were grown in LB broth at 37°C overnight. The bacteria were checked under the microscope for any signs of contamination and then DNA was extracted from 600 µl of the culture medium using the DNeasy extraction kit. The purity and concentration of the extracted DNA was determined using the Nanodrop spectrophotometer and then the purified DNA was diluted to 10.6 ng/µl (so that 5 µl would contain  $10^7$  gene copies) and 20 µl of this standard was aliquoted into individual PCR tubes and stored at -80°C until needed. A standard curve was created by making seven ten-fold serial dilutions of the standard. Five µl of each dilution, along with a no template control was run in duplicate for each qPCR run, giving concentrations ranging from  $10^7$  to  $10^0$  gene copies in water that could be used to confirm the qPCR was working and give a comparison for samples purified from blood.

Primer concentration optimization was performed according the procedure in the SYBR green user guide with the standard DNA using a 50 µl sample volume. Fifty nanomolar of the forward and reverse EcD primer set was found to be the most effective, showing only a single product with a size of approximately 150 BP and no amplification in the no-template wells.

qPCR analysis of the samples was conducted using 45 µL of SYBR green mastermix, containing 50 nM of the EcD primer set and 5 µl of sample. Amplification and fluorescent analysis was performed in a C1000 Thermocycler equipped with a CFX96 Real-Time System (BioRad) using the two step amplification recommended for the kit (10 minutes at 95°C to activate the hot start DNA polymerase, then 45 cycles with 15 seconds at 95°C to denature the double stranded DNA and 60 seconds at 60°C (for annealing and elongation). The intensity of the SYBR and FAM fluorescence was read after each cycle and a melt curve analysis was conducted after the final amplification step to check for non-specific amplification. The CFX manager 3.0 software calculated the threshold cycle (C<sub>q</sub>) from the measured fluorescence readings using the default settings. Gel electrophoresis (section 4.2.7) was conducted on individual samples to confirm the results of the melt curve analysis were accurate, particularly if any non-specific amplification was suspected.

#### **4.2.11 PCR detection of bacteria from food**

To show that the FcMBL beads could be used for a wide range of sample types, the FcMBL sample preparation procedure was adapted to work with homogenized food samples, including yogurt and oat cereal. For binding and detection of *E. coli* detection in yogurt, tests were conducted in plain nonfat yogurt (Dannon), Greek-style nonfat yogurt (Chobani) and Greek-style nonfat strawberry yogurt (Chobani). PCR with EcD primers was performed to make sure that the amplification was not inhibited by trace amounts of yogurt. Plain, nonfat yogurt was added into TBS-Tween 20 buffer with 5 mM calcium at 1 gm yogurt to 100 or 1000 ml buffer and added a range of *E. coli* concentrations (between 0 to 5000 cfu/ml). Then the DNA was extracted using the PrepGEM kit and PCR was performed on the samples (using the procedure laid out in section 4.2.7).

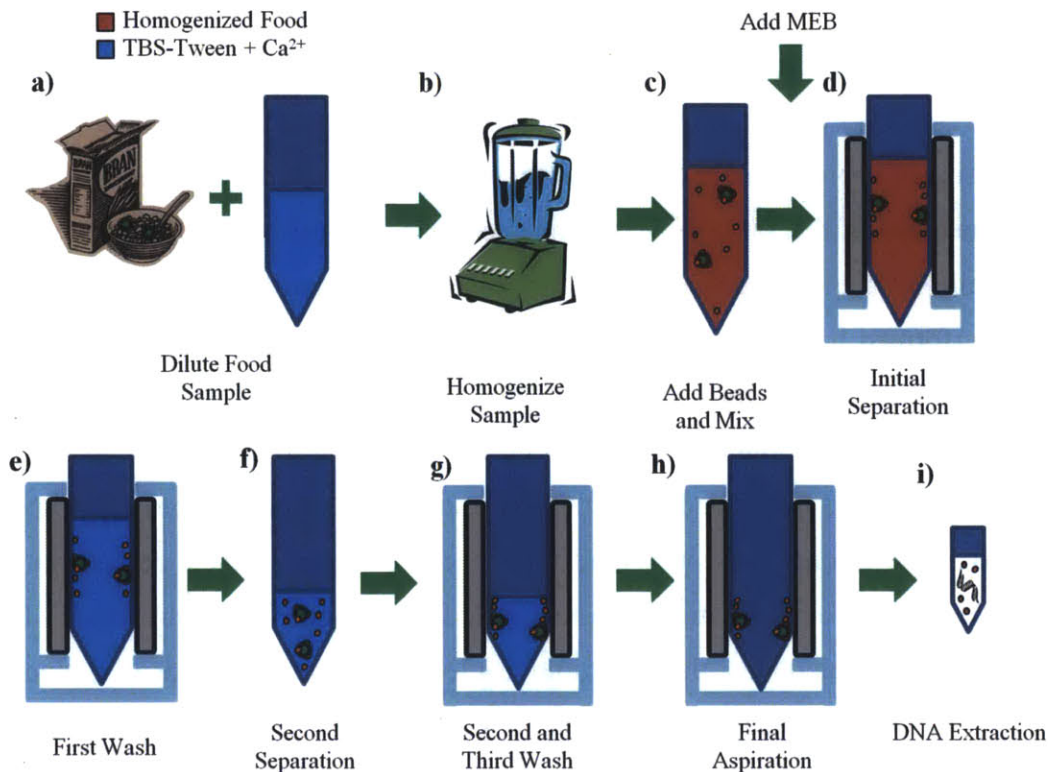


Figure 4.5 Modified FcMBL sample preparation method for isolating bacteria from food samples

Different dilutions of yogurt were tested to see how much the yogurt needed to be diluted with calcium buffer for binding of *E. coli* to be reliable. Dilutions of yogurt to buffer ranged from 1 gram: 1 ml to 1 gm: 9 ml with either 100 or 0 *E. coli* per ml (figure 4.5 a). The yogurt was mixed into the buffer by pipetting and then vortexing at full speed for 30 seconds (figure 4.5 b). Twenty five micrograms of 128 nm FcMBL beads/ml sample were added and the samples were placed in an inverting Hula Mixer (Invitrogen) for 20 minutes for binding (figure 4.5 c). The MEB were then added (12.5 µg 1 µm blocked beads/ ml) and the samples were placed in the Hex Rack for 20 minutes (figure 4.5 d). The yogurt solution was then aspirated and replaced with 3 ml of calcium buffer (figure 4.5 e). After five minutes, the first wash was removed and the sample resuspended in 1 ml of calcium buffer (figure 4.5 f) before being replaced in the rack (figure 4.5 g). The beads were given ten minutes to separate again and then the final wash was aspirated (figure 4.5 h). Then the tube was removed from the magnetic rack and the beads resuspended in 80 µl of water and submitted to the PrepGEM DNA extraction kit (figure 4.5 i) (section 4.2.6). Qualitative PCR analysis was then performed on all the different

samples, and only the highest dilution, 1 gram yogurt to 9 ml of TBS-Tween 20 buffer, showed a reliable PCR signal. This dilution factor was used for future experiments.

The approximate sensitivity of the assay was then determined using this dilution of yogurt (Plain nonfat from Dannon, Chobani 0% fat Greek-Style, Chobani 0% fat strawberry) by adding a range of *E. coli* to the 4.5 ml diluted samples and separating them out in with the Hex Rack (using the same binding conditions as the previous experiment). The wash procedure was the same as that used for blood (see section 4.2.3) and DNA extraction done using the PrepGEM kit (**figure 4.5**).

The same procedure was repeated with solid food samples as well (using General Mills oat cereal as an example). The optimization to determine a workable dilution factor was the same as with yogurt, but a different homogenization method was employed to prepare the solid food sample. In this case, oat cereal were measured out and placed in a Magic Bullet blender with TBS-Tween 20 with 5 mM calcium buffer and homogenized for 30 seconds (**figure 4.5 a-b**). The resulting slurry was filtered into a 50 ml tube using a 100  $\mu$ m cell strainer (BD falcon) to remove large particulates, after which the *E. coli* was added (bacteria were kept away from the homogenization blender to prevent contamination of negative control samples). It was found that 1 gm oat cereal to 48 ml buffer gave the best binding performance with the least sample dilution and used this to characterize the sensitivity of the assay with 4.5 ml diluted samples in the Hex Rack.

## **4.3 Results**

### **4.3.1 Building a better magnetic rack**

In my initial experiments with binding and separating bacteria out of blood with the FcMBL beads (Chapter 2), I found that the 1  $\mu$ m beads bound the smaller pathogens poorly but the 128 nm beads that could effectively bind to bacteria (more than 90% capture of both *E. coli* and *S. aureus*), but the bound bacteria proved difficult to extract out of blood with the DynaMag 2. Given that the bacteria could be separated out effectively in saline or plasma but not in blood, it appeared that the problem was not poor binding but difficulty in pulling the smaller beads, with their weaker induced dipole, out of blood. The magnetic force exerted on a bead depends on the number of iron oxide nanocrystals embedded in it, which have a roughly uniform concentration in the polymer matrix used to create the superparamagnetic beads we have

employed [142]. Consequently, the smaller volume of the bead volume, the lower the number magnetic crystals in it and the weaker net magnetic force.

Examination of the DynaMag 2 rack and the magnets in the KingFisher Flex Magnetic Particle Processor (employed for high throughput testing of the 1  $\mu\text{m}$  FcMBL beads [124]) showed that these system had been poorly optimized for creating the high magnetic field gradients required to pull out nanometer scale magnetic. The MACS column (Miltenyi Biotec) could recover these beads, but the high surface area of the column made high levels of non specific binding possible [79]. My work with the MFC showed that with the right setup, the magnetic gradient from a standard rare earth magnet like those used in both commercial systems could be greatly increased, so I developed a much more powerful magnetic rack to capture 128 nm beads and tagged bacteria out of blood.

Finite element modeling allowed me to reverse engineer the DynaMag 2 rack, evaluate its weaknesses and screen a large number of different magnet shapes and configurations create a better gradient. I found that over two millimeters of protective plastic separated the magnets of the sample in the DynaMag 2 rack, which was a problematic since magnetic force drops exponentially with distance from the magnets, so even a few hundred microns can make a large difference. The KingFisher has a similar problem; the protective plastic comb that sheathes the magnetic head is much thicker than it needs to be (over 1mm thick). The other primary weakness of the DynaMag 2 rack was that the magnets are only on one side of the tube, so magnetic particles on the far side of the tube are separated by the entire diameter of the tube ( $\sim 10$  mm). I worked on correcting these two weaknesses in my design. I first focused on getting the magnets as close as possible to the sample. The 5 ml FACS tube was selected for holding the sample because it has the thinnest wall of any conventional test tube (800  $\mu\text{m}$ ) and, in all configurations I examined, the magnets were placed in direct contact with the tube. To minimize the distance between the magnetic particles in the sample and the magnets, I surrounded the tubes with magnets rather than placing them one only one side, which led to the design of the Hex Rack (**figure 4.1 a-c**).

The Hex Rack contains six magnets arranged in a hexagonal pattern around the tube. Each is slightly offset so that the edge of the magnet is in contact with the tube, taking advantage of the high gradient spike at the edge of the magnet which I found to cause bead pile up in the early optical detection prototypes (Chapter 3). This created six equally spaced places around the



perimeter of the 5 ml tube with the high magnetic gradients. Alternating the direction of the magnetic poles into and out of the tube created an interlacing set of field lines in the sample volume (**figure 4.1 c**). Forcing the fields to bend in this manner created large changes in their magnitude and direction inside the tube, further increasing the field gradient.

Simulations showed that the Hex Rack produced a maximum magnetic field gradient nearly three times that of the commercial DynaMag 2 rack system from Invitrogen, making it much better suited for pulling out the smaller 128 nm beads that we work with for binding bacteria out of blood (**figure 4.1d**). The average magnetic gradient in the tube volume was boosted from 56 kg/Ams<sup>2</sup> to 119 kg/Ams<sup>2</sup>, boosting separation efficiency and decreasing bead losses during washes in the PCR sample prep procedure despite the increased diameter of the 5 ml tube. The 5 ml volume of the tubes also made it possible to handle a much larger sample volume than was previously possible, increasing the potential sensitivity our assay by allowing me to process a larger sample with more pathogens. The Hex Rack greatly improved the separation and retention of the 128 nm beads from blood; however, I developed an additional simple method to further improve retention.

#### **4.3.2 MEB and Improving Pathogen Separation**

When the magnetic beads are magnetized by an applied magnetic field (like in a magnetic rack), a magnetic dipole is induced in the bead, essentially turning the bead into a small magnet itself. As this induced dipole is pulled towards the magnet in the rack, the beads will also be attracted to other nearby beads in the samples [152]. The induced dipoles line up north to south, forming into needle-like aggregates (**figure 4.6 a-b**). The magnetic force on the bead aggregate increases linearly with the number of beads (assuming the magnetic beads area all the same size), but the drag on the ellipsoid increases at a much lower rate [142]. The net result is that the stochastic formation of these bead aggregates accelerates their separation out of the fluid. I decided to add larger magnetic beads after the binding was completed to accelerate this aggregation process of the 128 nm beads and create larger aggregates at the same time.

These larger magnetic enhancement beads (MEB) are added at the end of the binding process and briefly mixed into the sample before magnetic separation. When the larger beads are magnetized, they have a much larger magnetic dipole induced than smaller 128 nm beads, which results in the smaller beads nearby being attracted to the MEB, accelerating the aggregation process. The larger MEB beads play no role in the binding process themselves and were not

functionalized with FcMBL; they merely had their surface blocked with biotin and BSA to prevent non-specific adhesion.

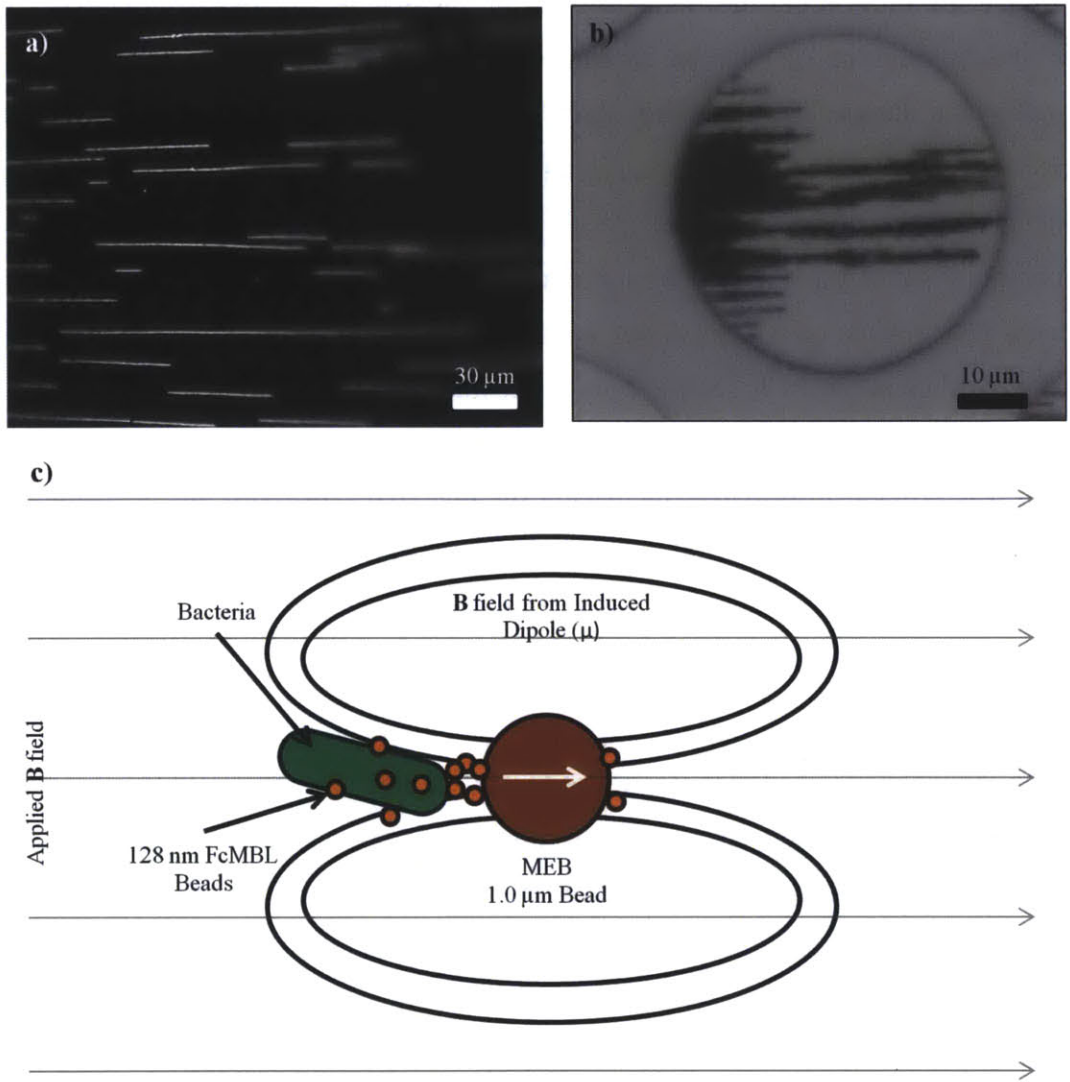


**Figure 4.6 Magnetic Enhancement Beads**

(a) Darkfield image showing 1 μm magnetic beads aggregating into needle like aggregates as their induced magnetic dipoles attract each other when magnetized by an applied field (b) Ellipsoid aggregates of 1 μm magnetic beads in a microwell of the optical detection microdevice (c) How the MEB work. The applied magnetic field induces a local dipole in all of the beads, but the stronger dipole in the 1 μm MEB bead attracts the smaller 128 nm FcMBL beads and tagged fungi to it, forming a large aggregate quickly. The white arrow represents the induced magnetic dipole ( $\mu$ ) in the MEB. The induced magnetic dipoles in the 128 nm FcMBL beads is not shown, nor is the local deformation of the applied  $B$  field caused by the beads aggregate.

There are three primary forces at work during the separation and washing process for the sample preparation procedure that need to be considered to understand why the MEB are

beneficial (**figure 4.7 a**). During separation, fluidic drag opposes the movement bead and tagged pathogen movement towards the magnet and during the washing process the surface tension will attempt to pull the beads down the tube away from the magnet during each fluid change. Neither the KingFisher system nor the DynaMag 2 was capable of reliably removing 128 nm beads from blood or holding them in place during wash steps. When I attempted to use the DynaMag rack, the vast majority of beads and tagged pathogens were lost during the washing process, leading to a very low detection rate with PCR.

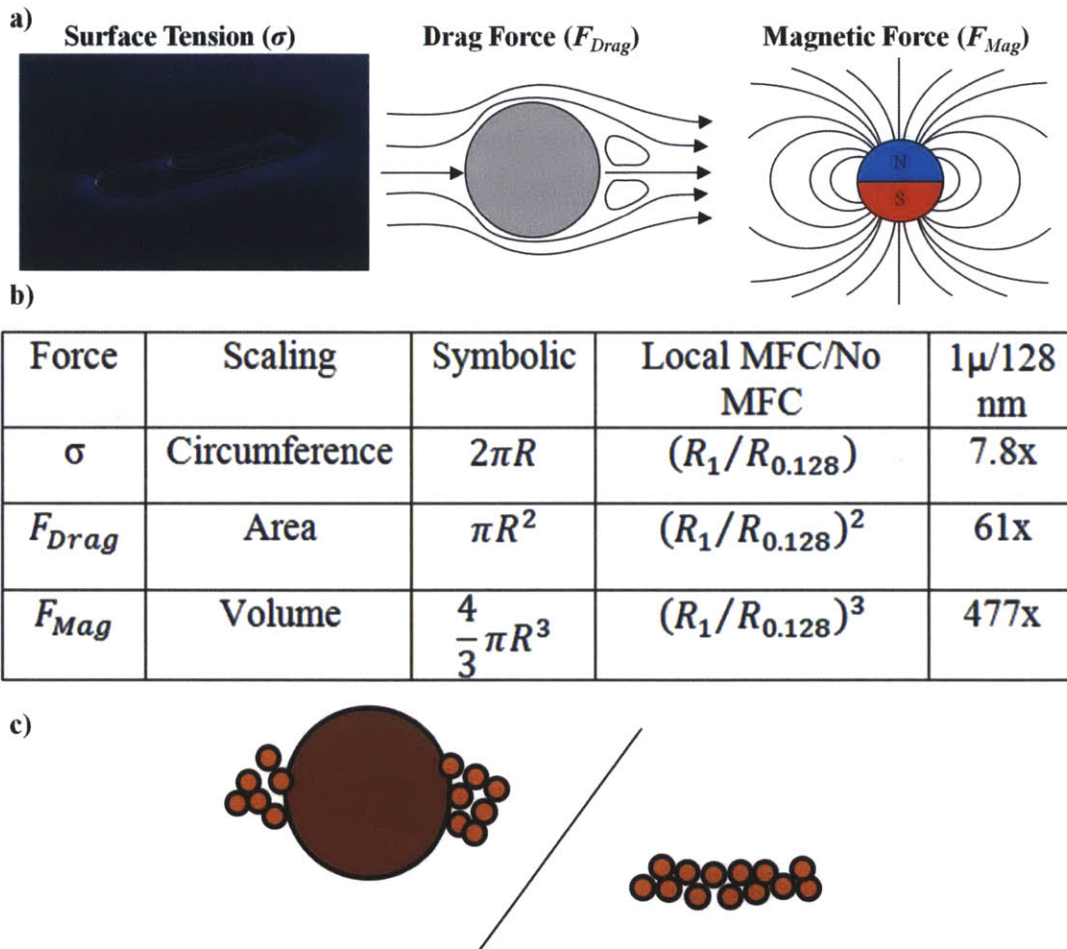
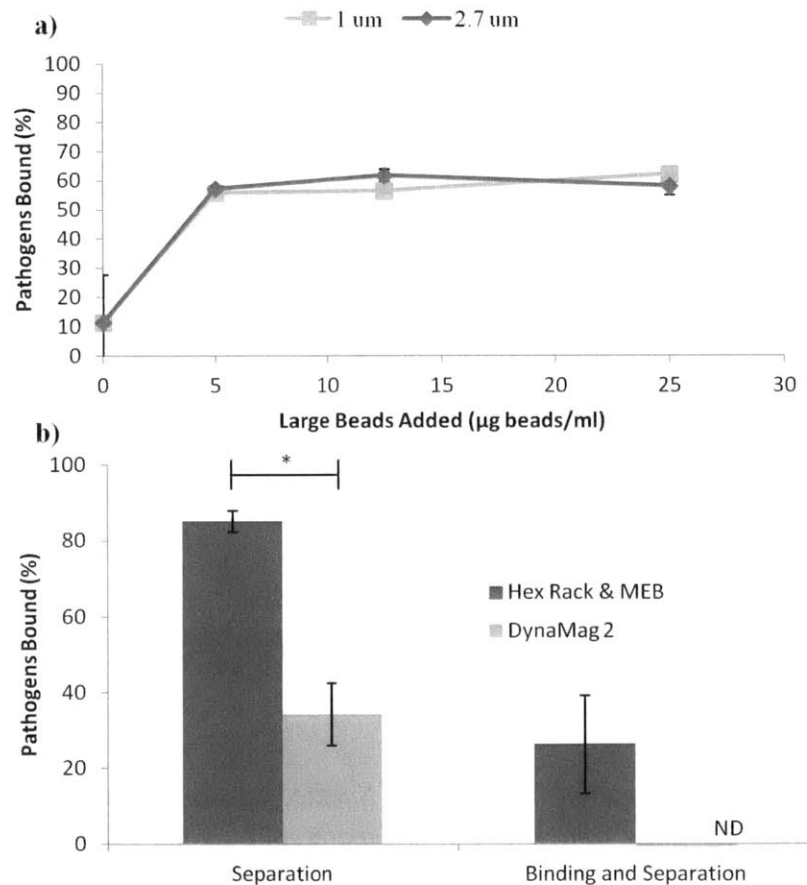


Figure 4.7MEB Theory

(a) Forces at work during separation and washes. Surface tension scales with the length of the object in contact with the fluid, which is the circumference in the case of a spherical bead. Images reprinted from [166, 167]. The drag force on an ellipsoid is higher than on a sphere in low Reynolds flow, being roughly equivalent to the minor axis cross section [152], which would be equivalent to the cross section of the MEB. Magnetic force scales with the number of magnetic nanocrystals in the bead, which is proportional to the volume of the MEB because the volume of the MEB is much larger than that of the 128 nm beads (b) Scaling analysis of the

MEB. This analysis assumes that the dimensions of the MEB dominate the behavior of the composite aggregates since they are much larger than the FcMBL beads used for pathogen binding (c) Illustration of how adding the 1  $\mu\text{m}$  MEB to 128 nm FcMBL beads (drawn to scale) increases the size of the magnetic bead aggregate.

The fluidic drag on the ellipsoid aggregate scales approximately with cross section of the MEB ( $\sim r^2$ ) and the surface tension on the aggregates scales approximately with the circumference of the MEB ( $\sim r$ ). The main advantage of this method is that the magnetic force on the aggregate scales with the volume ( $\sim r^3$ ), so there is a net increase in the magnetic force when the MEB are added that outweighs the increases in drag and surface tension (figure 4.7 b-c). For a mixture of 128 nm FcMBL beads with 1  $\mu\text{m}$  MEB, the net force on the beads should increase by a factor of  $\sim 8$  during the magnetic separation (magnetic force increases by  $\sim 477x$  and drag increases by  $\sim 61x$ ) and by a factor of  $\sim 61$  during the washing process.



**Figure 4.8 Effectiveness of the MEB and Hex Rack**

(a) Effect of adding different sizes and concentrations of MEB beads into diluted blood (1:4). All samples were bound with the same concentration of 128 nm FcMBL beads (25  $\mu\text{g per ml}$  sample) but different amounts of biotin and BSA blocked MEB beads were added. Magnetic

*separation was performed on the KingFisher in an adaptation of the method developed by Super et al. [124]. Adding the MEB significantly improved separation of E. coli out of blood ( $\alpha=0.05$ ), but no difference was observed between the two different MEB sizes tested or any of the three MEB concentrations tested.  $n=3$ , error bar: SEM (b) Binding and Separation of Bacteria in Blood with Hex Rack and MEB. Adding in the MEB and using the Hex Rack significantly improved separation of E. coli out of diluted blood (1:1) relative to the DynaMag 2 rack ( $\alpha=0.05$ ). It also showed an improvement when pathogen binding and separation (bacteria were not bound with beads before being added to blood). No separation of E. coli bound in blood were detectable with the DynaMag 2 while the Hex Rack and MEB showed  $26\% \pm 13\%$  binding and separation. These results indicate that the sample treatments (1:4 dilution, glucose treatment developed after my initial evaluations (Chapter 2) can boost the reliability of bacteria binding in blood [124].  $n=3$  error bar: SEM*

Experimental measurements with the KingFisher system showed that this simple strategy significantly improved separation after binding of bacteria in of diluted blood ( $\alpha=0.05$ ) and decreased the variability of the process, boosting recovery of pathogens bound with 128 nm FcMBL beads from  $11\% \pm 16\%$  to  $60\% \pm 2\%$ . Varying the MEB size (1  $\mu\text{m}$  or 2.7 $\mu\text{m}$ ) and concentration did not have any significant effect on the separation process (**figure 4.8 a**). Using the Hex Rack together MEB significantly improved separation of magnetically tagged bacteria out of diluted blood relative to the DynaMag 2 rack ( $\alpha=0.05$ ), boosting removal from  $34\% \pm 8\%$  to  $85\% \pm 3\%$  (**figure 4.8 b**). No bacteria were recovered with the DynaMag 2 rack when I attempted both binding and separation from diluted blood but the Hex Rack with MEB was able to recover  $34\% \pm 8\%$ . Using the new sample treatment conditions developed by other members of the sepsis group since my initial evaluations (Chapter 2) boosted the reliability of binding in blood as well [124]. These new conditions were used in the KingFisher MEB experiment, yielding  $60\% \pm 2\%$  of binding and separation of *E. coli* while the older sample treatment conditions only yielded  $26\% \pm 13\%$  binding and separation in the Hex Rack. This treatment will be used for subsequent binding and separation experiments. The following blood experiments examined only separation of bacteria and not binding and were conducted with the dilution and sample treatments outlined in Chapter 2 (1:1 dilution, cooling, heparin treatment). For subsequent experiments, the Hex Rack with 1  $\mu\text{g}$  of 1  $\mu\text{m}$  MEB beads per 2  $\mu\text{g}$  of 128 nm FcMBL (1  $\mu\text{g}$  MEB: 2  $\mu\text{g}$  Bind) added after binding were employed to boost the separation and minimize bead and pathogen losses during the washing process.

### 4.3.3 Results in Saline

The FcMBL beads are highly effective for binding and concentrating bacteria out of saline for PCR analysis. The FcMBL and MEB beads themselves did not interfere with the DNA extraction procedure at any concentration tested and showed no noticeable bacterial losses due to binding, magnetic separation and two washes relative to the control with the Hex Rack and MEB in saline (**figure 4.9**), evaluated with both PCR and qPCR. This was a major improvement over initial experiments with the commercial magnetic rack, which was able to adequately separate bacteria bound with 128 nm beads out of saline, but could not hold them in place against surface tension during the washes. As a result, the majority of the beads and tagged pathogens were lost after only two wash steps. Using the Hex Rack and MEB allowed me to virtually eliminate these losses, at least in saline, and concentrate all the pathogens from up to 5 ml of fluid down into 80  $\mu$ l of water for DNA extraction and PCR.

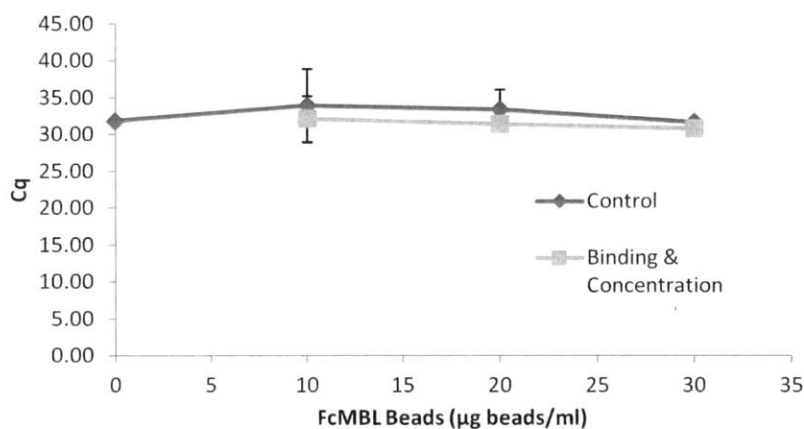


*Figure 4.9: Effect of FcMBL beads and MEB on DNA extraction*  
Control samples had different concentrations of 128 nm FcMBL beads and 1  $\mu$ m MEB beads added (in a ratio 1  $\mu$ g MEB: 2  $\mu$ g Binding beads) added to sample immediately before DNA extraction. No significant difference in the DNA concentration (determined using qPCR analysis) was found at any of the bead concentrations tested, indicating that neither the FcMBL beads nor MEB had a major effect on the DNA extraction. For the binding and concentration curve, the same amount of bacteria and beads were added to 1 ml of calcium buffer. The 128 FcMBL beads were then allowed to bind, the MEB added, the magnetic particles separated out with a magnetic rack and washed twice before being concentrated and resuspended for DNA extraction buffer. No significant bacteria losses relative to the control were observed, indicating in saline all of the *E. coli* in the sample and being bound and retained through the wash steps.  $n=3$ , error bar: SEM

#### 4.3.4 Sample Preparation in Blood and Comparison to Commercial Kit

With these improvements in bacteria separation and retention, it was possible to begin optimizing pathogen recovery out of diluted blood. These experiments were conducted using *E.*

*coli* tagged with 128 nm beads before they were added to blood to examine only the sample preparation procedure and not binding. Pathogen recovery at the end of the process was more difficult to measure than binding, since the beads caused cell aggregation (making plating inaccurate) and the inhibitors in blood made the qPCR suitable for comparing different methods but not for absolute quantification with the saline genomic standard employed. Bead recovery after the washing process in the Hex Rack with MEB was good (**fig 4.8a**), but in my preliminary tests, there was an issue with human DNA being recovered along with the beads and bacteria leading to non specific amplification. Repeating the tests in plasma showed virtually no non-specific amplification, indicating that the primary cause of the non-specific amplification was probably human DNA from phagocytes in the cellular fraction of blood.

Preparation	cfu/ml	Average Cq	Detection (%)	Cq STDEV
Hybrid	10000	29.6	100.0	2.2
Hybrid	1000	32.8	100.0	2.0
Hybrid	100	36.8	100.0	1.9
Hybrid	50	36.4	71.4	1.3
Hybrid	10	38.6	57.1	1.2
Hybrid	0	42.3	14.3	
MolYsis	10000	31.1	85.7	1.0
MolYsis	1000	34.2	85.7	1.0
MolYsis	100	38.0	85.7	1.0
MolYsis	50	39.6	71.4	2.6
MolYsis	10	41.3	57.1	0.3
MolYsis	0	41.3	14.3	
FcMBL	10000	34.7	71.4	2.4
FcMBL	1000	39.2	71.4	4.6
FcMBL	100	38.6	28.6	3.2
FcMBL	50	39.9	42.9	3.6
FcMBL	10	40.8	14.3	
FcMBL	0		0.0	
Con+	600,000	24.0	100.0	1.4
Con-	0	41.5	28.6	0.8

*Table 4.2 Summary of qPCR for the three different sample preparation method.*

*Preparation defines which of the three sample methods tested were used and cfu/ml indicates the E. coli concentration in each of the samples (2 ml of 1:1 diluted blood for the Hybrid and FcMBL methods, 1 ml of undiluted blood for the MolYsis method). Cq is the threshold cycle a fluorescent qPCR signal was detected. Detection is the percentage of the samples run at each concentration in which a signal was detected. STDEV is the standard deviation of the detected cycle threshold values. Blood from seven different donors was tested with each method. Positive and negative controls in saline (600,000 cfu/ml or 0 cfu/ml) were run with each assay to ensure*

*the DNA extraction procedure was working. The 0 cfu/ml blood samples served as negative controls for each sample preparation method.*

Selecting a different primer that was less prone to attaching to human DNA greatly reduced the non-specific amplification in the sample, making qPCR possible, but the remaining human DNA still had an inhibitory effect on the amplification that reduced both the amplification efficiency and the diagnostic sensitivity relative to the MoLYsis sample preparation method used for comparison. This reduced the reliability of the PCR amplification, so it could detect pathogen concentrations down to 50 cfu/ml, but in only 43% of the samples (3/7) (**table 4.2**).

To get a better idea of how well FcMBL bead sample prep compared to the current state-of-the-art systems for isolating bacterial DNA out of blood, I compared it to the MoLYsis sample prep kit (Molzym) (**figure 4.10**). This is one of the three kits commercially available for this purpose and has been found to have the best sensitivity [21, 160]. The MoLYsis kit relies on the pathogens having tougher cell walls so that the human cells in blood can be selectively lysed and their DNA enzymatically degraded without damaging the bacteria. Then the bacteria are pelleted by centrifugation and resuspended in fresh buffer for DNA extraction. The multiple centrifugation steps require a large amount of hands on time and the lysis is not completely successful at solubilizing all of the debris from the human blood. Therefore, in addition to the bacteria there is approximately 100  $\mu$ l of gelatinous byproduct recovered from a 1 ml blood sample after the final centrifugation, which requires 30 minutes of enzymatic degradation to break down. This byproduct appears to have a large amount of hemoglobin which must be removed during the DNA extraction process, so it requires proteinase K digestion and is not compatible with the PrepGEM kit. The DNeasy solid phase extraction kit works well for this purpose and was used for all samples in this comparison, including the FcMBL samples. However, despite these difficulties, the MoLYsis sample preparation method did work well for isolating bacterial DNA from donor blood for qPCR. I found comparable sensitivity to that found in the literature; at 50 cfu/ml the MoLYsis kit could detect 71% of the positive samples and 85% of the positives samples at higher bacterial loads [21, 160] (**table 4.2**). The FcMBL preparation method had a higher number of false negative results, indicating either failure to recover the bacteria or inhibition of the qPCR reaction.



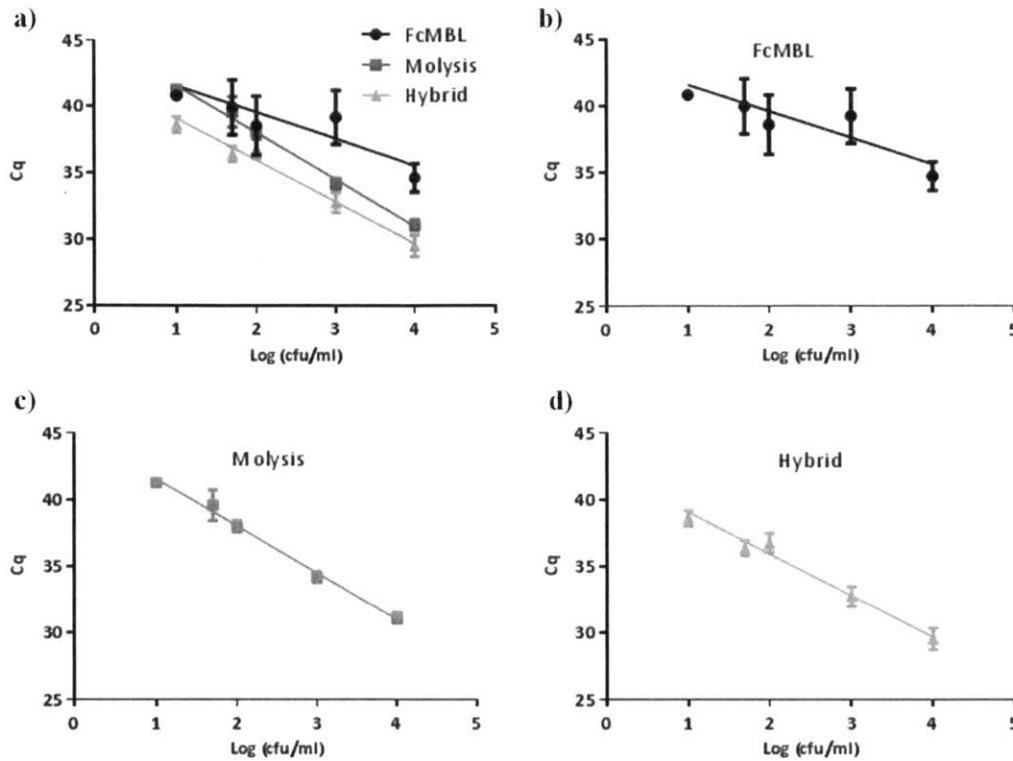


Figure 4.10 FcMBL vs. MolYsis Sample Preparation Methods,  $n=7$ , error bars: SEM

However, combining both the sample preparation methods to create a hybrid method increased the reliability of using the FcMBL. In this hybrid method, the FcMBL beads were used to concentrate the pathogens out of the blood so that the majority of the human cells could be removed immediately and then the MolYsis kit was used to degrade any of the remaining human DNA left in the sample. This eliminated the gelatinous blood debris and the human DNA, both of which interfered with PCR. Amplification efficiency went up and the number of false negatives went down (relative to the FcMBL method) using this method so that it was possible to detect bacterial loads down to 100 cfu/ml with 99% confidence ( $p=0.0078125$ ) [168]. However, I cannot say that the Hybrid and MolYsis sample preparation methods are significantly different. The Cq values with the Hybrid method are slightly lower than the MolYsis samples (indicating slightly higher amplification efficiency), but the standard deviations for those Cq values are higher than for the MolYsis samples (**table 4.2**). Applying additional statistics to the experimental design, probit analysis and a larger sample size would be required to conclusively establish the difference between the two [169].

Overall, the FcMBL sample preparation method was the least reliable of the three, with a lower detection rate at all pathogen concentrations. However, the effectiveness of the hybrid

version of the assay indicates that the bacteria are not being lost in the FcMBL sample preparation method. Instead it appears that the excess of human DNA extracted from white blood cells that phagocytose the beads is inhibiting amplification of the bacterial DNA causing a high rate of false negatives. Using the MolYsis treatment to remove this DNA after FcMBL bead separation prevents this inhibition and improves the reliability qPCR detection of the sample preparation method.

The hybrid method was also more reliable for detecting bacteria in heavily anticoagulated samples such as packed red blood cells from Blood Bank. These packed cells are treated with citrate phosphate dextrose adenine (CPDA), which contains a cocktail of anticoagulants and sugars [170], unlike the fresh donor samples used for the majority of the tests, which contained only heparin. The hybrid assay, with its more extensive sample cleaning procedure, could remove enough of these inhibitory molecules to make qPCR reliable for detecting *E. coli* spiked into these samples. Consequently, combining the two methods creates a simple sample preparation method that can both effectively remove human DNA and inhibitory substances from blood, increasing PCR sensitivity and reliability.

#### **4.3.5 Other Complex Samples**

The medical industry is not the only group trying to rapidly detect rare pathogens in complex samples. Detection of pathogenic bacteria in food currently uses techniques very similar to the methods used to diagnose sepsis (culture and AST) and suffers from many of the same limitations [32]. Every year in the United States, billions of dollars are spent screening food for bacterial and fungal contamination and millions of contaminated products still reach store shelves and cause millions of illnesses [171]. There are much fewer species of interest relative to sepsis as well. Most companies are primarily focused on detecting *E. coli* O157:H7, *C. difficile*, *Salmonella* and *Aspergillus*, so there is a smaller number of pathogens for which the sample preparation method must be tested [32, 35, 144, 172]. The primary limitation of current testing methods is that they are slow, so food must either be stored during the testing process or contaminated batches recalled after shipment, so there is great interest in a rapid diagnostic method to detect contamination before the food leaves the factory. I have shown that the FcMBL bead sample preparation method for PCR can rapidly detect bacteria in a few hours in blood. By comparison, most foods are much simpler sample matrices to work with, so we suspected it should be possible to adapt it to work with food.

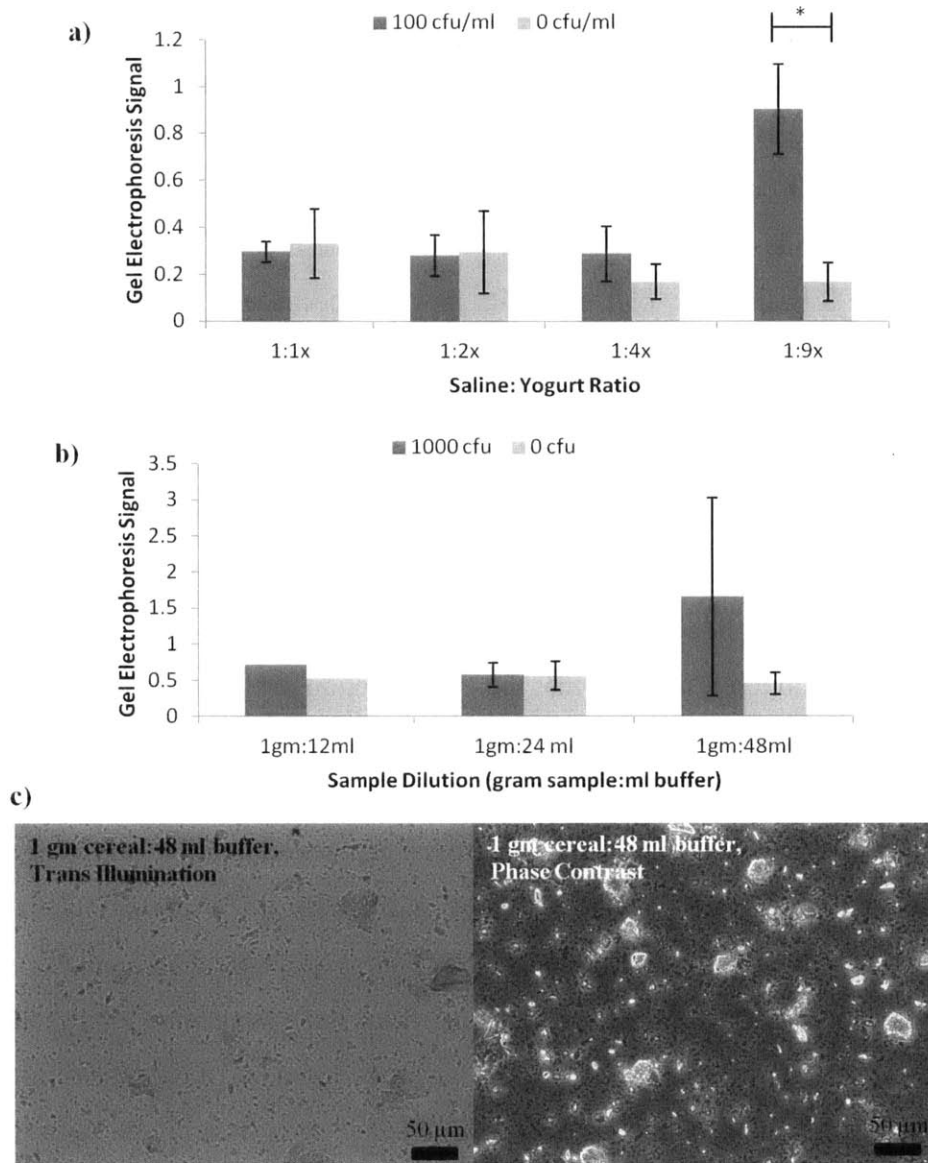


Figure 4.11 PCR detection of *E. coli* in different dilutions of food using FcMBL Sample Prep (a) Testing different buffer dilution factors in plain, nonfat yogurt. The 1 gm yogurt: 9 ml buffer was the only dilution factor tested that showed a specific PCR signal (assayed by gel electrophoresis) significantly above the background in the 0 cfu sample ( $\alpha=0.05$ ). One milliliter sample size,  $n=4$ , error bar: SEM (b) Testing different buffer dilution factors in oat cereal. The 1 gm cereal: 48 ml buffer was the only dilution factor tested that showed a specific PCR signal above the background in the 0 cfu sample). Four and half milliliter sample,  $n=2$ , error bar: SEM (c) Micrographs of homogenized oat cereal sample. Even at the 1:48 dilution factor, the homogenized cereal sample was still quite complex, with a similar volume fraction of the fluid ('hematocrit') occupied by solid particulates as the diluted blood samples

The main challenge with the switch to food was that it's much denser than blood, so dilution and homogenization were first required to make the sample liquid enough for the FcMBL beads to be able to circulate and bind bacteria. To determine the minimum sample dilution required for yogurt, I began by adding different ratios of calcium buffer to yogurt (1 ml buffer: 1 gram yogurt through 9 ml buffer: 1 gram yogurt), spiked in *E. coli* and determined if the 128 nm FcMBL beads could then bind the bacteria. The binding and recovery was assayed with qualitative PCR using *E. coli* specific primers because the large concentration of *Lactobacillus* in the yogurt would make the plate-based depletion assay unreliable. The bound pathogens were separated using the Hex Rack and MEB, and then washed before their DNA was extracted and amplified using PCR. I found that the minimum dilution for getting reliable binding and PCR detection was 1 gram yogurt: 9 ml buffer. None of the lower dilution factors showed a PCR signal above the negative control for that dilution, indicating binding and separation had failed (I had already established that trace amount of the yogurt did not inhibit the PCR reaction, so it was much less likely that the PCR reaction itself was failing). (**figure 4.11 a**). Diluting the sample with TBS-Tween 20 with 5 mM calcium ensured that there was enough ionic calcium present for the CRD in the FcMBL protein to form a stable bond with the sugar.

A similar procedure was repeated to determine the workable dilution for oat cereal, with the additional step that after the cereal was added to the buffer, it was homogenized for thirty seconds in a blender and then run through a 100  $\mu$ m filter (to remove particulates too large for the pipettes handling fluid transfer to remove). The cereal itself soaked up a large amount of the buffer, so I found that 1 gm cereal: 48 ml buffer was the minimum of the tested dilution (**figure 4.11 b**) in which the bacteria could be bound and detected with PCR. Even with this high of a dilution factor, the solid content of the sample was similar to the diluted hematocrit blood (**figure 4.11 c**), so the beads were most likely unable to circulate effectively through the solid particulates at lower dilution factors.

After a suitable dilution factor for pathogen binding and detection in the food samples had been determined, a range of successively lower pathogens concentrations were recovered and analyzed with PCR in 4.5 ml samples to determine the assay sensitivity. In yogurt, concentrations as low as 22 cfu/gm of *E. coli* (100 bacteria total added to the 4.5 ml diluted sample) could be bound, separated and detected with PCR (signal significantly above background,  $\alpha=0.05$ ) (**figure 4.12 a-b**). The detection threshold in oat cereal was similar; I could

reliably detect down to 100 cfu in the 4.5 ml diluted sample. However, because the oat cereal was diluted much more for binding, this translated to a sensitivity of 1067 cfu/gm cereal (**figure 4.12 c**). Unlike blood, the FcMBL beads alone were able to wash and purify the pathogens enough for PCR detection, without the need for a DNA degradation step, even in yogurt where a large number of *Lactobacillus* would be recovered by the beads as well as the target *E. coli*. This confirmed that the FcMBL beads could be employed to bind, separate and purify bacteria out of multiple types of food for rapid PCR detection once the correct buffer dilution factor had been found.

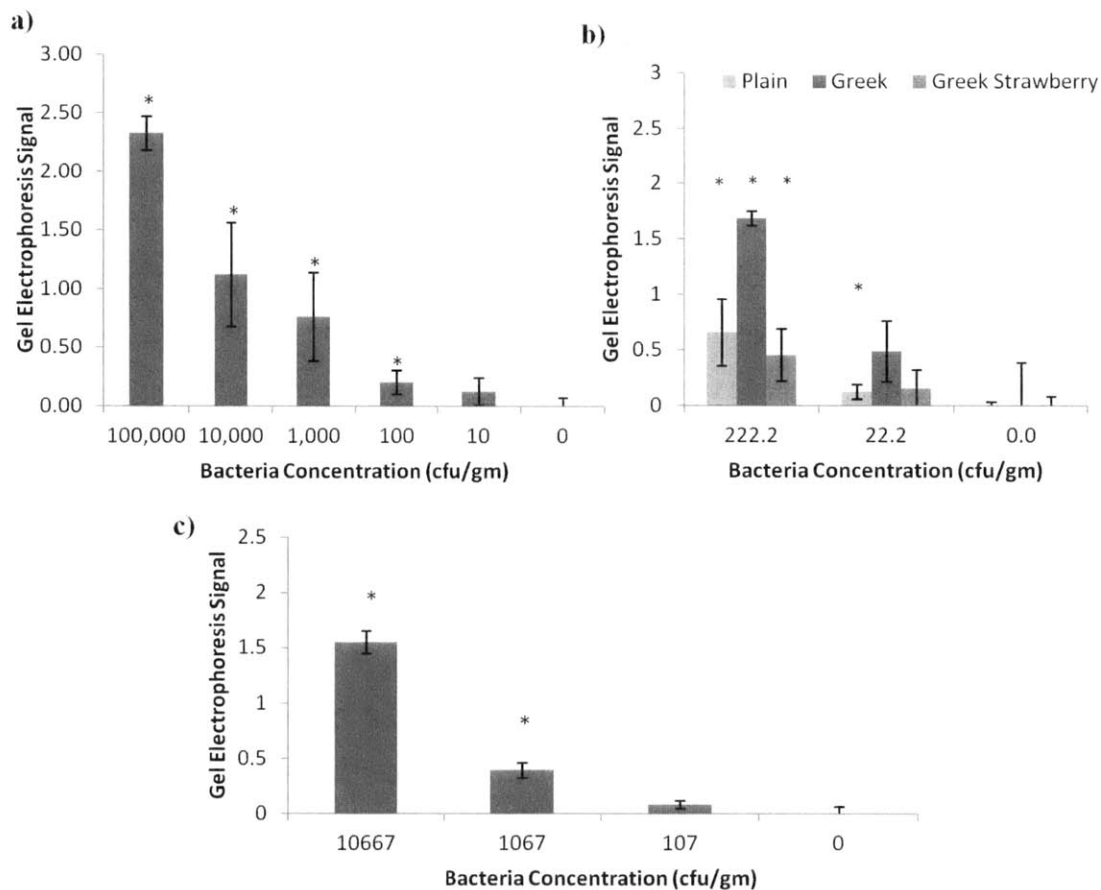


**Figure 4.12 : Bacteria Detection in Food using FcMBL Sample Prep Procedure**

(a) Detection of *E. coli* in plain, nonfat yogurt (1gm: 9 ml dilution factor, 1 ml diluted sample size). By using the FcMBL sample prep procedure, it was possible to concentrate the bacteria sufficiently to detect as little as 100 cfu/gm above background (\* indicates specific gel electrophoresis signal significantly above 0 cfu/gm sample,  $\alpha=0.05$ .)  $n=4$ , error bar: SEM (b) Detection of *E. coli* in different types of yogurt (1gm: 9 ml dilution factor, 4.5 ml diluted sample size). Detection in plain, nonfat yogurt, plain Greek-style yogurt and strawberry Greek-style yogurt was compared. Increasing the sample size to 4.5 ml allowed me to boost the sensitivity in

plain, non fat yogurt down to 22.2 cfu/gm (\* indicates specific gel electrophoresis signal significantly above 0 cfu/gm sample,  $\alpha=0.05$ ). Detection in Greek-Style yogurt was not as good, probably because this type of yogurt has a higher solid content than normal yogurt (part of the liquid is strained out), so a higher dilution factor may be required for optimal binding in future experiments. However, despite the increased protein and fruit content, the FcMBL beads were still able to bind to the *E. coli* added to the samples and isolate them for PCR detection.  $n=4$ , error bar: SEM (c) Detection of *E. coli* in oat cereal (1gm: 48 ml dilution factor, 4.5 ml diluted sample size). By using the FcMBL sample prep procedure, it was possible to concentrate the bacteria sufficiently to detect as little as 1067 cfu/gm above background (\* indicates specific gel electrophoresis signal significantly above 0 cfu/gm sample,  $\alpha=0.05$ ). Absolute number of bacteria in the sample detected was similar in both yogurt and oat cereal, but the higher dilution factor required for cereal meant the sensitivity in the undiluted sample was lower.

#### 4.4 Discussion

By combining the FcMBL beads with improvements in magnetic separation for nanometer scale beads, I have developed a simple sample preparation method to isolate bacteria from complex samples such as blood or food for rapid PCR detection. The magnetic beads provide a simple way to exert force on pathogens so that they can be concentrated and have PCR inhibitors removed at the same time, boosting the reliability of the PCR amplification.

The primary challenge for working with bacteria was that the smaller 128 nm FcMBL beads that bind them effectively are difficult to pull out of complex samples such as blood. These beads contain fewer magnetic nanocrystals, leading to a smaller magnetic force on the beads so that they are more difficult to pull through viscous, colloidal solutions like blood or homogenized food. The DynaMag 2 rack from Invitrogen could only separate out  $34\% \pm 8\%$  of the magnetically tagged *E. coli* from diluted blood, so a more effective method to recover the pathogens needed to be developed. I created the Hex Rack and MEB to boost the net magnetic force on the beads. The Hex Rack increased the strength of the magnetic gradient in the sample tube both by minimizing the distance between the sample and the magnets and by taking advantage of the gradient spikes at the edge of a rectangular magnet which caused problems with uniform bead spread in the optical detection microdevice (Chapter 3). Finite element modeling allowed me to evaluate several potential magnet geometries and pick the best one. This configuration more than doubled the average magnetic gradient strength throughout the sample volume and almost tripled the maximum gradient relative to the commercial rack.

The MEB acted as local magnetic flux concentrators in the sample fluid, drawing the smaller 128 nm beads towards them and accelerating the aggregation process of the magnetic

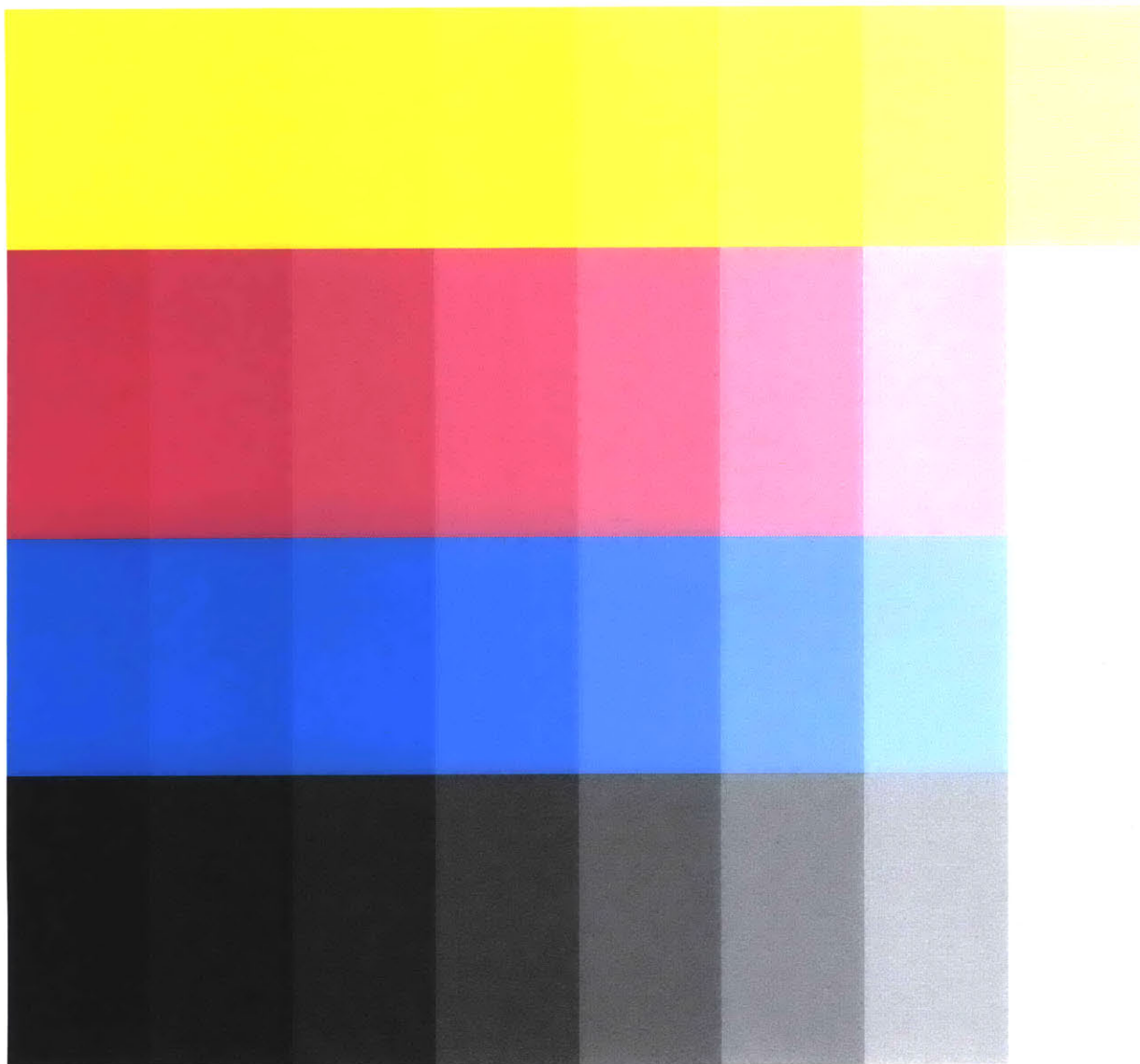
beads in the sample. This essentially gives the best features of both micron and nanometer scale beads: the better binding of the 128 nm beads to bacteria and the superior magnetic separation abilities of the larger 1  $\mu\text{m}$  beads. Adding the magnetic enhancement beads made it possible to use the 128 nm beads in the KingFisher system, which normally recovers only  $11\% \pm 16\%$  of the bacteria from blood, but was able to bind and separate over  $60\% \pm 2\%$  of *E. coli* spiked into the blood with this simple addition. Surprisingly, the MEB concentration and size (1  $\mu\text{m}$  or 2.7  $\mu\text{m}$ ) did not seem to affect the separation. From the scaling theory, it was expected that the 2.7  $\mu\text{m}$  would be more effective than the 1  $\mu\text{m}$  beads because ratio between the increase in magnetic force over the increase in surface tension and drag was greater, but no difference between the two was observed. The most likely explanation for this is that the same weight of 2.7  $\mu\text{m}$  beads actually has fewer beads than the same weight per ml 1  $\mu\text{m}$  beads. Magnetic dipole interactions drop off  $\sim 1/z^4$  (where  $z$  is the distance between beads). Adding more the MEB beads was also expected to boost the separation by reducing the average distance between the 128 beads and the MEB, but the lowest concentration tested (1  $\mu\text{g}$  MEB for every 5  $\mu\text{g}$  of 128 FcMBL beads) was still able to significantly improve separation in these experiments. This suggests that there are additional factors at work during the aggregation process which are not accounted for in the scaling estimates, such as the rate of aggregate formation, the average size of each aggregate and its configuration (in terms of MEB and FcMBL beads) which merit further study to optimize and understand the MEB phenomena. Overall the MEB greatly increased the reliability of the separation and retention of the FcMBL bead and bound bacteria during the sample prep procedure and they may prove useful for allowing many existing magnetic systems to work with much smaller magnetic beads than is currently possible. The Hex Rack and MEB technology both offer significant improvements on existing magnetic separation technologies. The Hex Rack technology can be scaled up or down for a wide range of tube sizes or adapted to fit around tubing for continuous separation applications. Together, they increase the separation speed and the holding force on the beads and tagged pathogens during the washes required in the sample preparation procedure.

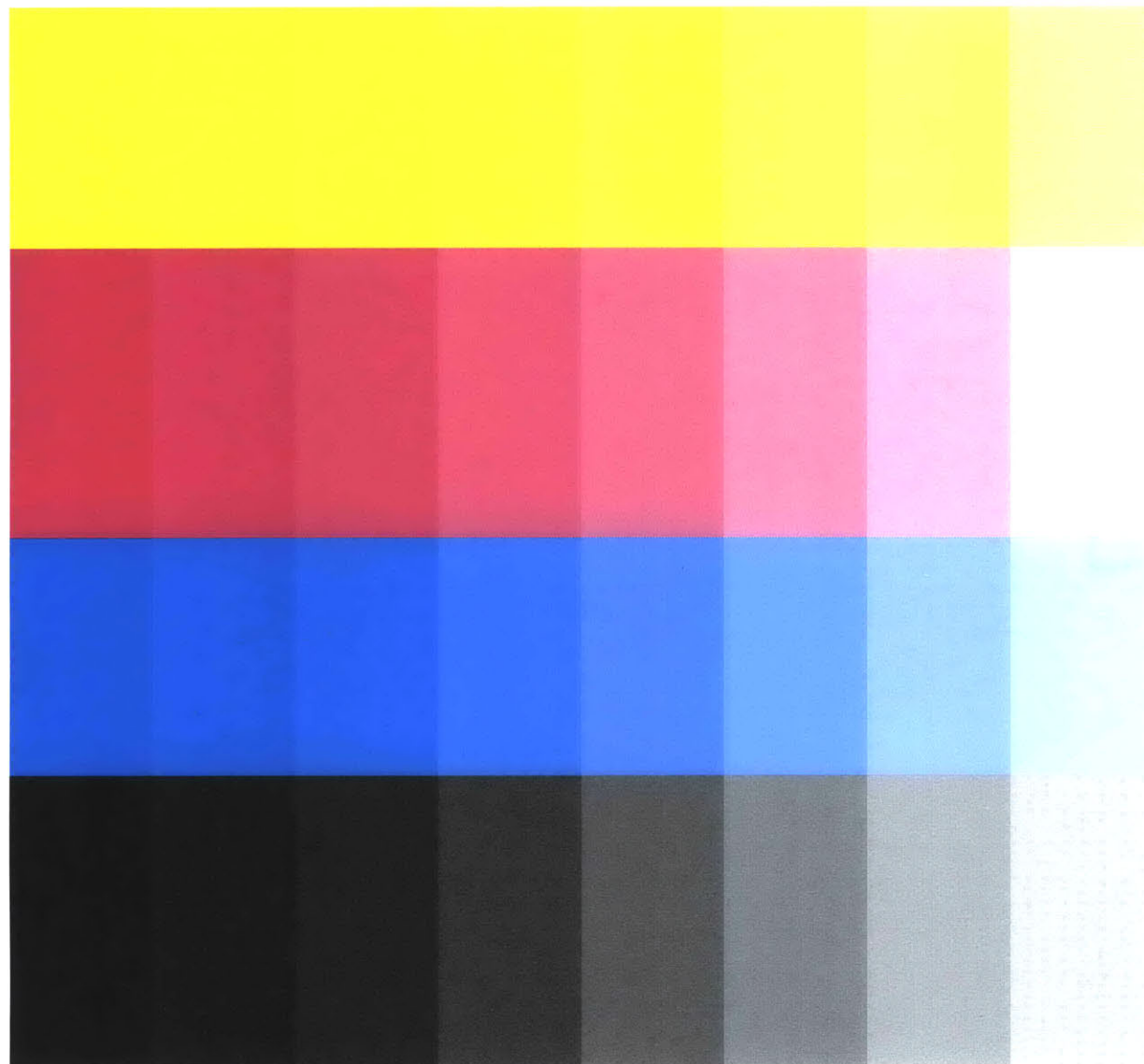
Two different DNA extraction kits were employed during these experiments to detect separated pathogens. The DNeasy Blood and Tissue kit (Qiagen) has been widely employed in literature [160]. It utilizes proteinase K to digest the bacterial cell wall and then uses solid phase extraction (SPE) on a silica column to bind the DNA, wash away contaminants and then elute

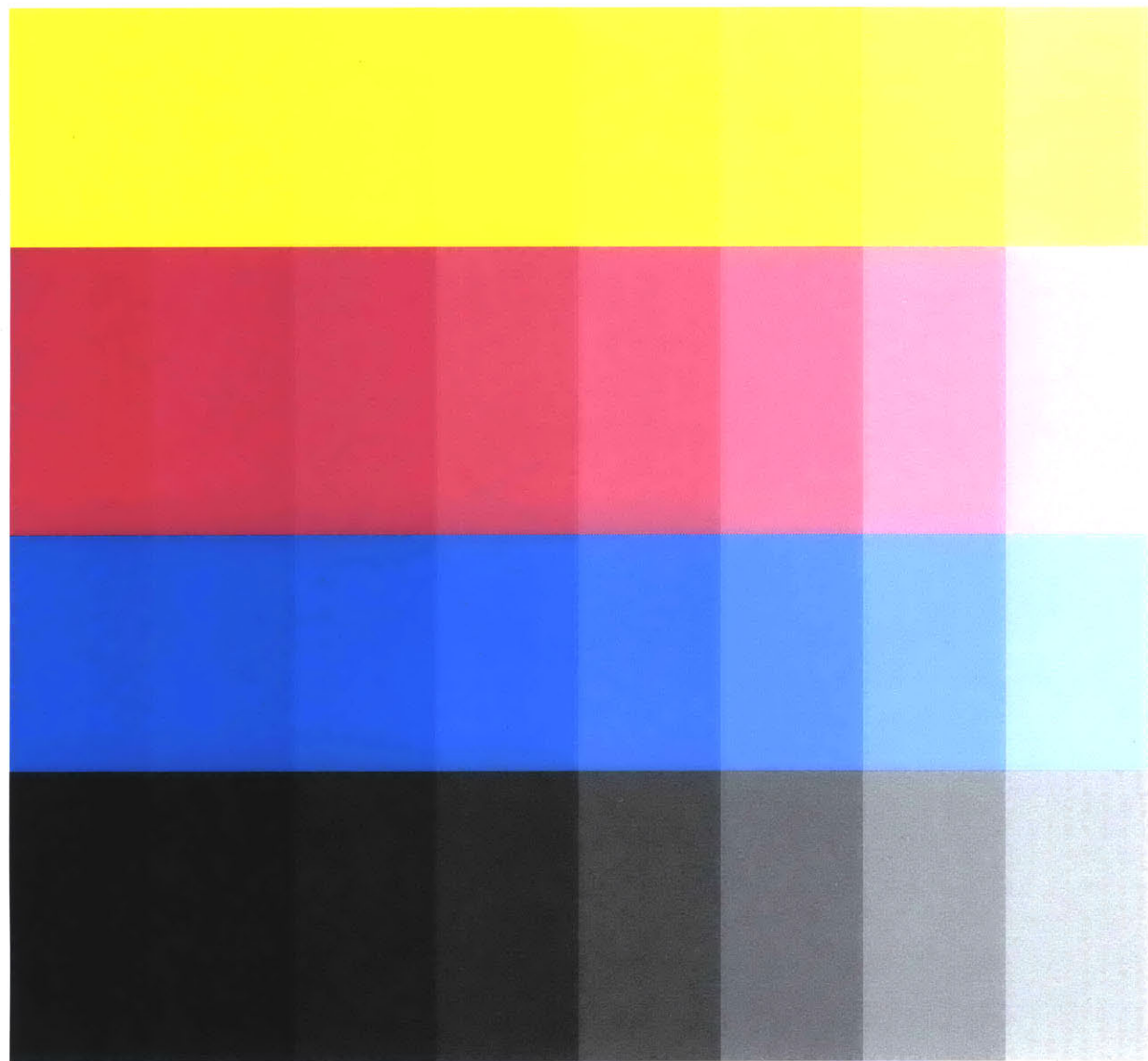
purified DNA [173]. It is quite effective but also quite costly in terms of hands on time and has several steps, making it more vulnerable to experimental error. The centrifugation steps make it difficult to automate without an elaborate robotic system. The PrepGEM kit (Zygem) employs a proprietary EA1 enzyme that is able to digest the cell and any nucleases to release the DNA in a closed tube assay. The digestion enzymes and buffer are added to the bacterial sample, and then incubated in the thermocycler to break down the bacterial cells and release the DNA. A final 95°C incubation denatures the extraction enzymes so that they do not interfere with the PCR reaction. This method takes the same amount of time as the SPE kit, but only has ~5 minutes of hands on time and is much easier to automate. Its main disadvantage is that the DNA is not as pure because the contaminating proteins are enzymatically degraded but not removed from the sample. Due to its simplicity, this method was employed for the majority of the tests except for the comparison with the commercial MoLYsis kit. Samples processed with the MoLYsis kit needed to be processed with proteinase K, so the DNeasy SPE kit was used for all three methods (FcMBL, MoLYsis, and Hybrid) to give a fair comparison. For all assays, extracted DNA was eluted or released into 100 µl of liquid and 5 µl of that solution was used for each qPCR reaction. This means that the PCR reactions from the 100 cfu/ml (containing 100 bacteria total in the starting sample), would have a maximum of 4-5 copies of the *E. coli* genome present. The 50 cfu/ml samples would contain 2-3 copies and the 10 cfu/ml samples would have between 0-1 genome copies. Therefore, the 50 cfu/ml samples are approaching the minimum copy number that it should be possible to detect with PCR with the 1 ml blood samples employed in this analysis. A larger sample size would be required to obtain enough genome copies to make detection at lower concentrations consistent.

My initial experiments to develop the FcMBL sample preparation procedure were evaluated with standard PCR and gel electrophoresis and compared to a 0 cfu/ml negative control to give a qualitative readout. This allowed me to find the correct treatments to determine an effective method to wash out the majority of PCR inhibitors in blood, check several *E. coli* specific primers and select the one that had the least non-specific amplification when exposed to human DNA from leukocytes, which would have given a large number of false positives in the SYBR green qPCR used to analyze later samples. Several universal primer sets have been used for attempting to detect bacteria out of blood using PCR, but these sets cannot differentiate between different pathogen species. For these initial characterizations, I wanted something more









specific and chose an *E. coli* specific target [29, 163]. This was particularly key for the yogurt samples, where DNA from the harmless *Lactobacillus* in the sample would be amplified with a universal primer set, regardless of the presence of *E. coli* in the sample. Cooling the blood samples to 4°C minimized leukocyte phagocytosis of the magnetic beads but did not entirely eliminate it, so the primary inhibitor remaining after the FcMBL procedure was human DNA from leukocytes that ingested or bound the FcMBL beads. Once a suitable primer set and primer concentration had been determined, there was minimal non specific amplification of human DNA in the processed samples (verified with both melt curve analysis and gel electrophoresis). Degrading this human DNA in the hybrid assay reduced this interference and increased the sensitivity and reliability of the FcMBL beads. Conversion to Taqman primers or fluorescent probes in the future would be prudent to minimize the risks from false positives due to non-specific amplification further [174-176]. We also plan to switch from using an *E. coli* specific primer in the near future to one of the universal 16s rDNA primers which amplifies a ribosomal DNA sequence that is highly conserved in most bacteria, at least for blood samples [53, 177, 178]. The added advantage of this approach is that each bacterium contains multiple copies of this sequence, making it easier to amplify than my current target (which has only one copy per genome) [179]. Work is ongoing in the sepsis group to optimize the bead surface and FcMBL properties to maximize pathogen binding and minimize non-specific adhesion or phagocytosis of human cells to further improve the purity of the recovered bacteria.

The FcMBL sample preparation procedure was not as dependable for detecting bacteria in blood as the MoLYsis kit, primarily due to the presence of human DNA inhibiting the PCR reaction for the FcMBL bead samples. The MoLYsis kit enzymatically degraded the majority of the human DNA in the sample, so it primarily suffered from contaminating proteins released by the lysed blood cells (such as hemoglobin). However, combining these two procedures created a hybrid sample preparation method increased the reliability of using the FcMBL beads. The pre-concentration of the pathogens with FcMBL beads allowed the vast majority of the blood cells and contaminating proteins to be removed before the lysis step and the MoLYsis kit destroyed the leukocytes separated with the beads and digested their DNA. The hybrid assay was able to detect down to 50 cfu/ml (2-3 gene copies/pcr) in 71% of the samples tested, very close to theoretical maximum sensitivity of the assay in its current form. So it appears the hybrid sample prep method is not only recovering nearly all the magnetically tagged pathogens, but also cleaning

their DNA sufficiently so that the PCR reaction can run at high efficiency. The hybrid method was also the only one of the three methods that could effectively remove the anticoagulant cocktail used to preserve packed red blood cells from the Blood Bank concentrates so that spiked bacteria could be detected with qPCR.

All of these experiments to compare the three methods were conducted using 1 ml blood samples due to limited availability of fresh blood for testing. I believe that the Hybrid method would have an advantage at higher sample volumes (5 or 10 ml of blood). The amount of contaminating proteins in the MoLYsis samples would rise with the sample volume, but the DNA contamination in the hybrid samples would be expected to stay constant, since the enzymatic digestion process would largely eliminate it. Currently, the chaotropic lysis buffer used in the MoLYsis kit causes a large fraction of the bound bacteria to detach from the FcMBL beads, so both magnetic and centrifugal separation methods must be employed in the hybrid method. Further testing should let us find a lysis buffer which does not compromise the FcMBL binding integrity so that the entire cleaning procedure can be done using magnetic separation alone. The FcMBL beads offer an effective method to remove the majority of blood contaminants and concentrate pathogens for PCR analysis, but more work to minimize bead phagocytosis and degrade human DNA should increase the reliability of this method even further and make it practical for use as a rapid PCR diagnostic for sepsis.

A simple adaptation of the FcMBL bead sample prep method also made it possible to bind, separate and purify bacteria from food (both yogurt and oat cereal) for rapid PCR detection. This demonstrates that these general opsonin beads have potential applications outside of the medical field for rapidly detecting bacterial contamination in other complex samples. Despite the yogurt samples containing a larger number of harmless *lactobacillus* bacteria, the beads bound and recovered enough of the spiked *E. coli* to detect down 22 cfu/gm in yogurt (1 gene copy/PCR). The high dilution factor required to homogenize the oat cereal limited the sensitivity to 1067 cfu/gm (5 gene copies/PCR) with a 4.5 ml sample. Concentrating bacteria out of larger sample volumes should boost the sensitivity further. It was much easier to obtain large amounts of food for testing (relative to blood), so these characterizations were carried out with 4.5 ml of the diluted food homogenates. The foods tested also contained fewer PCR inhibitors than blood, so sample preparation procedure was actually much more reliable in these samples than it was in blood.

Blood culture is currently the gold standard for sepsis diagnosis, but it is both slow and inaccurate [28, 29]. PCR offers an amplification method sensitive enough to directly detect pathogens and is believed by many clinicians to be the technology most likely to supplant blood culture systems in the near future. An added advantage over blood culture is that PCR can detect dead and damaged pathogens as well as viable ones, giving it a much larger sample population to detect [52]. However, the presence of inhibitors in blood currently limits its utility [69]. I have shown that the FcMBL magnetic beads offer a simple way to bind and hold pathogens from blood or other complex samples and wash away the majority of PCR inhibitors present. When combined with a method to remove contaminating human DNA from the bacteria, it forms a robust sample preparation method that can detect clinically relevant pathogen concentrations from blood with qPCR in less than four hours. These beads can bind and concentrate bacteria out of diverse food types, offering a rapid method to test for pathogenic bacterial contamination. Both PCR and AST testing methods are currently approved by the FDA for identifying bacteria in food, but both analysis methods still require at least one to two days of culture to obtain enough bacteria for identification [32, 34, 35]. During this time, the food must be stored at considerable expense. The FcMBL sample prep method has the potential to speed this process up so that contaminated food can be detected and destroyed before it leaves the processing plant without significantly interrupting the workflow by requiring storage for multiple days.

The primary limitation of PCR is that there is currently no reliable method to assess the antibiotic susceptibility of the detected pathogens in most cases. The sequence of resistance genes for methicillin and vancomycin are known and can be used to detect Methicillin-resistant *Staphylococcus aureus* (MRSA) and vancomycin-resistant *enterococci* (VRE), but the majority of them mutate rapidly, making them difficult to assess with fixed PCR primers [180, 181]. FcMBL beads can isolate viable pathogens, so it is possible that part of the concentrated bacteria can be set aside for subsequent testing if the PCR amplification identifies an infection.

## **Chapter 5 Conclusions**

### **5.1 Thesis Contributions**

The goal of this thesis was to develop general magnetic opsonin beads and show their potential applications for rapidly detecting sepsis, using both optical detection methods for detecting fungi and PCR amplification for detecting bacteria. The accomplishments in each of these areas are outlined below.

#### **5.1.1 General Magnetic Opsonins**

I have shown that the FcMBL beads can bind to a wide range of pathogens, including fungi, gram positive and gram negative bacteria. Bead size, concentration and FcMBL density was determined to give good binding to both bacteria and fungi in saline. Judging from experimental measurements and collision theory, for effective capture, the magnetic opsonin should be much smaller than the target pathogen (one tenth its radius or less). This minimizes the relative velocity of the bead and pathogen during their initial contact so that the FcMBL can establish binding avidity and allows a large number of the beads to attach to the surface of each pathogen. Consequently, the 1  $\mu\text{m}$  beads are more effective for binding to fungi ( $\sim 5\text{-}10 \mu\text{m}$  in diameter) while 128 nm beads are more effective for binding to bacteria ( $\sim 1\text{-}2 \mu\text{m}$ ) in diameter.

I also showed that these general magnetic opsonins could bind to bacteria and fungi in blood, although additional sample treatments were required to improve the binding because blood is a complex colloidal fluid. Diluting the blood 1:1 with saline increased the average spacing between the red blood cells, reducing the hydrodynamic shielding effect and letting the FcMBL beads circulate more effectively. Cooling the sample minimized the bead phagocytosis. Bead concentrations, mixing times and separation times for pathogen binding were also determined. With the correct treatment conditions, I was able to bind 86% of the fungi spiked into diluted blood. Bacteria proved more difficult because the smaller beads were more difficult to mechanically separate out of blood, which led me to design an improved separation system for them in chapter 4.

This is the first time that a single set of beads has been able to bind a diverse range of pathogens in blood. Previous immunomagnetic separation systems have relied on antibodies or lectins not compatible with blood [101-103]. I then go on to show that both fungi and bacteria can be rapidly isolated and detected from blood using the FcMBL general magnetic opsonins. Since these initial investigations, other members of the sepsis group have carried on these experiments and found sample treatments and bead chemistries for blood that have boosted the reproducibility and reliability of bacteria binding in blood [124].

### **5.1.2 Optical Detection of Fungi**

I developed the Magnetic Flux Concentrator and microdevice to balance the magnetic and convective forces on the FcMBL beads and magnetically tagged fungi. Capturing and concentrating magnetically tagged pathogens is a relatively simple matter, but trying to optically detect the captured pathogens is much more difficult because the large excess of magnetic beads required for capture interferes with the analysis. Other groups have developed microfluidic separation systems for isolating magnetically tagged cells from flowing fluid, but none of them have been able to optically detect the captured cells in the same device [72, 78, 82, 84]. The MFC and microdevice system allowed the fungi and excess beads to be concentrated out of blood and spread into a thin layer. After fluorescent staining, the captured fungi could be quantified by scanning over the microdevice with an epifluorescent microscope. Using this method, I was able to detect 67% of the magnetically tagged fungi in a 5 ml blood sample in less than three and a half hours and should be able to detect pathogen loads as low as 1 fungus/ml.

### **5.1.3 Rapid PCR Detection of Bacteria**

Using the FcMBL beads, I developed a sample preparation method to rapidly concentrate and purify pathogens out of complex samples for rapid PCR detection. To effectively isolate bacteria tagged with nanometer scale magnetic beads, I developed a novel magnetic rack system (the Hex Rack) that boosted the average and maximum magnetic gradients in the sample volume, leading to more effective pathogen separation. I also developed the Magnetic Enhancement Beads, which act as local magnetic flux concentrators inside of the sample to boost the separation efficiency of the nanometer scale beads and their retention during multiple wash steps. I showed that the combination of these two new separation technologies significantly improved separation and retention of magnetically tagged bacteria out of blood over the commercial



magnetic separation systems tested. These two technologies could have applications in a wide range of magnetic separation applications.

Using these two new separation technologies, I developed a simple protocol to rapidly separate bacteria out of complex samples such as blood or food matrices, concentrating the bacteria and removing PCR inhibitors from the sample at the same time. This protocol could rapidly separate the tagged pathogens out of blood and, when combined with an enzymatic treatment to remove inhibitory human DNA, was able to detect down to 100 cfu/ml with 99% confidence and down to 50 cfu/ml in the majority of samples. Performance of this Hybrid method was comparable to the existing state of the art method (MolYsis).

By adding a sample homogenization step, the FcMBL sample preparation method could also be readily adapted to bind, concentrate and purify bacteria out of different types of food samples. This demonstrates that the general magnetic opsonins can not only bind a wide range of pathogens, but also operate in wide range of different sample types. This is the first time that a single sample preparation method for PCR detection has been shown to function in blood, dairy and cereal samples.

## **5.2 Future Directions**

Both the general opsonin magnetic beads and magneto-fluidic separation technologies developed in this thesis have a wide range of potential future applications for concentrating and detecting rare cells out of large, complex samples.

Despite the impressive results already obtained with the general magnetic opsonin beads, work is ongoing at the Wyss Institute to optimize binding in blood and other complex samples. New recombinant versions of MBL and other lectins are being studied to develop an opsonin that can bind encapsulated bacteria (which neither wild type nor FcMBL can reliably bind) and other pathogens resistant to MBL. Different bead surface coatings are under investigation to further decrease the phagocytosis rate and perhaps dispense with the need to cool the sample. An in depth investigation of the optimal bead concentrations, size combinations (to enable simultaneous capture of bacteria and fungi) and sample additives is also underway. It has already been found that adding 10 mM glucose reduces non-specific binding to the FcMBL beads [124]. This work should allow us to lower the bead concentration and binding time while still retaining good pathogen binding in blood. The effect of different food components (simple and complex carbohydrates, proteins, fats) will be systematically investigated to determine the complete range

of sample types that the FcMBL beads can operate in and appropriate sample preparation methods for each food type of interest. Improvements in binding will also increase the versatility and reliability of the optical detection device and the sample preparation method for PCR.

For the optical detection microdevice, we will work on improving fluorescent pathogen labeling, probably using FISH, to provide a more versatile confirmation of the calcofluor staining in blood and determine species at the same time [28]. The system will then be automated and combined with an inexpensive epifluorescent microscope developed at the Wyss Institute to create a benchtop unit suitable for testing with clinical samples.

We will boost the sensitivity of the FcMBL bead sample preparation by combining aspects of the optical detection micro device with the MEB technology so that magnetically tagged bacteria from much larger blood and food sample volumes (up to 50 ml) can be concentrated and purified for PCR detection. In blood, we can already detect down to 50 cfu/ml in a one milliliter blood sample, so we should be able to boost this down to 1 cfu/ml by increasing the sample size. We are currently establishing collaborations with several companies in the food industry to develop a parallel project to detect bacterial and fungal contamination in a range of different food types, including yogurt, cereal, cookie dough, milk, and fruit juice, using PCR and optical detection methods.

In addition to improving pathogen separation, we will also improve the PCR reaction chemistry. The current qPCR assay used for amplification is basic, so we will be collaborating with experts in the PCR field to optimize the reaction conditions and prevent non-specific amplification. The use of universal PCR primers and multiplex PCR detection will be investigated to determine to create a diagnostic assay that can capture, concentrate, detect and identify bacteria in septic blood samples. This system will then be tested with clinical samples from local hospitals to show improved speed and reliability over blood culture diagnostics.

We also plan to continue investigating pathogen capture and detection with the FcMBL beads in other samples, including sputum (upper respiratory infections), urine (urinary tract infection), cerebrospinal fluid (meningitis) and platelet concentrates [33, 86, 131]. Platelet concentrates have a very short shelf life, of which a large percentage is consumed waiting for culture results to come back showing that they are safe for infusion [33, 86]. The FcMBL beads have the potential to reduce this testing time to a few hours so that the concentrates can be tested on the same day they will be used, greatly decreasing both storage costs and waste from

concentrates expiring during the testing process. The strategies for binding and separating magnetic beads out of blood can also be applied assays using antibody based beads as well, so the MFC microdevice, Hex rack and MEB may be of use in immunomagnetic separations to rapidly isolate and detect circulating tumor cells, viruses and protein biomarkers from biological samples.

## Chapter 6 References

1. Xia, N., et al., *Combined microfluidic-micromagnetic separation of living cells in continuous flow*. Biomedical Microdevices, 2006. **8**(4): p. 299-308.
2. Yung, C.W., et al., *Micromagnetic-microfluidic blood cleansing device*. Lab on a Chip, 2009. **9**(9): p. 1171-1177.
3. Jack, D.L., N.J. Klein, and M.W. Turner, *Mannose-binding lectin: targeting the microbial world for complement attack and opsonophagocytosis*. Immunological Reviews, 2001. **180**: p. 86-99.
4. Gupta, K., R.K. Gupta, and K. Hajela, *Disease associations of mannose-binding lectin & potential of replacement therapy*. Indian Journal of Medical Research, 2008. **127**(5): p. 431-440.
5. Turner, M.W., *Mannose-binding lectin: The pluripotent molecule of the innate immune system*. Immunology Today, 1996. **17**(11): p. 532-540.
6. Bone, R.C., *The Pathogenesis of Sepsis*. Annals of Internal Medicine, 1991. **115**(6): p. 457-469.
7. Reimer, L.G., M.L. Wilson, and M.P. Weinstein, *Update on detection of bacteremia and fungemia*. Clinical Microbiology Reviews, 1997. **10**(3): p. 444-&.
8. Cohen, J., *The immunopathogenesis of sepsis*. Nature, 2002. **420**(6917): p. 885-891.
9. Laforgia, N., et al., *Rapid detection of neonatal sepsis using polymerase chain reaction*. Acta Paediatrica, 1997. **86**(10): p. 1097-1099.
10. Dellinger, R.P., et al., *Surviving Sepsis Campaign: International guidelines for management of severe sepsis and septic shock: 2008*. Critical Care Medicine, 2008. **36**(1): p. 296-327.
11. Bone, R.C., et al., *Definitions for Sepsis and Organ Failure and Guidelines for the Use of Innovative Therapies in Sepsis*. Chest, 1992. **101**(6): p. 1644-1655.
12. Morace, G. and E. Borghi, *Fungal infections in ICU patients: epidemiology and the role of diagnostics*. Minerva Anestesiologica, 2010. **76**(11): p. 950-956.
13. Vergnano, S., et al., *Neonatal sepsis: an international perspective*. Archives of Disease in Childhood-Fetal and Neonatal Edition, 2005. **90**(3): p. 220-224.
14. Hall, M.J., Ph.D.; Sonja N. Williams, M.P.H.; Carol J. DeFrances, Ph.D.; and Aleksandr Golosinskiy, M.S., *Inpatient Care for Septicemia or Sepsis: A Challenge for Patients and Hospitals*. NCHS Data Brief, 2011. **62**.
15. Rangelfrausto, M.S., et al., *The Natural-History of the Systemic Inflammatory Response Syndrome (SIRS) - A Prospective-Study*. Jama-Journal of the American Medical Association, 1995. **273**(2): p. 117-123.
16. Kellogg, J.A., J.P. Manzella, and D.A. Bankert, *Frequency of low-level bacteremia in children from birth to fifteen years of age*. Journal of Clinical Microbiology, 2000. **38**(6): p. 2181-2185.
17. Doern, G.V., *Clinical Impact of Rapid In-Vitro Susceptibility Testing and Bacterial Identification - Reply*. Journal of Clinical Microbiology, 1995. **33**(2): p. 508-508.
18. Garnacho-Montero, J., et al., *Timing of adequate antibiotic therapy is a greater determinant of outcome than are TNF and IL-10 polymorphisms in patients with sepsis*. Critical Care, 2006. **10**(4): p. 12.
19. Guery, B., et al., *Management of invasive candidiasis and candidemia in adult non-neutropenic intensive care unit patients: Part II. Treatment*. Intensive Care Medicine, 2009. **35**(2): p. 206-214.
20. Davis, T.E., D.D. Fuller, and E.C. Aeschleman, *Rapid, Direct Identification of Sraphylococcus-Aureus and Streptococcus-Pneumoniae from Blood Cultures Using Commercial Immunological Kits and Modified Conventional Tests*. Diagnostic Microbiology and Infectious Disease, 1992. **15**(4): p. 295-300.
21. Pletz, M.W., N. Wellinghausen, and T. Welte, *Will polymerase chain reaction (PCR)-based diagnostics improve outcome in septic patients? A clinical view*. Intensive Care Medicine, 2011. **37**(7): p. 1069-1076.
22. Kaufman, D. and K.D. Fairchild, *Clinical microbiology of bacterial and fungal sepsis in very-low-birth-weight infants*. Clinical Microbiology Reviews, 2004. **17**(3): p. 638-+.
23. Lee, A., et al., *Detection of bloodstream infections in adults: How many blood cultures are needed?* Journal of Clinical Microbiology, 2007. **45**(11): p. 3546-3548.
24. *Guidelines for the management, of adults with hospital-acquired, ventilator-associated, and healthcare-associated pneumonia*. American Journal of Respiratory and Critical Care Medicine, 2005. **171**(4): p. 388-416.
25. Weinstein, M.P., et al., *The Clinical-Significance of Positive Blood Cultures - A Comprehensive Analysis of 500 Episodes of Bacteremia and Fungemia in Adults .I. Laboratory and Epidemiologic Observations*. Reviews of Infectious Diseases, 1983. **5**(1): p. 35-53.
26. Schelonka, R.L., et al., *Volume of blood required to detect common neonatal pathogens*. Journal of Pediatrics, 1996. **129**(2):

- p. 275-278.
27. Carrigan, S.D., G. Scott, and M. Tabrizian, *Toward resolving the challenges of sepsis diagnosis*. *Clinical Chemistry*, 2004. **50**(8): p. 1301-1314.
  28. Peters, R.P.H., et al., *New developments in the diagnosis of bloodstream infections*. *Lancet Infectious Diseases*, 2004. **4**(12): p. 751-760.
  29. Pammi, M., et al., *Molecular Assays in the Diagnosis of Neonatal Sepsis: A Systematic Review and Meta-analysis*. *Pediatrics*, 2011. **128**(4): p. E973-E985.
  30. Stoll, B.J. and N. Hansen, *Infections in VLBW infants: Studies from the NICHD Neonatal Research Network*. *Seminars in Perinatology*, 2003. **27**(4): p. 293-301.
  31. Montag, T., *Strategies of bacteria screening in cellular blood components*. *Clinical Chemistry and Laboratory Medicine*, 2008. **46**(7): p. 926-932.
  32. Swaminathan, B. and P. Feng, *Rapid Detection of Food-Borne Pathogenic Bacteria*. *Annual Review of Microbiology*, 1994. **48**: p. 401-426.
  33. Blajchman, M.A., M. Goldman, and F. Baeza, *Improving the bacteriological safety of platelet transfusions*. *Transfusion Medicine Reviews*, 2004. **18**(1): p. 11-24.
  34. Liming, S.H., et al., *Detection of Listeria monocytogenes in fresh produce using molecular beacon - Real-time PCR technology*. *Journal of Food Science*, 2004. **69**(8): p. M240-M245.
  35. Tice, G., et al., *DuPont Qualicon BAX (R) System Polymerase Chain Reaction Assay*. *Journal of Aoac International*, 2009. **92**(6): p. 1902-1905.
  36. Todar, K. *Control of Microbial Growth*. *Todar's Online Textbook of Bacteriology* 2012 [cited; Available from: [http://textbookofbacteriology.net/control\\_6.html](http://textbookofbacteriology.net/control_6.html)].
  37. Klouche, M. and U. Schroder, *Rapid methods for diagnosis of bloodstream infections*. *Clinical Chemistry and Laboratory Medicine*, 2008. **46**(7): p. 888-908.
  38. *SepsiTest*. Goffin Molecular Technologies [cited 2013 March 21]; Available from: <http://www.goffinmoleculartechnologies.com/sepsitest-selectna/>.
  39. Giamarellos-Bourboulis, E.J., et al., *Should procalcitonin be introduced in the diagnostic criteria for the systemic inflammatory response syndrome and sepsis?* *Journal of Critical Care*, 2004. **19**(3): p. 152-157.
  40. Moussaoui, W., et al., *Matrix-assisted laser desorption ionization time-of-flight mass spectrometry identifies 90% of bacteria directly from blood culture vials*. *Clinical Microbiology and Infection*, 2010. **16**(11): p. 1631-1638.
  41. Drancourt, M., *Detection of microorganisms in blood specimens using matrix-assisted laser desorption ionization time-of-flight mass spectrometry: a review*. *Clinical Microbiology and Infection*, 2010. **16**(11): p. 1620-1625.
  42. Prod'hom, G., et al., *Matrix-Assisted Laser Desorption Ionization-Time of Flight Mass Spectrometry for Direct Bacterial Identification from Positive Blood Culture Pellets*. *Journal of Clinical Microbiology*, 2010. **48**(4): p. 1481-1483.
  43. Christner, M., et al., *Rapid Identification of Bacteria from Positive Blood Culture Bottles by Use of Matrix-Assisted Laser Desorption-Ionization Time of Flight Mass Spectrometry Fingerprinting*. *Journal of Clinical Microbiology*, 2010. **48**(5): p. 1584-1591.
  44. Ferroni, A., et al., *Real-Time Identification of Bacteria and Candida Species in Positive Blood Culture Broths by Matrix-Assisted Laser Desorption Ionization-Time of Flight Mass Spectrometry*. *Journal of Clinical Microbiology*, 2010. **48**(5): p. 1542-1548.
  45. La Scola, B. and D. Raoult, *Direct Identification of Bacteria in Positive Blood Culture Bottles by Matrix-Assisted Laser Desorption Ionisation Time-of-Flight Mass Spectrometry*. *Plos One*, 2009. **4**(11).
  46. Lagace-Wiens, P.R.S., et al., *Identification of Blood Culture Isolates Directly from Positive Blood Cultures by Use of Matrix-Assisted Laser Desorption Ionization-Time of Flight Mass Spectrometry and a Commercial Extraction System: Analysis of Performance, Cost, and Turnaround Time*. *Journal of Clinical Microbiology*, 2012. **50**(10): p. 3324-3328.
  47. Szabados, F., et al., *The sensitivity of direct identification from positive BacT/ALERT (TM) (bioMerieux) blood culture bottles by matrix-assisted laser desorption ionization time-of-flight mass spectrometry is low*. *Clinical Microbiology and Infection*, 2011. **17**(2): p. 192-195.
  48. Loeffler, J., et al., *Automated extraction of genomic DNA from medically important yeast species and filamentous fungi by using the MagNA pure LC system*. *Journal of Clinical Microbiology*, 2002. **40**(6): p. 2240-2243.
  49. Marinach-Patrice, C., et al., *Use of mass spectrometry to identify clinical Fusarium isolates*. *Clinical Microbiology and Infection*, 2009. **15**(7): p. 634-642.
  50. Marklein, G., et al., *Matrix-Assisted Laser Desorption Ionization-Time of Flight Mass Spectrometry for Fast and Reliable Identification of Clinical Yeast Isolates*. *Journal of Clinical Microbiology*, 2009. **47**(9): p. 2912-2917.
  51. Metwally, L., et al., *Improving molecular detection of Candida DNA in whole blood: comparison of seven fungal DNA*

- extraction protocols using real-time PCR.* Journal of Medical Microbiology, 2008. **57**(3): p. 296-303.
52. Wilmore, D.W., *Polymerase chain reaction surveillance of microbial DNA in critically ill patients: Exploring another new frontier.* Annals of Surgery, 1998. **227**(1): p. 10-11.
  53. Wu, Y.D., et al., *Gram stain-specific-probe-based real-time PCR for diagnosis and discrimination of bacterial neonatal sepsis.* Journal of Clinical Microbiology, 2008. **46**(8): p. 2613-2619.
  54. Burns, M.A., et al., *An integrated nanoliter DNA analysis device.* Science, 1998. **282**(5388): p. 484-487.
  55. Easley, C.J., et al., *A fully integrated microfluidic genetic analysis system with sample-in-answer-out capability.* Proceedings of the National Academy of Sciences of the United States of America, 2006. **103**(51): p. 19272-19277.
  56. Kaigala, G.V., et al., *Automated screening using microfluidic chip-based PCR and product detection to assess risk of BK virus-associated nephropathy in renal transplant recipients.* Electrophoresis, 2006. **27**(19): p. 3753-3763.
  57. Lagally, E.T., C.A. Emrich, and R.A. Mathies, *Fully integrated PCR-capillary electrophoresis microsystem for DNA analysis.* Lab on a Chip, 2001. **1**(2): p. 102-107.
  58. Lagally, E.T., et al., *Integrated portable genetic analysis microsystem for pathogen/infectious disease detection.* Analytical Chemistry, 2004. **76**(11): p. 3162-3170.
  59. Legendre, L.A., et al., *A simple, valveless microfluidic sample preparation device for extraction and amplification of DNA from nanoliter-volume samples.* Analytical Chemistry, 2006. **78**(5): p. 1444-1451.
  60. Munchow, G., et al., *Automated chip-based device for simple and fast nucleic acid amplification.* Expert Review of Molecular Diagnostics, 2005. **5**(4): p. 613-620.
  61. Park, S., et al., *Advances in microfluidic PCR for point-of-care infectious disease diagnostics.* Biotechnology Advances, 2011. **29**(6): p. 830-839.
  62. Pippner, J., et al., *Clockwork PCR including sample preparation.* Angewandte Chemie-International Edition, 2008. **47**(21): p. 3900-3904.
  63. Young, B., et al., *Wheater's Functional Histology* 5ed. 2007, China: Elsevier Limited.
  64. Lien, K.Y., et al., *Extraction of genomic DNA and detection of single nucleotide polymorphism genotyping utilizing an integrated magnetic bead-based microfluidic platform.* Microfluidics and Nanofluidics, 2009. **6**(4): p. 539-555.
  65. Liu, R.H., et al., *Self-contained, fully integrated biochip for sample preparation, polymerase chain reaction amplification, and DNA microarray detection.* Analytical Chemistry, 2004. **76**(7): p. 1824-1831.
  66. Pippner, J., et al., *Catching bird flu in a droplet.* Nature Medicine, 2007. **13**(10): p. 1259-1263.
  67. Wilding, P., et al., *Integrated cell isolation and polymerase chain reaction analysis using silicon microfilter chambers.* Analytical Biochemistry, 1998. **257**(2): p. 95-100.
  68. Yuen, P.K., et al., *Microchip module for blood sample preparation and nucleic acid amplification reactions.* Genome Research, 2001. **11**(3): p. 405-412.
  69. Abu al-Soud, W. and P. Radstrom, *Purification and characterization of PCR-inhibitory components in blood cells.* Journal of Clinical Microbiology, 2001. **39**(2): p. 485-493.
  70. Molday, R.S., S.P.S. Yen, and A. Rembaum, *Application of Magnetic Microspheres in Labeling and Separation of Cells.* Nature, 1977. **268**(5619): p. 437-438.
  71. Sinha, A., R. Ganguly, and I.K. Puri, *Magnetic separation from superparamagnetic particle suspensions.* Journal of Magnetism and Magnetic Materials, 2009. **321**(14): p. 2251-2256.
  72. Fallesen, T., et al., *Magnet polepiece design for uniform magnetic force on superparamagnetic beads.* Review of Scientific Instruments, 2010. **81**(7).
  73. Guo, J.M., et al., *Combined use of positive and negative immunomagnetic isolation followed by real-time RT-PCR for detection of the circulating tumor cells in patients with colorectal cancers.* Journal of Molecular Medicine-Jmm, 2004. **82**(11): p. 768-774.
  74. Wang, N., J.P. Butler, and D.E. Ingber, *Mechanotransduction Across the Cell-Surface and Through the Cytoskeleton.* Science, 1993. **260**(5111): p. 1124-1127.
  75. Wills, T.B., et al., *Immunomagnetic isolation of canine circulating endothelial and endothelial progenitor cells.* Veterinary Clinical Pathology, 2009. **38**(4): p. 437-442.
  76. Cebers, A. and M. Ozols, *Dynamics of an active magnetic particle in a rotating magnetic field.* Physical Review E, 2006. **73**(2).
  77. Kinnunen, P., et al., *Monitoring the growth and drug susceptibility of individual bacteria using asynchronous magnetic bead rotation sensors.* Biosensors & Bioelectronics, 2010. **26**(5): p. 2751-2755.
  78. Weddemann, A., et al., *A hydrodynamic switch: Microfluidic separation system for magnetic beads.* Applied Physics Letters, 2009. **94**(17).
  79. Grutzkau, A. and A. Radbruch, *Small But Mighty: How the MACS (R)-Technology Based on Nanosized Superparamagnetic*

- Particles has Helped to Analyze the Immune System Within the Last 20 Years. Cytometry Part A, 2010. 77A(7): p. 643-647.*
80. Furlani, E.P., et al., *A model for predicting magnetic particle capture in a microfluidic bioseparator*. Biomedical Microdevices, 2007. **9**(4): p. 451-463.
  81. Modak, N., A. Datta, and R. Ganguly, *Cell separation in a microfluidic channel using magnetic microspheres*. Microfluidics and Nanofluidics, 2009. **6**(5): p. 647-660.
  82. Pekas, N., et al., *Magnetic particle diverter in an integrated microfluidic format*. Journal of Magnetism and Magnetic Materials, 2005. **293**(1): p. 584-588.
  83. Smistrup, K., et al., *Magnetic separation in microfluidic systems using microfabricated electromagnets-experiments and simulations*. Journal of Magnetism and Magnetic Materials, 2005. **293**(1): p. 597-604.
  84. Baier, T., et al., *Modelling immunomagnetic cell capture in CFD*. Microfluidics and Nanofluidics, 2009. **7**(2): p. 205-216.
  85. Mikkelsen, C. and H. Bruus, *Microfluidic capturing-dynamics of paramagnetic bead suspensions*. Lab on a Chip, 2005. **5**(11): p. 1293-1297.
  86. Mohanty, S., T. Baier, and F. Schonfeld, *Three-dimensional CFD modelling of a continuous immunomagnetophoretic cell capture in BioMEMs*. Biochemical Engineering Journal, 2010. **51**(3): p. 110-116.
  87. Antolovic, D., et al., *Heterogeneous detection of circulating tumor cells in patients with colorectal cancer by immunomagnetic enrichment using different EpCAM-specific antibodies*. Bmc Biotechnology, 2010. **10**.
  88. Zigeuner, R.E., et al., *Isolation of circulating cancer cells from whole blood by immunomagnetic cell enrichment and unenriched immunocytochemistry in vitro*. Journal of Urology, 2003. **169**(2): p. 701-705.
  89. Condiotti, R., et al., *Ex vivo expansion of CD56(+) cytotoxic cells from human umbilical cord blood*. Experimental Hematology, 2001. **29**(1): p. 104-113.
  90. Xia, N., et al., *Combined microfluidic-micromagnetic separation of living cells in continuous flow*. Biomed. Microdevices, 2006. **8**(4): p. 299-308.
  91. Yung, C.W., et al., *Micromagnetic-microfluidic blood cleansing device*. Lab Chip, 2009. **9**(9): p. 1171-1177.
  92. El-Boubbou, K., C. Gruden, and X. Huang, *Magnetic glyco-nanoparticles: A unique tool for rapid pathogen detection, decontamination, and strain differentiation*. Journal of the American Chemical Society, 2007. **129**(44): p. 13392-+.
  93. Devi, R.V., M.R. Basilrose, and P.D. Mercy, *Prospect for lectins in arthropods*. Italian Journal of Zoology, 2010. **77**(3): p. 254-260.
  94. Kawabata, S., et al., *Role of tachylectins in host defense of the Japanese horseshoe crab Tachypleus tridentatus, in Phylogenetic Perspectives on the Vertebrate Immune System*. 2001. p. 195-202.
  95. Koizumi, N., et al., *Lipopolysaccharide-binding proteins and their involvement in the bacterial clearance from the hemolymph of the silkworm Bombyx mori*. European Journal of Biochemistry, 1997. **248**(1): p. 217-224.
  96. Kawasaki, K., T. Kubo, and S. Natori, *A Novel Role of Periplaneta Lectin as an Opsonin to Recognize 2-Keto-3-Deoxy Octonate Residues of Bacterial Lipopolysaccharides*. Comparative Biochemistry and Physiology B-Biochemistry & Molecular Biology, 1993. **106**(3): p. 675-680.
  97. Wilson, R., C.W. Chen, and N.A. Ratcliffe, *Innate immunity in insects: The role of multiple, endogenous serum lectins in the recognition of foreign invaders in the cockroach, Blaberus discoidalis*. Journal of Immunology, 1999. **162**(3): p. 1590-1596.
  98. Boswell, C.A. and C.J. Bayne, *Isolation, Characterization and Functional Assessment of a Hemagglutinin from the Plasmid of Biomphalaria-Glabrata, Intermediate Host of Schistosoma-Mansoni*. Developmental and Comparative Immunology, 1984. **8**(3): p. 559-568.
  99. Ip, W.K.E., et al., *Mannose-binding lectin and innate immunity*. Immunological Reviews, 2009. **230**: p. 9-21.
  100. Lackie, A.M., *The Specificity of the Serum Agglutinins of Periplaneta-Americana and Schistocerca-Gregaria and Its Relationship to the Insects Immune-Response*. Journal of Insect Physiology, 1981. **27**(2): p. 139-143.
  101. Chattera.A and W.C. Boyd, *A Specific Anti-B Lectin for Routine Diagnostic Purposes*. Journal of Immunology, 1966. **96**(5): p. 898-&.
  102. Coombe, D.R., P.L. Ey, and C.R. Jenkin, *Self Non-Self Recognition in Invertebrates*. Quarterly Review of Biology, 1984. **59**(3): p. 231-255.
  103. Tripp, M.R., *How Do Invertebrates Recognize Foreignness - A Citation-Classic Commentary on Hemagglutinin in the Blood of the Oyster, Crassostrea-Virginica* Current Contents/Agriculture Biology & Environmental Sciences, 1991(26): p. 8-8.
  104. Anders, E.M., C.A. Hartley, and D.C. Jackson, *Bovine and Mouse Serum Beta-Inhibitors of Influenza-A Viruses are Mannose-Binding Lectins*. Proceedings of the National Academy of Sciences of the United States of America, 1990. **87**(12): p. 4485-4489.

105. Epstein, J., et al., *The collectins in innate immunity*. Current Opinion in Immunology, 1996. **8**(1): p. 29-35.
106. Kuhlman, M., K. Joiner, and R.A.B. Ezekowitz, *The Human Mannose-Binding Protein Functions as an Opsonin*. Journal of Experimental Medicine, 1989. **169**(5): p. 1733-1745.
107. Takahashi, K., et al., *The mannose-binding lectin: a prototypic pattern recognition molecule*. Current Opinion in Immunology, 2006. **18**(1): p. 16-23.
108. Fujita, T., M. Matsushita, and Y. Endo, *The lectin-complement pathway - its role in innate immunity and evolution*. Immunological Reviews, 2004. **198**: p. 185-202.
109. Turner, M.W., *Mannose-binding lectin: The pluripotent molecule of the innate immune system (vol 17, pg 532, 1996)*. Immunology Today, 1997. **18**(2): p. 98-98.
110. Endo, Y., M. Takahashi, and T. Fujita, *Lectin complement system and pattern recognition*. Immunobiology, 2006. **211**(4): p. 283-293.
111. Drickamer, K., *Engineering Galactose-Binding Activity into a C-Type Mannose-Binding Protein*. Nature, 1992. **360**(6400): p. 183-186.
112. Weis, W.I., K. Drickamer, and W.A. Hendrickson, *Structure of a C-Type Mannose-Binding Protein Complexed with an Oligosaccharide* Nature, 1992. **360**(6400): p. 127-134.
113. Kilpatrick, D.C., *Phospholipid-binding activity of human mannan-binding lectin*. Immunology Letters, 1998. **61**(2-3): p. 191-195.
114. Palaniyar, N., et al., *Nucleic acid is a novel ligand for innate, immune pattern recognition collectins surfactant proteins A and D and mannose-binding lectin*. Journal of Biological Chemistry, 2004. **279**(31): p. 32728-32736.
115. Palaniyar, N., J. Nadesalingam, and K.B.M. Reid, *Innate immune collectins bind nucleic acids and enhance DNA clearance in vitro*, in *Apoptosis: from Signaling Pathways to Therapeutic Tools*. 2003, New York Acad Sciences: New York. p. 467-470.
116. Gadjeva, M., K. Takahashi, and S. Thiel, *Mannan-binding lectin - a soluble pattern recognition molecule*. Molecular Immunology, 2004. **41**(2-3): p. 113-121.
117. Iobst, S.T., et al., *Binding of Sugar Ligands to Ca<sup>2+</sup>-Dependent Animal Lectin .I. Analysis of Mannose-Binding by Site-Directed Mutagenesis and NMR*. Journal of Biological Chemistry, 1994. **269**(22): p. 15505-15511.
118. Kawasaki, N., T. Kawasaki, and I. Yamashina, *Isolation and Characterization of a Mannan-Binding Protein from Human-Serum*. Journal of Biochemistry, 1983. **94**(3): p. 937-947.
119. Eisen, D.P., et al., *Low serum mannose-binding lectin level increases the risk of death due to pneumococcal infection*. Clinical Infectious Diseases, 2008. **47**(4): p. 510-516.
120. Takahashi, K., et al., *Mannose-binding lectin and its associated proteases (MASPs) mediate coagulation and its deficiency is a risk factor in developing complications from infection, including disseminated intravascular coagulation*. Immunobiology, 2011. **216**(1-2): p. 96-102.
121. Valdimarsson, H., et al., *Human plasma-derived mannose-binding lectin: A phase I safety and pharmacokinetic study*. Scandinavian Journal of Immunology, 2004. **59**(1): p. 97-102.
122. *Electrophoresis*. Biology Reference 2013 [cited; Available from: <http://www.biologyreference.com/Dn-Ep/Electrophoresis.html>].
123. Barelle, C.J., et al., *GFP as a quantitative reporter of gene regulation in Candida albicans*. Yeast, 2004. **21**(4): p. 333-340.
124. Super, M., et al., *An engineered mannose-binding lectin (FcMBL) opsonin for generic pathogen capture and sepsis diagnosis* IN PREPARATION, 2013.
125. Truskey, G.A., F. Yuan, and D.F. Katz, *Transport Phenomena in Biological Systems*. 2004, Upper Saddle River, NJ: Pearson Prentice Hall.
126. Porter, J., et al., *An evaluation of lectin-mediated magnetic bead cell sorting for the targeted separation of enteric bacteria*. Journal of Applied Microbiology, 1998. **84**(5): p. 722-732.
127. Scott, M.A., J.M. Davis, and K.A. Schwartz, *Staphylococcal protein A binding to canine IgG and IgM*. Veterinary Immunology and Immunopathology, 1997. **59**(3-4): p. 205-212.
128. Kaibara, M., *Rheological Studies on Blood-Coagulation and Network Formation of Fibrin*. Polymer Gels and Networks, 1994. **2**(1): p. 1-28.
129. Koeppe, B.M. and B.A. Stanton, *Berne & Levy Physiology*. 6 ed. 2008, Philadelphia, PA: Mosby Elsevier.
130. *Blood Components*. 2011 [cited 2013 March 21]; Available from: <http://www.tbceb.net/a-1273.htm>.
131. Kumar, V., et al., *Robbins and Cotran Pathological Basis of Disease*. 8 ed. 2010, Philadelphia, PA: Elsevier Inc. .
132. Gomez, S.M., et al., *Capture of rare cells in suspension with antibody-coated polystyrene beads*. Biotechnology Progress, 1999. **15**(2): p. 238-244.



133. Kundu, P.K. and I.M. Cohen, *Fluid Mechanics*. 4 ed. 2008, Burlington, MA: Elsevier Inc.
134. Kim, D., et al., *Amphiphilic polymer-coated hybrid nanoparticles as CT/MRI dual contrast agents*. *Nanotechnology*, 2011. **22**(15).
135. Ma, H.L., et al., *Magnetic targeting after femoral artery administration and biocompatibility assessment of superparamagnetic iron oxide nanoparticles*. *Journal of Biomedical Materials Research Part A*, 2008. **84A**(3): p. 598-606.
136. Kaim, A.H., et al., *MR imaging with ultrasmall superparamagnetic iron oxide particles in experimental soft-tissue infections in rats*. *Radiology*, 2002. **225**(3): p. 808-814.
137. Lee, H.Y., et al., *Synthesis and characterization of PVP-coated large core iron oxide nanoparticles as an MRI contrast agent*. *Nanotechnology*, 2008. **19**(16).
138. Ugaki, H., et al., *Safety and efficacy of lower-dose unfractionated heparin for prophylaxis of deep vein thrombosis and pulmonary embolism in an Asian population*. *Blood Coagulation & Fibrinolysis*, 2008. **19**(6): p. 585-589.
139. Elalamy, I., M.H. Horellou, and M.M. Samama, *Pharmacological Characteristics of Heparins*. *Semaine Des Hopitaux*, 1995. **71**(13-14): p. 389-400.
140. Koepfen, B.M. and B.A. Stanton, *Renal Physiology* 4ed. The Mosby Physiology Monograph Series. 2007, Philadelphia: Mosby Elsevier.
141. Mellau, L.S.B. and R.J. Jorgensen, *Does EDTA-infusion affect calcium homeostasis leading to increased resistance to challenge?* *Acta Veterinaria Scandinavica*, 2003: p. 29-34.
142. Fonnun, G., et al., *Characterisation of Dynabeads (R) by magnetization measurements and Mossbauer spectroscopy*. *Journal of Magnetism and Magnetic Materials*, 2005. **293**(1): p. 41-47.
143. Kang, J.H., et al., *Bioinspired Spleen-On-A-Chip for Sepsis Therapy*. IN PREPARATION, 2013.
144. Deponte, S., et al., *Biomagnetic separation of Escherichia coli by use of anion-exchange beads: measurement and modeling of the kinetics of cell-bead interactions*. *Analytical and Bioanalytical Chemistry*, 2004. **379**(3): p. 419-426.
145. McCloskey, K.E., J.J. Chalmers, and M. Zborowski, *Magnetic cell separation: Characterization of magnetophoretic mobility*. *Analytical Chemistry*, 2003. **75**(24): p. 6868-6874.
146. Spielman, L.A., *Particle Capture from Low-Speed Laminar Flows*. *Annual Review of Fluid Mechanics*, 1977. **9**: p. 297-319.
147. Vito, R.P. and S.A. Dixon, *Blood vessel constitutive models-1995-2002*. *Annual Review of Biomedical Engineering*, 2003. **5**: p. 413-439.
148. Xia, Y.N. and G.M. Whitesides, *Soft lithography*. *Annual Review of Materials Science*, 1998. **28**: p. 153-184.
149. *Countess - A small, cheap and handy automated cell counter*. Groco ehf. 2008 [cited 2013 March 21]; Available from: [http://www.groco.is/groco/is/search/news/Default.asp?ew\\_0\\_a\\_id=317160](http://www.groco.is/groco/is/search/news/Default.asp?ew_0_a_id=317160).
150. *Just Released-November, 2010—Our Newest Cellular Analysis Products and Technologies*. 2013 [cited 2013 March 21]; Available from: <http://www.invitrogen.com/site/us/en/home/References/Newsletters-and-Journals/BioProbes-Journal-of-Cell-Biology-Applications/BioProbes-Issues-2010/BioProbes-63/Newest-Cellular-Analysis-Products-and-Technologies-Nov-2010.html>.
151. *NE-1000 Programmable Single Syringe Pump*. 2013 [cited 2013 March 21]; Available from: <http://www.syringepump.com/NE-1000.php>.
152. Schaller, V., et al., *Motion of nanometer sized magnetic particles in a magnetic field gradient*. *Journal of Applied Physics*, 2008. **104**(9).
153. Jaeger, R.C., *Introduction to Microelectronic Fabrication*. 2 ed. Modular Series on Solid State Devices ed. G.W. Neudeck and R.F. Pierret. Vol. V. 2002.
154. Young, E.W.K., et al., *Rapid Prototyping of Arrayed Microfluidic Systems in Polystyrene for Cell-Based Assays*. *Analytical Chemistry*, 2011. **83**(4): p. 1408-1417.
155. Rostaing, H., et al., *A micromagnetic actuator for biomolecule manipulation*. *Sensors and Actuators a-Physical*, 2007. **135**(2): p. 776-781.
156. Fedosov, D.A., et al., *Blood Flow and Cell-Free Layer in Microvessels*. *Microcirculation*, 2010. **17**(8): p. 615-628.
157. Mach, A.J. and D. Di Carlo, *Continuous Scalable Blood Filtration Device Using Inertial Microfluidics*. *Biotechnology and Bioengineering*, 2010. **107**(2): p. 302-311.
158. Pfaller, M.A. and D.J. Diekema, *Epidemiology of invasive candidiasis: a persistent public health problem*. *Clinical Microbiology Reviews*, 2007. **20**(1): p. 133-+.
159. Worth, L.J., et al., *Optimizing antifungal drug dosing and monitoring to avoid toxicity and improve outcomes in patients with hematological disorders*. *Internal Medicine Journal*, 2008. **38**(6B): p. 521-537.
160. Hansen, W.L.J., C.A. Bruggeman, and P.F.G. Wolfs, *Evaluation of New Preanalysis Sample Treatment Tools and*

- DNA Isolation Protocols To Improve Bacterial Pathogen Detection in Whole Blood. *Journal of Clinical Microbiology*, 2009. **47**(8): p. 2629-2631.
161. *Magnets for Molecular and Cell Separation Applications*. 2011 [cited 2013 March 21]; Available from: <http://www.b2b.invitrogen.com/site/us/en/home/brands/Dynal/Magnets.html>.
162. *Technology - Pathogen DNA Isolation*. MolYsis [cited 2013 March 21]; Available from: <http://www.molzym.com/products/dna-isolation-products/pathogen-dna-molysis/molysis-technology.html>.
163. Maheux, A.F., et al., *Analytical comparison of nine PCR primer sets designed to detect the presence of Escherichia coli/Shigella in water samples*. *Water Research*, 2009. **43**(12): p. 3019-3028.
164. Alocilja, E.C., E. Dreelin, and J.B. Rose, *Rapid and Quantitative Detection of Helicobacter Pylori and E. Coli O157 in Well Water Using a Nano-Wired Biosensor and QPCR*, E.P. Agency, Editor. 2008.
165. *Escherichia coli ATCC 8739*. Genome Atlas Database 2013 [cited 2013 01/31/2013]; Available from: <http://www.cbs.dtu.dk/services/GenomeAtlas-3.0/?action=acct&pid=18083&k=Bacteria&pt=g>.
166. *Surface Tension*. Flickr 2013 [cited 2013 March 21]; Available from: <http://www.flickr.com/photos/placbo/1269184231/>.
167. Balmer, D. *Separation of Boundary Layers*. [cited 2013 March 21]; Available from: <http://www.see.ed.ac.uk/~johnc/teaching/fluidmechanics4/2003-04/fluids14/separation.html>.
168. Hospodsky, D., N. Yamamoto, and J. Peccia, *Accuracy, Precision, and Method Detection Limits of Quantitative PCR for Airborne Bacteria and Fungi*. *Applied and Environmental Microbiology*, 2010. **76**(21): p. 7004-7012.
169. Finney, D.J., *Probit Analysis*. 3 ed. 1980, Cambridge: Cambridge University Press.
170. Latham, J.T., J.R. Bove, and F.L. Weirich, *Chemical and Hematological Changes in Stored CPDA-1 Blood*. *Transfusion*, 1982. **22**(2): p. 158-159.
171. Ravindranath, S.P., et al., *Biofunctionalized Magnetic Nanoparticle Integrated Mid-infrared Pathogen Sensor for Food Matrixes*. *Analytical Chemistry*, 2009. **81**(8): p. 2840-2846.
172. Zhao, Y., et al., *Simultaneous Detection of Multifood-Borne Pathogenic Bacteria Based on Functionalized Quantum Dots Coupled with Immunomagnetic Separation in Food Samples*. *Journal of Agricultural and Food Chemistry*, 2009. **57**(2): p. 517-524.
173. Price, C.W., D.C. Leslie, and J.P. Landers, *Nucleic acid extraction techniques and application to the microchip*. *Lab on a Chip*, 2009. **9**(17): p. 2484-2494.
174. Kilic, A., et al., *Triplex real-time polymerase chain reaction assay for simultaneous detection of Staphylococcus aureus and coagulase-negative staphylococci and determination of methicillin resistance directly from positive blood culture bottles*. *Diagnostic Microbiology and Infectious Disease*. **66**(4): p. 349-355.
175. Lehmann, L.E., et al., *A multiplex real-time PCR assay for rapid detection and differentiation of 25 bacterial and fungal pathogens from whole blood samples*. *Medical Microbiology and Immunology*, 2008. **197**(3): p. 313-324.
176. Ohlin, A., et al., *Real-time PCR of the 16S-rRNA gene in the diagnosis of neonatal bacteraemia*. *Acta Paediatrica*, 2008. **97**(10): p. 1376-1380.
177. Barghouthi, S.A., *A Universal Method for the Identification of Bacteria Based on General PCR Primers*. *Indian Journal of Microbiology*, 2011. **51**(4): p. 430-444.
178. Greisen, K., et al., *PCR PRIMERS AND PROBES FOR THE 16S RIBOSOMAL-RNA GENE OF MOST SPECIES OF PATHOGENIC BACTERIA, INCLUDING BACTERIA FOUND IN CEREBROSPINAL-FLUID*. *Journal of Clinical Microbiology*, 1994. **32**(2): p. 335-351.
179. Lee, C.M., et al., *Estimation of 16S rRNA gene copy number in several probiotic Lactobacillus strains isolated from the gastrointestinal tract of chicken*. *Fems Microbiology Letters*, 2008. **287**(1): p. 136-141.
180. Rajan, L., E. Smyth, and H. Humphreys, *Screening for MRSA in ICU patients. How does PCR compare with culture?* *Journal of Infection*, 2007. **55**(4): p. 353-357.
181. Patel, R., et al., *Multiplex PCR detection of vanA, vanB, vanC-1, and vanC-2/3 genes in enterococci*. *Journal of Clinical Microbiology*, 1997. **35**(3): p. 703-707.